

THE ANALYSIS OF  
THE DOUBLE-KELVIN TRANSMISSION LINE  
AND SOME APPLICATIONS

A THESIS

Presented to  
The Faculty of the Graduate Division  
by  
Joseph Morris Googe

In Partial Fulfillment  
of the Requirements for the Degree  
Doctor of Philosophy in the School of  
Electrical Engineering

Georgia Institute of Technology

February 1963

In presenting the dissertation as a partial fulfillment of the requirements for an advanced degree from the Georgia Institute of Technology, I agree that the Library of the Institution shall make it available for inspection and circulation in accordance with its regulations governing materials of this type. I agree that permission to copy from, or to publish from, this dissertation may be granted by the professor under whose direction it was written, or, in his absence, by the dean of the Graduate Division when such copying or publication is solely for scholarly purposes and does not involve potential financial gain. It is understood that any copying from, or publication of, this dissertation which involves potential financial gain will not be allowed without written permission.

---

0 1 0

2000  
68  
12P

THE ANALYSIS OF  
THE DOUBLE-KELVIN TRANSMISSION LINE  
AND SOME APPLICATIONS

Approved:

\_\_\_\_\_  
\_\_\_\_\_  
\_\_\_\_\_  
\_\_\_\_\_  
\_\_\_\_\_

U

Date Approved by Chairman: March 14, 1963

## ACKNOWLEDGMENT

I wish to thank my thesis advisor, Dr. K. L. Su, for his guidance and encouragement during this investigation. I also express my appreciation to the Ford Foundation for their financial assistance. A special thanks is tendered my family for their patience and understanding.

## TABLE OF CONTENTS

	Page
ACKNOWLEDGMENTS . . . . .	ii
LIST OF TABLES . . . . .	v
LIST OF ILLUSTRATIONS . . . . .	vi
SUMMARY . . . . .	ix
CHAPTER	
I. INTRODUCTION . . . . .	1
Definition and Purpose of the Problem	
History Leading to the Problem	
II. THE DOUBLE-KELVIN LINE BOUNDARY VALUE PROBLEM . . . . .	8
The Partial Differential Equations for the Double Line	
Ordinary Differential Equations for the Steady State Case	
Solution of the Ordinary Differential Equations for the Line	
Boundary Conditions	
III. THE DOUBLE-KELVIN LINE AS A TWOPORT . . . . .	15
Open-Circuit Characteristics	
The u-Plane Behavior of the Double-Kelvin Line	
Real-Frequency Zero	
Real-Frequency Zero Parameter Locus	
Poles of the Open-Circuit Transfer Function	
The Frequency Response of the Double-Kelvin Transmission Line	
IV. THE DOUBLE-KELVIN LINE TWOPORT WITH A SERIES ELEMENT . . . . .	40
The General Case of Series Element	
The Case for a Series Resistance	
The Case for a Series Capacitance	
The Case for a Series Inductance	
Applications of the Double-Line Twoport	
V. EXPERIMENTAL WORK . . . . .	61
Lumped Constant Realization	
Thin-Film Realization	
Parallel Plate Circuit Model	

CHAPTER	Page
VI. CONCLUDING REMARKS . . . . .	80
Results of the Research	
Applications of the Double-Kelvin Line	
Recommendations for Future Research	
APPENDICES . . . . .	83
I. DETAILED SOLUTION OF THE DOUBLE-KELVIN BOUNDARY VALUE PROBLEM . . . . .	84
II. COMPUTATIONAL METHOD FOR THE ROOTS OF TRANSCENDENTAL EQUATIONS . . . . .	94
BIBLIOGRAPHY . . . . .	97
VITA . . . . .	99

LIST OF TABLES

Table	Page
1. Summary of Notation Introduced in Appendix I . . . . .	91

## LIST OF ILLUSTRATIONS

Figure	Page
1. The Double-Kelvin Transmission Line . . . . .	1
2. Circuit Symbols and Diagrams for the Double-Kelvin Line . .	2
3. The Kelvin-Line Twoport . . . . .	3
4. The Kelvin Line with a Series Resistance . . . . .	4
5. Monolithic Distributed Parameter Circuit . . . . .	6
6. Three-Layer Thin-Film Circuits . . . . .	6
7. Section of a Double-Kelvin Line . . . . .	8
8. An Elementary Length of a Double Line . . . . .	8
9. Locations of Boundary Points on the Double Line . . . . .	13
10. Two-Port Notation for the Double Line . . . . .	15
11. Parameter Families for the Double-Kelvin Line . . . . .	19
12. Map of Transfer Function Behavior for the Double-Kelvin Line . . . . .	20
13. RC Ladder Network . . . . .	22
14. RC Loci for the Double-Kelvin Line . . . . .	26
15. u-Plane Root Locus for Variable $c_2/c_1$ . . . . .	27
16. u-Plane Root Locus for Variable $r_2/r_1$ . . . . .	28
17. u-Plane Root Locus for Family of Double-Kelvin Lines Having $K = 23.12$ . . . . .	29
18. Frequency Response of Single and Double Lines . . . . .	34
19. Frequency Response for Family of Double Lines Having $K = 23.12$ . . . . .	35
20. Frequency Response for Three Double Lines with Real- Frequency Zero But Not Having $K = 23.12$ . . . . .	36

Figure	Page
21. Typical Phase Shift Characteristics for Double Lines . . .	37
22. Polar Diagram of the Transfer Function for a Double Line Having a Near Real-Frequency Zero . . . . .	39
23. The Double-Line Twoport with Series Element . . . . .	40
24. Sketch of Typical $z_{12}(u)$ for the Double-Kelvin Twoport . . .	42
25. Frequency Response of Double Line with Series Resistance, Case for $r_2/r_1 = 1.0$ and $c_2/c_1 = 1.0$ . . . . .	46
26. Frequency Response of Double Line with Series Resistance Case for $r_2/r_1 = 0.01$ and $c_2/c_1 = 8.0$ . . . . .	47
27. Frequency Response of Double Line with Series Capacitance. Case for $r_2/r_1 = 1.0$ and $c_2/c_1 = 1.0$ . . . . .	50
28. Frequency Response of Double Line with Series Capacitance. Case for $r_2/r_1 = 0.01$ and $c_2/c_1 = 8.0$ . . . . .	51
29. Frequency Response of Double Line with Series Capacitance. Case for $r_2/r_1 = 1.0$ and $c_2/c_1 = 5.0$ . . . . .	52
30. Frequency Response of Double Line with Series Inductance. Case for $r_2/r_1 = 1.0$ and $c_2/c_1 = 1.0$ . . . . .	54
31. Frequency Response of Double Line with Series Inductance. Case for $r_2/r_1 = 0.01$ and $c_2/c_1 = 8.0$ . . . . .	55
32. Frequency Response of Double Line with Series Inductance. Case for $r_2/r_1 = 0.01$ and $c_2/c_1 = 4.7$ . . . . .	56
33. Frequency Response of a Double Line with Series Resistance Giving a Band-Elimination Characteristic . . . .	60
34. Lumped Approximation of a Double-Kelvin Line . . . . .	62
35. Frequency Response of a Lumped Approximate Double Line, Case for $r_2/r_1 = 1.0$ and $c_2/c_1 = 1.0$ . . . . .	64
36. Frequency Response of a Lumped Approximate Double Line. Case for $r_2/r_1 = 0.01$ and $c_2/c_1 = 4.7$ . . . . .	66
37. High Frequency Equivalent Circuits for the Approximate Double-Kelvin Line when Used with Series R . . . . .	67
38. Frequency Response of Lumped Approximate Double Line With Series Resistance. Case for $r_2/r_1 = 1.0$ and $c_2/c_1 = 1.0$ . . . . .	68

Figure	Page
39. High Frequency Approximate Equivalent Circuit . . . . .	69
40. Frequency Response of Lumped Approximate Double Line with Series Capacitance. Case for $r_2/r_1 = 1.0$ , $c_2/c_1 =$ $1.0$ , and $R_0 = 2.4$ . . . . .	70
41. Frequency Response of Lumped Approximate Double Line with Series Inductance. Case for $r_2/r_1 = 1.0$ , $c_2/c_1 =$ $1.0$ , and $L_0 = 10^{-4}$ . . . . .	71
42. Thin-Film Double-Kelvin Transmission Line . . . . .	72
43. Frequency Response of Thin-Film Double Line. Case for $r_2/r_1 = 1.54$ and $c_2/c_1 = 1.15$ . . . . .	74
44. Frequency Response of Thin-Film Double Line. Case for $r_2/r_1 \rightarrow \infty$ and $c_2/c_1 = 1.0$ . . . . .	75
45. Frequency Response of Parallel Plate Double Line. Case for $r_2/r_1 = 1.0$ and $c_2/c_1 = 1.18$ . . . . .	77
46. Frequency Response of Parallel Plate Double Line. Case for $r_2/r_1 = 0.0117$ and $c_2/c_1 = 5.65$ . . . . .	78

## SUMMARY

The double-Kelvin transmission line is formed when two layers of dielectric and two layers of resistive material of uniform width and thickness are placed on top of a conductive layer. Such a transmission line finds realization in a variety of physical forms, one of which is the thin-film electrical circuit. Four electrical terminals are attached to the device, one at each end of the top and bottom layers, to form a twoport.

In this study, the equilibrium equations for the double-Kelvin line are derived and solved for the steady-state case to obtain expressions for the voltages and currents associated with the double line. These expressions are then used to obtain the open-circuit impedance functions for the twoport formed by the double line. Then, the impedance functions are employed to derive the open-circuit voltage transfer function for the twoport. The resulting transfer function is examined in terms of the amplitude and phase shift of its real-frequency response.

The existence of real-frequency transmission zeros for the double-Kelvin twoport is studied in detail. An important result of the study is the derivation of a parameter locus for the family of double lines having real-frequency zeros. The effect of parameter variations on the transmission zeros of the twoport is also discussed, and real-frequency response data for typical double-line twoports are calculated and displayed.

The versatility of the double-line twoport is extended by the addition of an impedance element in series with the double-line twoport.

This leads to the derivation of the transfer function for the combination double-line with series impedance and the examination of three special cases.

The first special case is that of the resistance which has a transfer function which can be made to have a real-frequency zero for a suitable value of series resistance. Approximate equations for the location of the real-frequency zero and the magnitude of the resistance to produce the zero are derived. Families of transfer functions are calculated and displayed showing the type of frequency response produced by this combination twoport and resistance. The notch filter and band-elimination filter are the types produced by the double line with series resistance.

The second case is that of a double-line twoport with a series capacitance which is also analyzed to obtain the transfer function of the combination twoport. Approximate design formulas and typical frequency response data for this configuration are given. The typical frequency response of this circuit arrangement is of the low-pass type or low-pass type with a notch.

For the third case, the twoport with series inductance is analyzed. This configuration produces an interesting band-elimination filter. Examples of this filter characteristic are calculated and displayed.

The transfer function for the double-Kelvin line and double-Kelvin twoport with series element are verified by comparison with experimental data. The verification was performed with three experimental circuit types, the double line being realized by a lumped approximate circuit, a thin-film circuit, and a parallel plate circuit. Good agree-

ment between calculated and experimental results is demonstrated for all three realizations. Results obtained with the approximate design formulas are also compared with the measured results and the limitations of the lumped approximate double line are examined and discussed.

Suitable applications of the double-Kelvin twoport are discussed. The double line produces filters of the low-pass, band-elimination, notch, and low-pass with notch characteristic. Suggestions for additional applications are made.

The double-Kelvin boundary value problem is solved in detail in an Appendix. A numerical method for calculating the roots of transcendental equations is derived in another Appendix.

CHAPTER I

INTRODUCTION

Definition and Purpose of the Problem

The double-Kelvin transmission line, as it will be called, is formed when two layers of dielectric and two layers of resistive material of uniform width and thickness are placed on top of a conductive layer. Such a transmission line finds realization in a variety of physical forms, one of which is the thin-film electrical circuit. The double-Kelvin line is modeled in Figure 1.

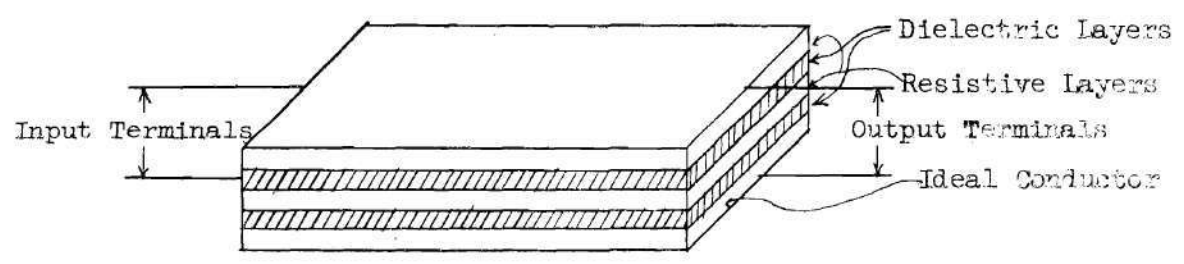


Figure 1. The Double-Kelvin Transmission Line.

The resistive and dielectric layers of the double line are considered to be uniform and isotropic so that the problem is one dimensional. Four electrical terminals are attached to the device, one at each end of the top and bottom layers, to form a twoport. The research is centered about the electrical properties of this twoport with emphasis

on the open-circuit voltage transfer function.

The versatility of the double-Kelvin twoport is extended by the addition of a single impedance element in series with the double line. The circuit diagram for the double line and the circuit diagram for the double line with series element are shown in Figure 2.

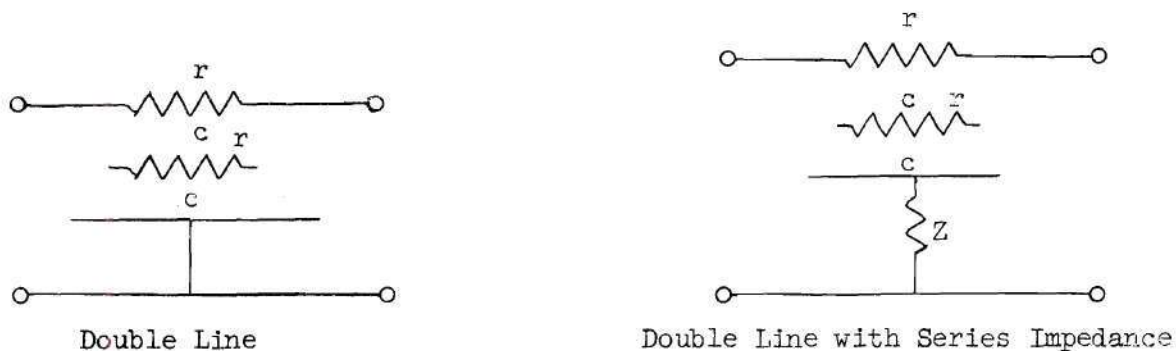


Figure 2. Circuit Symbols and Diagrams for the Double-Kelvin Line.

### History Leading to the Problem

Transmission lines have been of interest as electrical wave filters since their conception. The distributed filter was at first not intentionally inserted, but it was a result of the large physical dimensions of a device. This was the case with Lord Kelvin and the undersea cable. In many other cases, however, a transmission line is deliberately introduced for its particular characteristics of wave shaping or delay.

In 1854 Sir William Thompson, later to become the Lord Kelvin, began an investigation of the practicality of a proposed transoceanic telegraph system.<sup>1</sup> The submarine cables of that period were essentially leakage-free, high-resistance coaxial cables. The conductors were copper, and the dielectric material was gutta-percha which is a sap from a

variety of Malaysian tree.

Lord Kelvin developed formulas for the electrical parameters of the cable and formulated a mathematical model of the telegraph system. His solution of the transmission problem was instrumental in the success of early long distance transmission lines. The results of his analysis are well known and the RC transmission line is often called the Kelvin line.

The Kelvin line has found wide application as a twoport. The circuit for the Kelvin filter is shown in Figure 3.

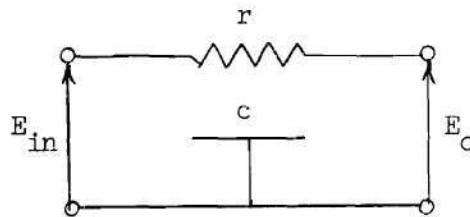


Figure 3. The Kelvin-Line Twoport.

The open-circuit voltage transfer function for the Kelvin line is given by

$$T(s) = \frac{1}{\cosh(\gamma\lambda)} \quad (1-1)$$

where

$$\gamma = \sqrt{src} \quad (1-2)$$

and

$$s = \sigma + j\omega \quad (1-3)$$

and  $\lambda$  is the length of the line. The line constants  $r$  and  $c$  are the per unit length resistance and capacitance of the line.

It is convenient to express Equation (1-1) in the form

$$T(u) = \frac{1}{\cosh(u)} \quad (1-4)$$

where  $u$  is given by

$$u = \sqrt{rc\lambda^2 s} \quad (1-5)$$

which, for real frequencies, is

$$u = \sqrt{rc\lambda^2 \omega} \epsilon^{j\frac{\pi}{4}} \quad (1-6)$$

Tables of  $\cosh(u)$  for both complex and real frequencies were published as early as 1913.<sup>2</sup>

The Kelvin line with series resistance has been analyzed and design formulas are given for its application as a twoport.<sup>3</sup> The behavior of this network is similar to that of the bridged-T filter. Figure 4 shows the circuit diagram of the Kelvin line with a series resistance.

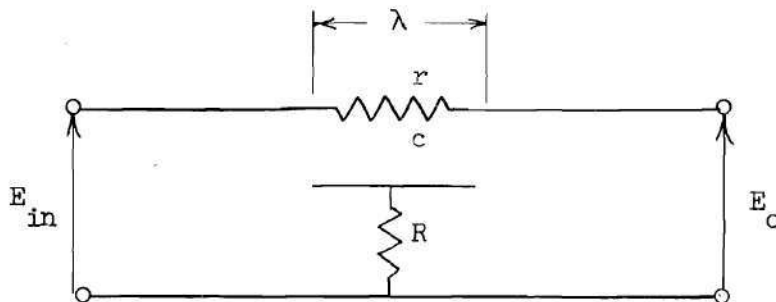


Figure 4. The Kelvin Line with a Series Resistance.

The transfer function of the network in Figure 4 is

$$T(u) = \frac{u \sinh(u) + D}{u \sinh(u) + D \cosh(u)} \quad (1-7)$$

where

$$D = \frac{r\lambda}{R} \quad (1-8)$$

Much effort has been expended in the past few years toward the reduction of the sizes and weights of electrical equipment. The art of miniturization has advanced to the point where circuit components with dimensions in the order of atomic dimensions are employed. Circuits of this dimensional order are called microcircuits and the description of such circuits requires distributed parameter electrical models.

Two of the structures used in passive microcircuits are the thin-film structure and the monolithic structure. The thin-film structure consists of layers or strata of various materials deposited onto a suitable supporting medium or substrate. The Kelvin line of Figure 3 is realizable as a three-strata thin-film circuit.<sup>4</sup>

The monolithic structure for the realization of distributed electrical networks consists of layers of semiconductor materials formed in a small block. The Kelvin line twoport of Figure 5 is an example of a monolithic circuit structure. Distributed resistance is obtained from a lightly doped semiconductor. Distributed capacitance is obtained from a p-n junction with reverse bias potential applied.

Microcircuits are limited to distributed resistance and capacitance for, up to this date, no practical method of producing inductance values has been developed.

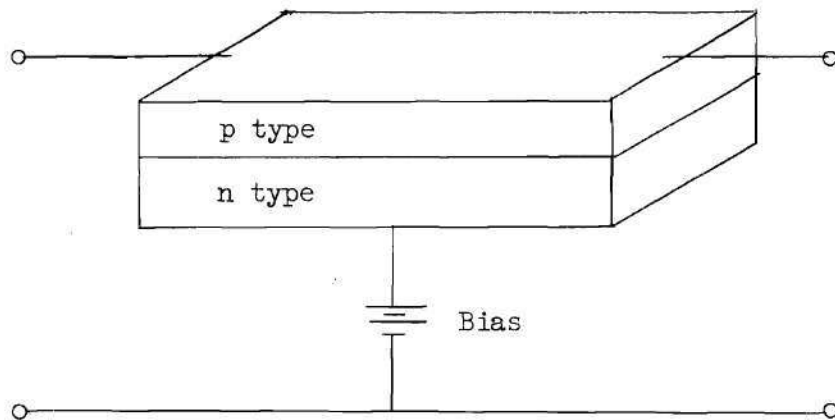


Figure 5. Monolithic Distributed Parameter Circuit.

The Kelvin-line twoport has found wide application both as three-strata film and monolithic circuits. One group of investigators has reported on the morphology of three-layer RC thin-film circuits and catalogued the behavior of the various twoports which can be obtained from this four-terminal network.<sup>5</sup> The two forms of the network discussed in their investigation are shown in Figure 6. The twoports of Figure 6 are only slightly more general than the Kelvin line and add little to its versatility.

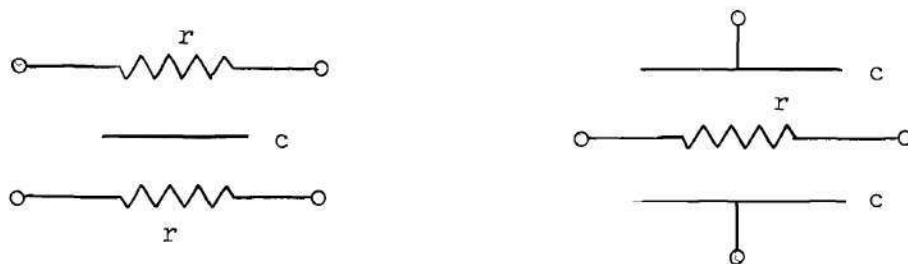


Figure 6. Three-Layer Thin-Film Circuits.

Throughout the past forty years the nonuniform transmission line has been examined as a twoport with possibilities of useful characteristics. J. R. Carson in 1921<sup>6</sup> and A. T. Starr<sup>7</sup> in 1932 contributed much to the general understanding of the nonuniform or tapered transmission line. Recent interest in microcircuits has focused attention on the class of tapered RC lines. Tapered two-wire RC lines are used in electronic oscillators with advantages over lumped circuit elements.<sup>8</sup>

A class of RC transmission line whose parameters vary trigonometrically has been analyzed by K. L. Su.<sup>9</sup> The trigonometric line can be used to obtain an improved notch filter as compared with a uniform line.

Unfortunately, most attempts to improve the versatility of the distributed RC twoport by tapering result in a model without solution in closed form.

An alternative to tapering the line constants has been selected for this research. The logical evolution of the Kelvin line or three strata thin-film circuit is the double-Kelvin line or five-strata thin-film circuit. The complexity and the design freedom of the RC line is consequently extended by the addition of the two strata and the model remains linear with constant coefficients. A solution in closed form is assured and a new configuration is analyzed.

## CHAPTER II

## THE DOUBLE-KELVIN LINE BOUNDARY VALUE PROBLEM

The Partial Differential Equations for the Double Line

The double-Kelvin transmission line has been described in Chapter

I. A section of such a line is shown in Figure 7.

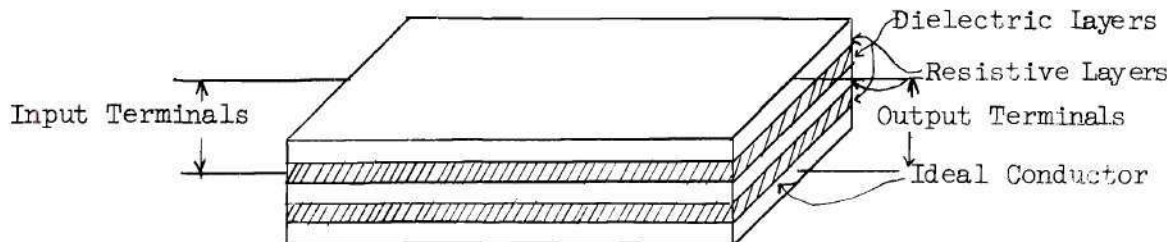


Figure 7. Section of a Double-Kelvin Line.

An elementary length of such a line is shown in Figure 8 and will be used

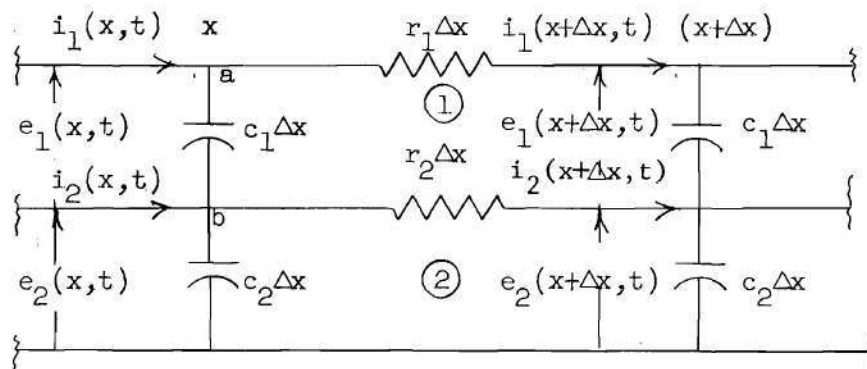


Figure 8. An Elementary Length of a Double Line.

to obtain the electrical equilibrium equations for the line. By applying Kirchoff's law around meshes 1 and 2 and at nodes a and b in the circuit of Figure 8, the following equilibrium equations are written:

$$i_1(x + \Delta x, t)r_1\Delta x + e_1(x + \Delta x, t) - i_2(x + \Delta x)r_2\Delta x - e_1(x, t) = 0 \quad (2-1)$$

$$i_2(x + \Delta x, t)r_2\Delta x + e_2(x + \Delta x, t) - e_2(x, t) = 0 \quad (2-2)$$

$$i_1(x, t) - i_1(x + \Delta x, t) - c_1\Delta x \frac{\partial e_1(x, t)}{\partial t} = 0 \quad (2-3)$$

$$i_2(x, t) + c_1\Delta x \frac{\partial e_1(x, t)}{\partial t} - i_2(x + \Delta x, t) - c_2\Delta x \frac{\partial e_2(x, t)}{\partial t} = 0 \quad (2-4)$$

In the limit as  $\Delta x$  approaches zero these equations become Partial Differential Equations (2-5), (2-6), (2-7), and (2-8).

$$\frac{\partial e_1(x, t)}{\partial x} = r_2 i_2(x, t) - r_1 i_1(x, t) \quad (2-5)$$

$$\frac{\partial e_2(x, t)}{\partial x} = -r_2 i_2(x, t) \quad (2-6)$$

$$\frac{\partial i_1(x, t)}{\partial x} = -c_1 \frac{\partial e_1(x, t)}{\partial t} \quad (2-7)$$

$$\frac{\partial i_2(x, t)}{\partial x} = c_1 \frac{\partial e_1(x, t)}{\partial x} - c_2 \frac{\partial e_2(x, t)}{\partial t} \quad (2-8)$$

#### Ordinary Differential Equations for the Steady State Case

The system of partial differential equations can be reduced to ordinary differential equations with respect to the distance variable  $x$

by assuming sinusoidal forcing functions.

$$\frac{dE_1(x)}{dx} = r_2 I_2(x) - r_1 I_1(x) \quad (2-9)$$

$$\frac{dE_2(x)}{dx} = -r_2 I_2(x) \quad (2-10)$$

$$\frac{dI_1(x)}{dx} = j\omega c_1 E_1(x) \quad (2-11)$$

$$\frac{dI_2(x)}{dx} = j\omega c_1 E_1(x) - j\omega c_2 E_2(x) \quad (2-12)$$

The characteristic determinant for the system of Equations, (2-9) through (2-12), is evaluated as follows.

$$\begin{vmatrix} D & r_1 & 0 & -r_2 \\ 0 & 0 & D & r_2 \\ j\omega c_1 & D & 0 & 0 \\ -j\omega c_1 & 0 & j\omega c_2 & D \end{vmatrix} = D^4 - j\omega(r_1 c_1 + r_2 c_2 + r_2 c_1)D^2 - \omega^2 r_1 c_1 r_2 c_2 \quad (2-13)$$

Since this determinant is not zero, the system is independent and the general solution has four arbitrary constants.<sup>10</sup>

#### Solution of the Ordinary Differential Equations for the Line

Equations (2-9), (2-10), (2-11), and (2-12) can be solved by first manipulating them into diagonal form. The results of this process are shown below.

$$\frac{d^4 I_1}{dx^4} - j\omega(r_1 c_1 + r_2 c_2 + r_2 c_1) \frac{d^2 I_1}{dx^2} - \omega^2 r_1 c_1 r_2 c_2 I_1 = 0 \quad (2-14)$$

$$\frac{dI_1}{dx} + j\omega c_1 E_1 = 0 \quad (2-15)$$

$$r_1 I_1 + \frac{dE_1}{dx} - r_2 I_2 = 0 \quad (2-16)$$

$$-j\omega c_1 E_1 + \frac{dI_2}{dx} + j\omega c_2 E_2 = 0 \quad (2-17)$$

The solutions for the currents and voltages follow directly from the preceding diagonal system. The details of the solution are contained in Appendix I.

$$I_1(x) = A_1 e^{-\alpha x} + A_2 e^{-\beta x} + A_3 e^{\alpha x} + A_4 e^{\beta x} \quad (2-18)$$

$$E_1(x) = \frac{\alpha}{j\omega c_1} A_1 e^{-\alpha x} + \frac{\beta}{j\omega c_1} A_2 e^{-\beta x} - \frac{\alpha}{j\omega c_1} A_3 e^{\alpha x} - \frac{\beta}{j\omega c_1} A_4 e^{\beta x} \quad (2-19)$$

$$I_2(x) = \left[ \frac{r_1}{r_2} - \frac{\alpha^2}{j\omega r_2 c_1} \right] A_1 e^{-\alpha x} + \left[ \frac{r_1}{r_2} - \frac{\beta^2}{j\omega r_2 c_1} \right] A_2 e^{-\beta x} \quad (2-20)$$

$$+ \left[ \frac{r_1}{r_2} - \frac{\alpha^2}{j\omega r_2 c_1} \right] A_3 e^{\alpha x} + \left[ \frac{r_1}{r_2} - \frac{\beta^2}{j\omega r_2 c_1} \right] A_4 e^{\beta x}$$

$$E_2(x) = \frac{r_2}{\alpha} \left[ \frac{r_1}{r_2} - \frac{\alpha^2}{j\omega r_2 c_1} \right] A_1 e^{-\alpha x} + \frac{r_2}{\beta} \left[ \frac{r_1}{r_2} - \frac{\beta^2}{j\omega r_2 c_1} \right] A_2 e^{-\beta x} \quad (2-21)$$

$$- \frac{r_2}{\alpha} \left[ \frac{r_1}{r_2} - \frac{\alpha^2}{j\omega r_2 c_1} \right] A_3 e^{\alpha x} - \frac{r_2}{\beta} \left[ \frac{r_1}{r_2} - \frac{\beta^2}{j\omega r_2 c_1} \right] A_4 e^{\beta x}$$

where

$$\alpha = \sqrt{j\omega \frac{(r_1 c_1 + r_2 c_2 + r_2 c_1)}{2}} \left\{ 1 + \sqrt{1 - \frac{4r_1 c_1 r_2 c_2}{(r_1 c_1 + r_2 c_2 + r_2 c_1)^2}} \right\} \quad (2-22)$$

and

$$\beta = \sqrt{j\omega \frac{(r_1 c_1 + r_2 c_2 + r_2 c_1)}{2}} \left\{ 1 - \sqrt{1 - \frac{4r_1 c_1 r_2 c_2}{(r_1 c_1 + r_2 c_2 + r_2 c_1)^2}} \right\} \quad (2-23)$$

In order to simplify the evaluation of the arbitrary constants, the preceding equations are written in matrix form.

$$\begin{bmatrix} I_1(x) \\ E_1(x) \\ I_2(x) \\ E_2(x) \end{bmatrix} = \begin{bmatrix} f_1(x) & f_2(x) & f_3(x) & f_4(x) \\ f_5(x) & f_6(x) & f_7(x) & f_8(x) \\ f_9(x) & f_{10}(x) & f_{11}(x) & f_{12}(x) \\ f_{13}(x) & f_{14}(x) & f_{15}(x) & f_{16}(x) \end{bmatrix} \begin{bmatrix} A_1 \\ A_2 \\ A_3 \\ A_4 \end{bmatrix} \quad (2-24)$$

In Equation (2-24), each function in the square matrix represents the corresponding function in Equations (2-18) through (2-21). For the exact definitions of these functions, see Table 1 of Appendix I. For convenience, the following notation will be used to indicate the value of a function at the sending or input end of the double line.

$$f_k(x) \Big|_{x=0} = f_k \quad (2-25)$$

#### Boundary Conditions

The boundary conditions for the evaluation of the four arbitrary constants in the solution to the homogeneous system are listed below.

$$I_1(\lambda) = 0 \quad (2-26)$$

$$I_2(0) = 0 \quad (2-27)$$

$$I_2(\lambda) = 0 \quad (2-28)$$

$$E_1(0) + E_2(0) = E_{in} \quad (2-29)$$

The locations of these boundary points are indicated in the diagram of the double line shown in Figure 9.

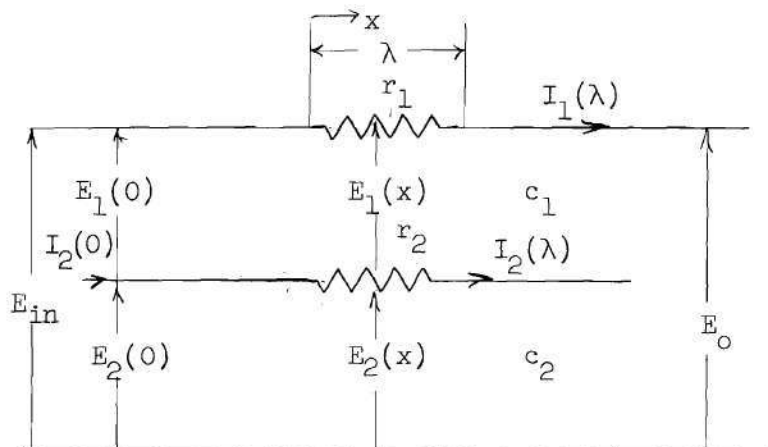


Figure 9. Locations of Boundary Points on the Double Line.

Applying the specified boundary conditions to Equations (2-18) through (2-21) produces the matrix equation shown below.

$$\begin{bmatrix} e^{-\alpha\lambda} & e^{-\beta\lambda} & e^{\alpha\lambda} & e^{\beta\lambda} \\ f_9 & f_{10} & f_9 & f_{10} \\ f_9 e^{-\alpha\lambda} & f_{10} e^{-\beta\lambda} & f_9 e^{\alpha\lambda} & f_{10} e^{\beta\lambda} \\ \frac{r_1}{\alpha} & \frac{r_1}{\beta} & -\frac{r_1}{\alpha} & -\frac{r_1}{\beta} \end{bmatrix} \begin{bmatrix} A_1 \\ A_2 \\ A_3 \\ A_4 \end{bmatrix} = \begin{bmatrix} 0 \\ 0 \\ 0 \\ E_{in} \end{bmatrix} \quad (2-30)$$

The evaluation of the constants  $A_1$ ,  $A_2$ ,  $A_3$ , and  $A_4$  and the simplification of the resulting terms yield the expressions for the steady-state currents and voltages of interest on the double-Kelvin transmission line.

$$I_1(x) = E_{in} \frac{f_9 \sinh(\alpha\lambda) \sinh(\lambda-x)\beta - f_{10} \sinh(\beta\lambda) \sinh(\lambda-x)\alpha}{\frac{r_1 f_9}{\beta} \sinh(\alpha\lambda) \cosh(\beta\lambda) - \frac{r_1 f_{10}}{\alpha} \sinh(\beta\lambda) \cosh(\alpha\lambda)} \quad (2-31)$$

$$I_2(x) = E_{in} \frac{f_9 f_{10} \sinh(\alpha\lambda) \sinh(\lambda-x)\beta - f_9 f_{10} \sinh(\beta\lambda) \sinh(\lambda-x)\alpha}{\frac{r_1 f_9}{\beta} \sinh(\alpha\lambda) \cosh(\beta\lambda) - \frac{r_1 f_{10}}{\alpha} \sinh(\beta\lambda) \cosh(\alpha\lambda)} \quad (2-32)$$

$$E_1(x) = E_{in} \frac{f_6 f_9 \sinh(\alpha\lambda) \sinh(\lambda-x) - f_5 f_{10} \sinh(\beta\lambda) \cosh(\lambda-x)\alpha}{\frac{r_1 f_9}{\beta} \sinh(\alpha\lambda) \cosh(\beta\lambda) - \frac{r_1 f_{10}}{\alpha} \sinh(\beta\lambda) \cosh(\alpha\lambda)} \quad (2-33)$$

$$E_2(x) = E_{in} \frac{f_9 f_{14} \sinh(\alpha\lambda) \cosh(\lambda-x) - f_{10} f_{13} \sinh(\beta\lambda) \cosh(\lambda-x)\alpha}{\frac{r_1 f_9}{\beta} \sinh(\alpha\lambda) \cosh(\beta\lambda) - \frac{r_1 f_{10}}{\alpha} \sinh(\beta\lambda) \cosh(\alpha\lambda)} \quad (2-34)$$

Addition of Equations (2-33) and (2-34) produces an expression for the voltage between the top and bottom wires of the line.

$$E(x) = E_{in} \frac{\alpha f_9 \sinh(\alpha\lambda) \cosh(\lambda-x)\beta - \beta f_{10} \sinh(\beta\lambda) \cosh(\lambda-x)\alpha}{\alpha f_9 \sinh(\alpha\lambda) \cosh(\beta\lambda) - \beta f_{10} \sinh(\beta\lambda) \cosh(\alpha\lambda)} \quad (2-35)$$

The detailed solution of the problem which is outlined in this Chapter is given in Appendix I.

## CHAPTER III

## THE DOUBLE-KELVIN LINE AS A TWOPORT

Open-Circuit Characteristics

The solution of the boundary value problem described in Chapter II produced the expressions for the voltages and currents in the model of the double line. The expressions required to derive the open-circuit impedance functions for the double line are:

$$I_1(x) = E_{in} \frac{f_9 \sinh(\alpha\lambda) \sinh(\lambda-x) - f_{10} \sinh(\beta\lambda) \sinh(\lambda-x)\alpha}{\frac{r_1 f_9}{\beta} \sinh(\alpha\lambda) \cosh(\beta\lambda) - \frac{r_1 f_{10}}{\alpha} \sinh(\beta\lambda) \cosh(\alpha\lambda)} \quad (3-1)$$

$$E(x) = E_{in} \frac{f_9 \sinh(\alpha\lambda) \cosh(\lambda-x)\beta - \beta f_{10} \sinh(\beta\lambda) \cosh(\lambda-x)\alpha}{\alpha f_9 \sinh(\alpha\lambda) \cosh(\beta\lambda) - \beta f_{10} \sinh(\beta\lambda) \cosh(\alpha\lambda)} \quad (3-2)$$

The open-circuit impedance functions are defined by the following expressions which use the notation shown in Figure 10.

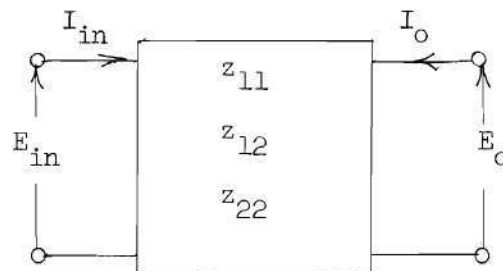


Figure 10. Two-Port Notation for the Double Line.

$$z_{11} = \left. \frac{E_{in}}{I_{in}} \right|_{I_o=0} = \frac{E_{in}}{I_1(0)} \quad (3-3)$$

For the double line, Equation (3-3) becomes

$$z_{11} = \frac{k_1 \sinh(\alpha\lambda) \cosh(\beta\lambda) + k_2 \sinh(\beta\lambda) \cosh(\alpha\lambda)}{\sinh(\alpha\lambda) \sinh(\beta\lambda)} \quad (3-4)$$

where  $k_1$  and  $k_2$  are defined as

$$k_1 = \frac{r_1 f_9}{(f_9 - f_{10})} \quad (3-5)$$

and

$$k_2 = \frac{r_1 f_{10}}{(f_9 - f_{10})} \quad (3-6)$$

The open-circuit transfer impedance is

$$z_{12} = \left. \frac{E_o}{I_{in}} \right|_{I_o=0} = \frac{E(\lambda)}{I_1(0)} \quad (3-7)$$

which becomes

$$z_{12} = \frac{k_1 \sinh(\alpha\lambda) + k_2 \sinh(\beta\lambda)}{\sinh(\alpha\lambda) \sinh(\beta\lambda)} \quad (3-8)$$

for the double-Kelvin line. The double-line is a symmetrical twoport and, therefore, requires only two open-circuit impedance functions for its description.

The open-circuit voltage transfer function can be calculated using the relationship

$$T(s) = \frac{E_o}{E_{in}} \Big|_{I_o=0} = \frac{z_{12}}{z_{11}} \quad (3-9)$$

Substitution of Equations (3-4) and (3-8) into (3-9) yields

$$T(s) = \frac{k_1 \sinh(\alpha\lambda) + k_2 \sinh(\beta\lambda)}{k_1 \sinh(\alpha\lambda) \cosh(\beta\lambda) + k_2 \sinh(\beta\lambda) \cosh(\alpha\lambda)} \quad (3-10)$$

#### The u-Plane

If a new independent variable  $u$  is defined which is related to the complex frequency variable  $s$  by Equation (3-11), Equation (3-9) can be put into the form shown in Equation (3-12).

$$u = \sqrt{sr_1c_1}\lambda^2 \quad (3-11)$$

$$T(u) = \frac{K_1 \sinh(Au) + K_2 \sinh(Bu)}{K_1 \sinh(Au) \cosh(Bu) + K_2 \sinh(Bu) \cosh(Au)} \quad (3-12)$$

The following new parameters and variables have been defined in the process of reducing Equation (3-10) to the form of Equation (3-12).

$$\tau' = \frac{1}{2} \left( 1 + \frac{r_2}{r_1} + \frac{r_2c_2}{r_1c_1} \right) \quad (3-13)$$

$$A = \sqrt{\tau' + \sqrt{\tau'^2 - \frac{r_2c_2}{r_1c_1}}} \quad (3-14)$$

$$B = \sqrt{\tau' - \sqrt{\tau'^2 - \frac{r_2 c_2}{r_1 c_1}}} \quad (3-15)$$

$$K_1 = \frac{A^2 - 1}{B(A^2 - B^2)} \quad (3-16)$$

$$K_2 = \frac{1 - B^2}{A(A^2 - B^2)} \quad (3-17)$$

The behavior of the open-circuit voltage transfer function can now be more conveniently examined in the  $u$ -plane which is normalized, square root, and complex frequency domain.

#### The $u$ -Plane Behavior of the Double-Kelvin Line

The newly introduced parameters,  $K_1$ ,  $K_2$ ,  $A$  and  $B$ , of Equation (3-12) are related to the resistance and capacitance constants of the double line by nonlinear algebraic formulas which are developed in Appendix I. The relationships between these parameters and the line constants are shown graphically in Figure 11. Families of curves for constant  $K_1$ ,  $K_2$ ,  $A$  and  $B$  are drawn on logarithmic axes with  $r_2/r_1$  for the abscissa and  $c_2/c_1$  for the ordinate.

Information relative to the behavior of the double-line transfer function can be deduced from Figure 11. A study of the comparative magnitudes of the parameters  $K_1$ ,  $K_2$ ,  $A$  and  $B$  over wide ranges of  $r_2/r_1$  and  $c_2/c_1$  allows approximations to be made in the transfer function expression for certain ranges of line constants. The salient features of this study are discussed in the following paragraphs and also shown in the map of Figure 12.

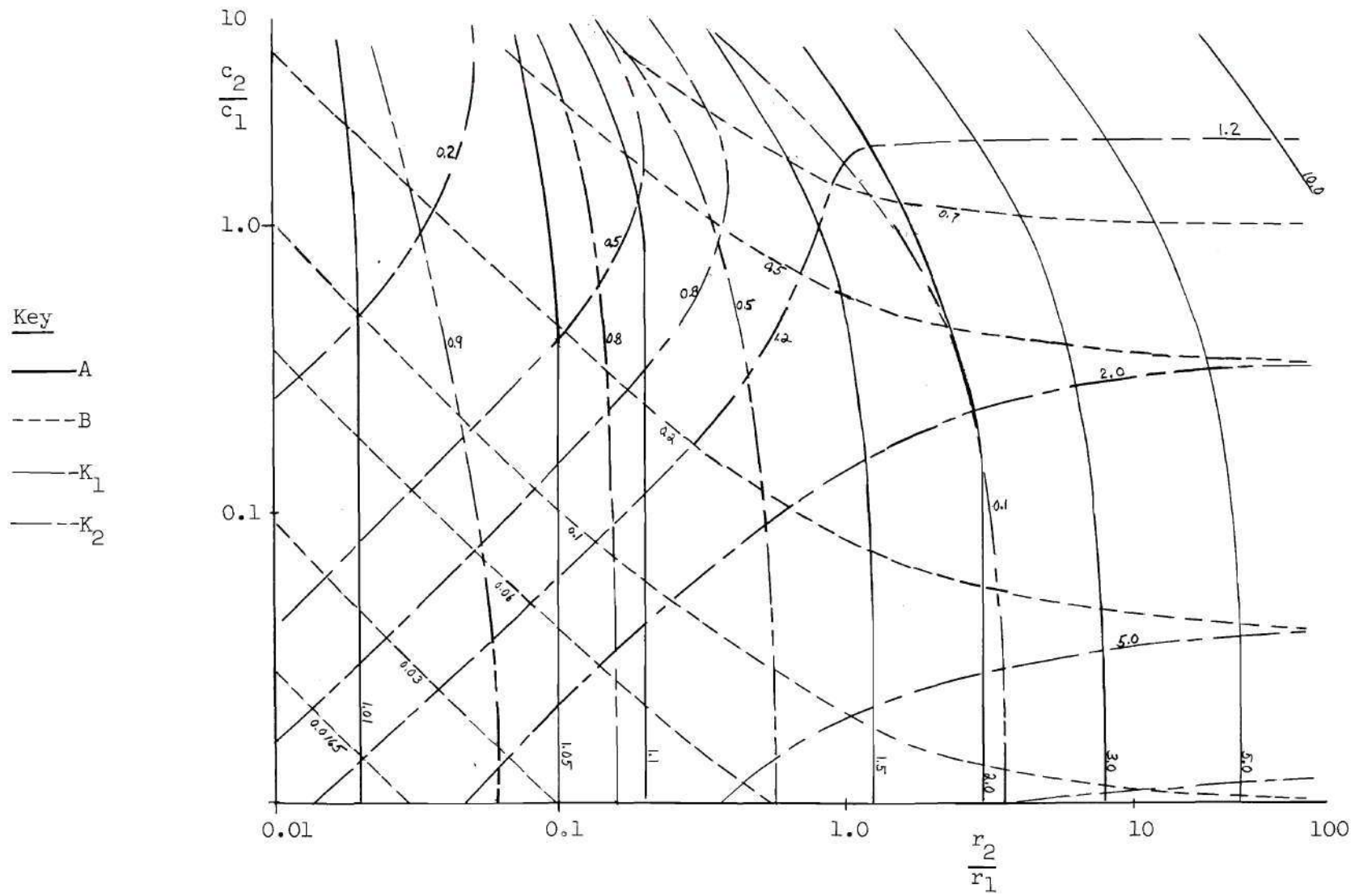


Figure 11. Parameter Families for the Double-Kelvin Line.

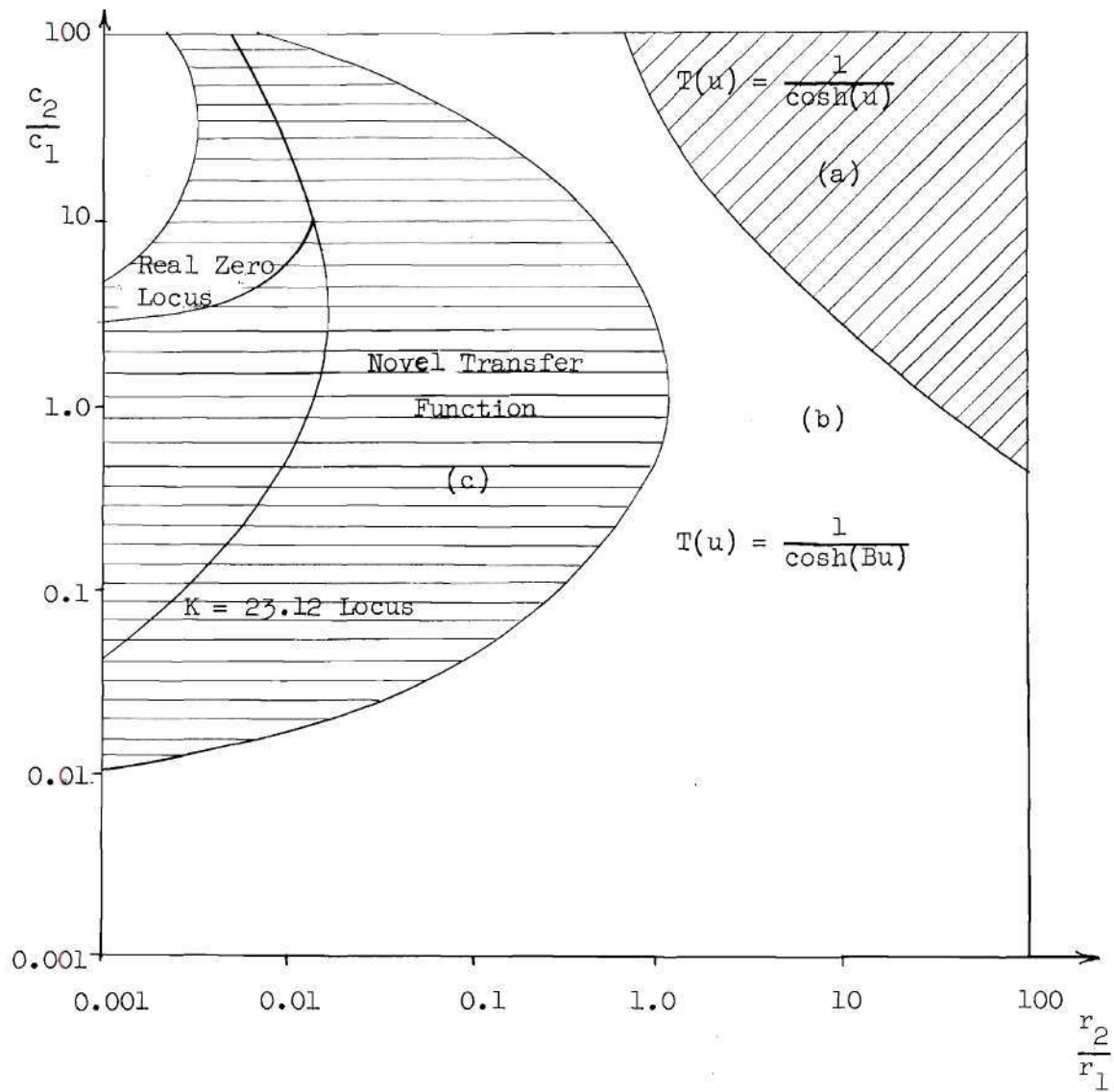


Figure 12. Map of Transfer Function Behavior for the Double-Kelvin Line.

When the resistance ratio  $r_2/r_1$  is large, that is greater than unity, the double line behaves as a single line with a modified frequency scale. This includes the regions (a) and (b) in Figure 12. Since the current in the  $r_2$  stratum is always constrained to zero at the sending and receiving ends of the line, it is not surprising that the  $r_2/r_1$  ratio must be small before the effects of the additional strata are noticeable.

The double line is identical in behavior to a single line when both  $r_2/r_1$  and  $c_2/c_1$  are large. The region where these conditions are satisfied occupies the upper right portion of Figure 12 and is marked as region (a).

The region defined by a very small  $r_2/r_1$  ratio, (not shown on the map) that is 0.001 or less, contains parameters for lines which behave similar to single lines having a series capacitance of magnitude  $c_2\lambda$  farads. The behavior of a single-line twoport with series capacitance is discussed elsewhere.<sup>11</sup>

The range of  $r_2/r_1$  and  $c_2/c_1$  parameters producing novel behavior is indicated in Figure 12 as region (c). It is to this region of unique behavior that the most attention is focused.

#### Real-Frequency Zero

The open-circuit transfer function of the single-Kelvin or RC two-wire transmission line is described in the  $u$ -domain by

$$T(u) = \frac{1}{\cosh(u)} \quad (3-18)$$

The function in Equation (3-18) has an infinite number of simple poles on

the imaginary axis in the  $u$ -plane. These singularities are located on the negative real axis in the  $s$ -plane.

The lumped-circuit element counterpart of the single-Kelvin line, the RC ladder network of Figure 13, has no transfer function poles at the origin or infinity and a finite number of simple poles on the negative real axis in the  $s$ -plane. The transfer function zeros of the RC ladder are restricted to the negative real axis also, but may be of any order.<sup>12</sup>

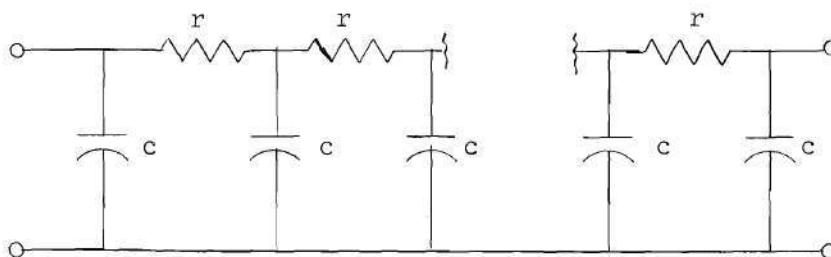


Figure 13. RC Ladder Network.

In the case of the double-Kelvin transmission line the poles and zeros of the voltage transfer function are the roots of transcendental equations formed by the numerator and denominator of Equation (3-12). The numerator of this equation can be written as

$$N(u) = \sinh(Au) + K \sinh(Bu) \quad (3-19)$$

where

$$K = \frac{K_1}{K_2} > 0 \quad (3-20)$$

The roots of Equation (3-19) are infinite in number but can never be

real because of the physical limitations on the line parameters. No explicit method exists for obtaining the roots of Equation (3-19), but it is possible to find some of its roots by numerical techniques. Of particular interest is the possibility of roots in the  $u$ -plane which transform to real-frequency roots in the  $s$ -plane. The locus of real frequency roots in the  $s$ -plane is the 45 degree line in the first quadrant in the  $u$ -plane. This can be seen from a consideration of the transformation between  $u$  and  $s$  given by Equation (3-11).

Setting Equation (3-19) equal to zero and using the relationship

$$u = x + jy \quad (3-21)$$

produce the following pair of real equations

$$\cos(Ay) \sinh(Ax) + K \cos(By) \sinh(Bx) = 0 \quad (3-22)$$

$$\sin(Ay) \cosh(Ax) + K \sin(By) \cosh(Bx) = 0 \quad (3-23)$$

Since the complex frequency  $s$  is proportional to  $u^2$ , the existence of real frequency roots for Equation (3-19) is evidenced by the existence of real roots in the simultaneous solution of Equations (3-22) and (3-23) when  $x$  is set equal to  $y$ . Setting  $x$  equal to  $y$  in these equations yields

$$\cos(Ay) \sinh(Ay) + K \cos(By) \sinh(By) = 0 \quad (3-24)$$

$$\sin(Ay) \cosh(Ay) + K \sin(By) \cosh(By) = 0 \quad (3-25)$$

At this point in the analysis it is useful to introduce the approximations

$$\cosh(Ay) = \sinh(Ay) = \frac{1}{2} e^{Ay} \quad (3-26)$$

$$\cosh(By) = \sinh(By) = \frac{1}{2} \epsilon^{By} \quad (3-27)$$

which are reasonable for large arguments. The resulting approximate equations are

$$\cos(Ay)\epsilon^{(A-B)y} = -K \cos(By) \quad (3-28)$$

$$\sin(Ay)\epsilon^{(A-B)y} = -K \sin(By) \quad (3-29)$$

Equations (3-28) and (3-29) have a solution under the following conditions:

$$(A-B)y = n\pi \quad n = \pm 1, \pm 3, \pm 5, \dots \quad (3-30)$$

$$K = \epsilon^{n\pi} \quad n = \pm 1, \pm 3, \pm 5, \dots \quad (3-31)$$

The value of  $u$  given by this solution  $u_{on}$ , and the corresponding real frequency root,  $\omega_{on}$ , are

$$u_{on} = \frac{\sqrt{2} n\pi}{A-B} \epsilon^{j\frac{\pi}{4}} \quad (3-32)$$

$$\omega_{on} = \frac{|u_{on}|^2}{r_{1c} \lambda^2} \text{ rad/sec} \quad (3-33)$$

The case which proves to be of practical interest is that for  $n=1$ . This value of  $n$  requires

$$K = e^{\pi} = 23.12 \quad (3-34)$$

and produces a real-frequency zero at

$$\omega_{01} = \frac{2\pi^2}{(A-B)^2 r_1 c_1 \lambda^2} \text{ rad/sec} \quad (3-35)$$

#### Real-Frequency Zero Parameter Locus

The condition necessary for a real-frequency root to exist in the numerator of the transfer function of the double-Kelvin transmission line, specified by Equation (3-34), is satisfied only for certain values of the line constants. The locus of all values of  $c_2/c_1$  and  $r_2/r_1$  which produce a  $K = 23.12$  has been calculated and is shown in Figure 14.

Since this value of  $K$  applies only to the approximate equation, the roots corresponding to the lines with parameters on this locus were calculated to check the approximation. The check shows the approximation to be accurate when  $c_2/c_1$  is greater than 5. When the  $c_2/c_1$  ratio is less than 5 the exact locus for real-frequency roots has been calculated. Both loci are shown in Figure 14. The numerical method used to compute the roots of the transcendental equations in this study is described in Appendix II. The actual and approximate loci are seen to merge as the magnitude of the real-frequency root increases.

The effect of parameter variations on the location of the transmission zero was investigated and the results are shown in Figures 15, 16, and 17. Figure 15 shows the root locus in the  $u$ -plane for a particular double-Kelvin line as the  $c_2/c_1$  ratio of the line is varied around the value required for a real-frequency zero. The  $r_2/r_1$  ratio for the line is held constant. The locus crosses the 45 degree line twice. These two crossings occur for values of line parameters which satisfy the  $K$  equal to 23.12 condition.

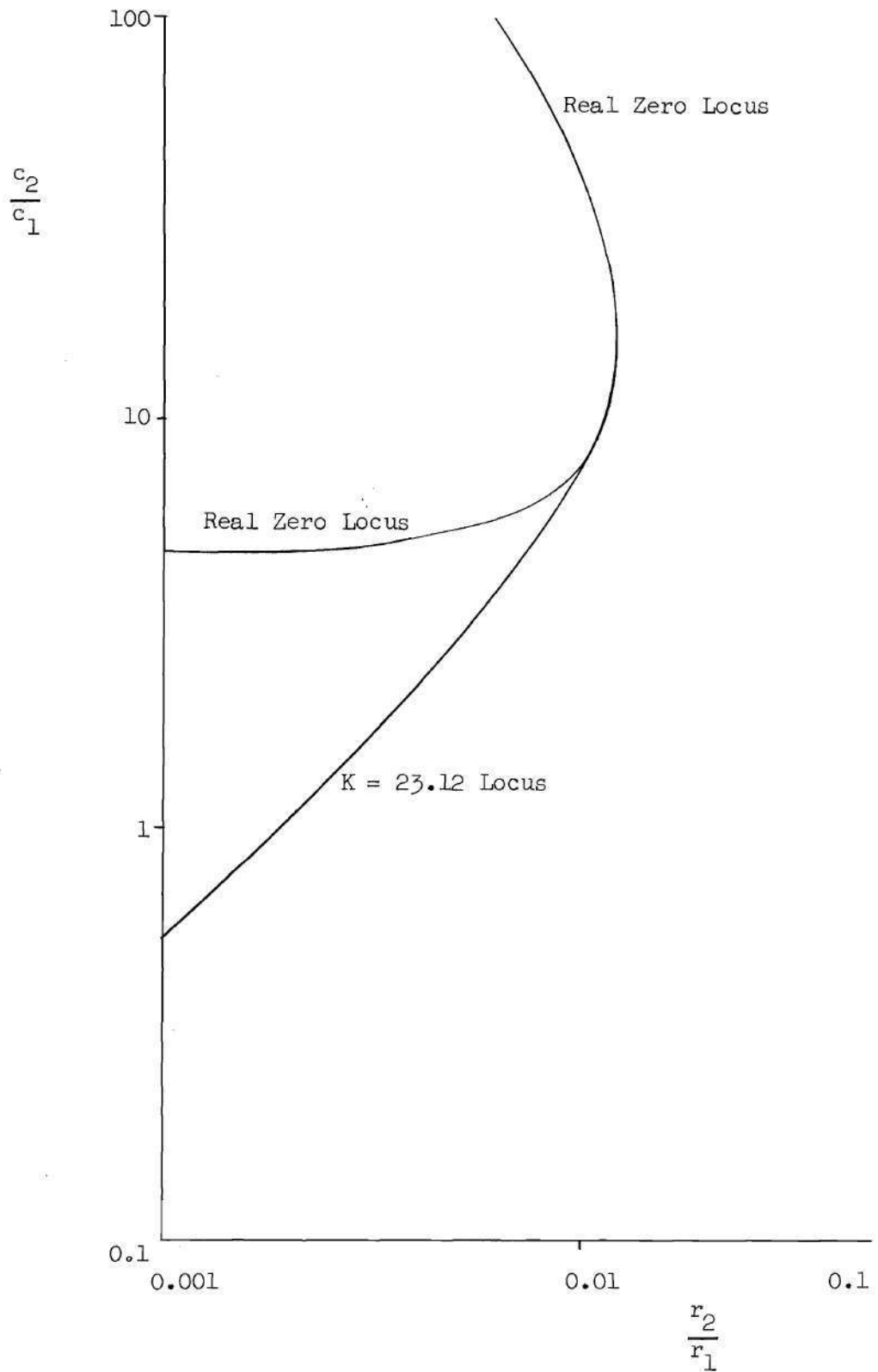


Figure 14. RC Loci for the Double-Kelvin Line.

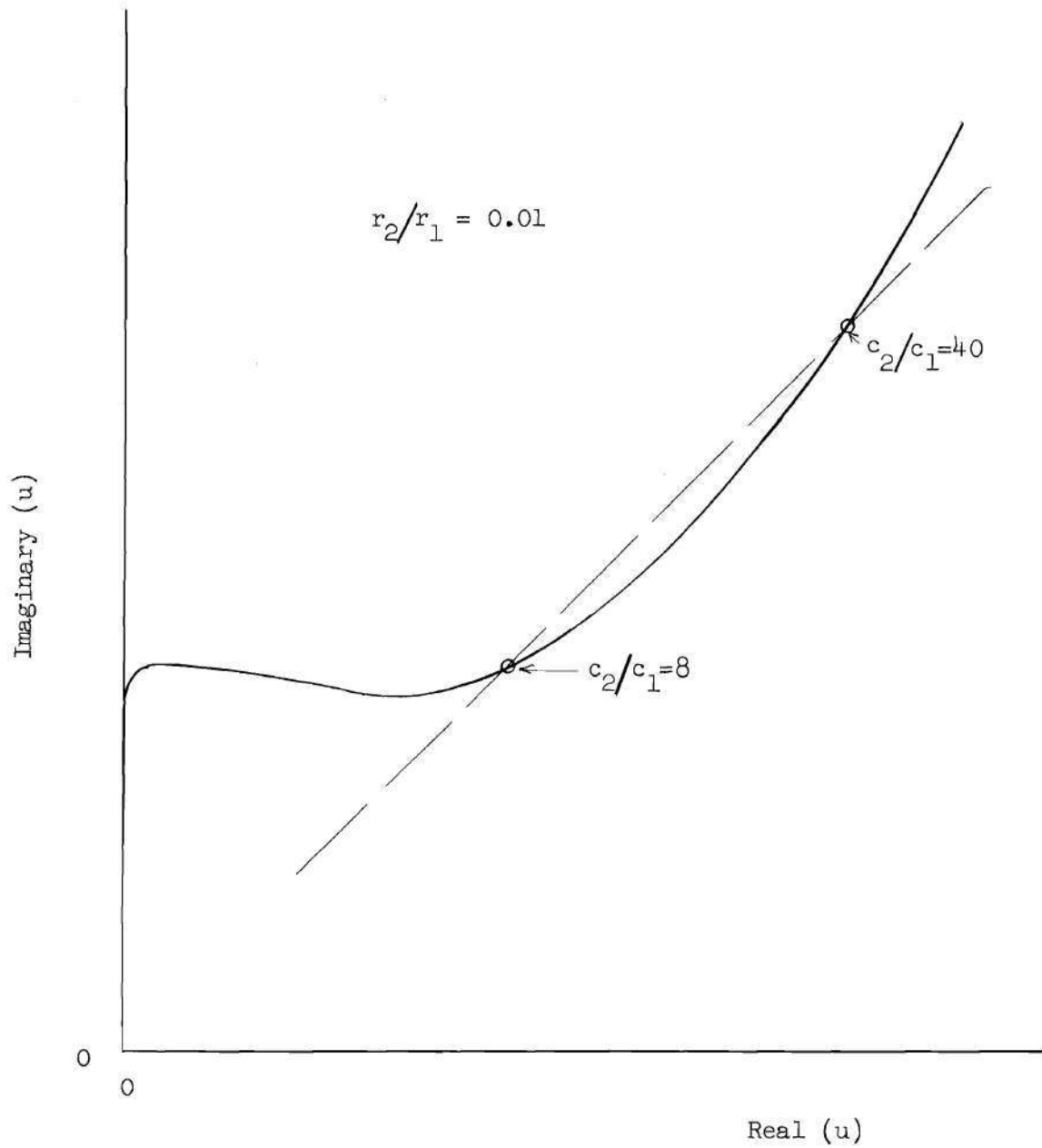


Figure 15.  $u$ -Plane Root Locus for Variable  $c_2/c_1$ .

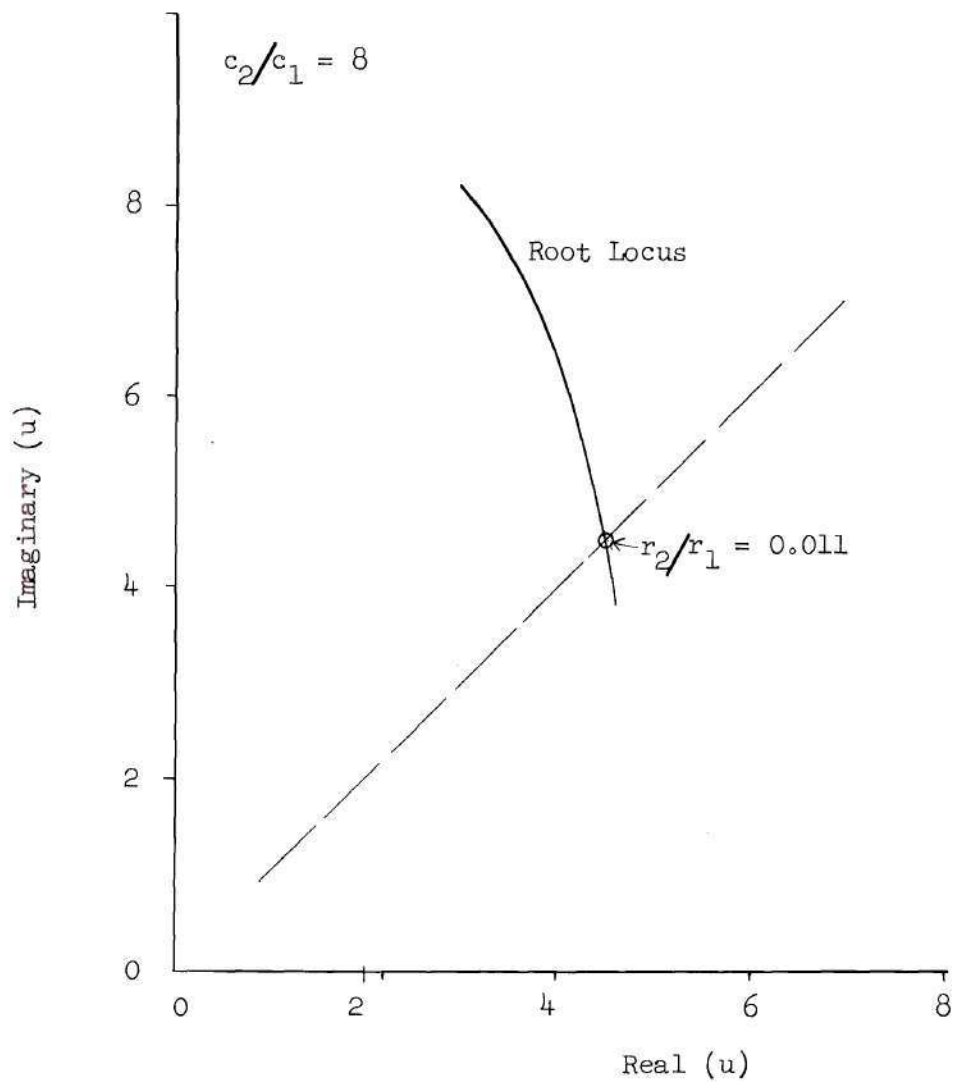


Figure 16.  $u$ -Plane Root Locus for Variable  $r_2/r_1$ .

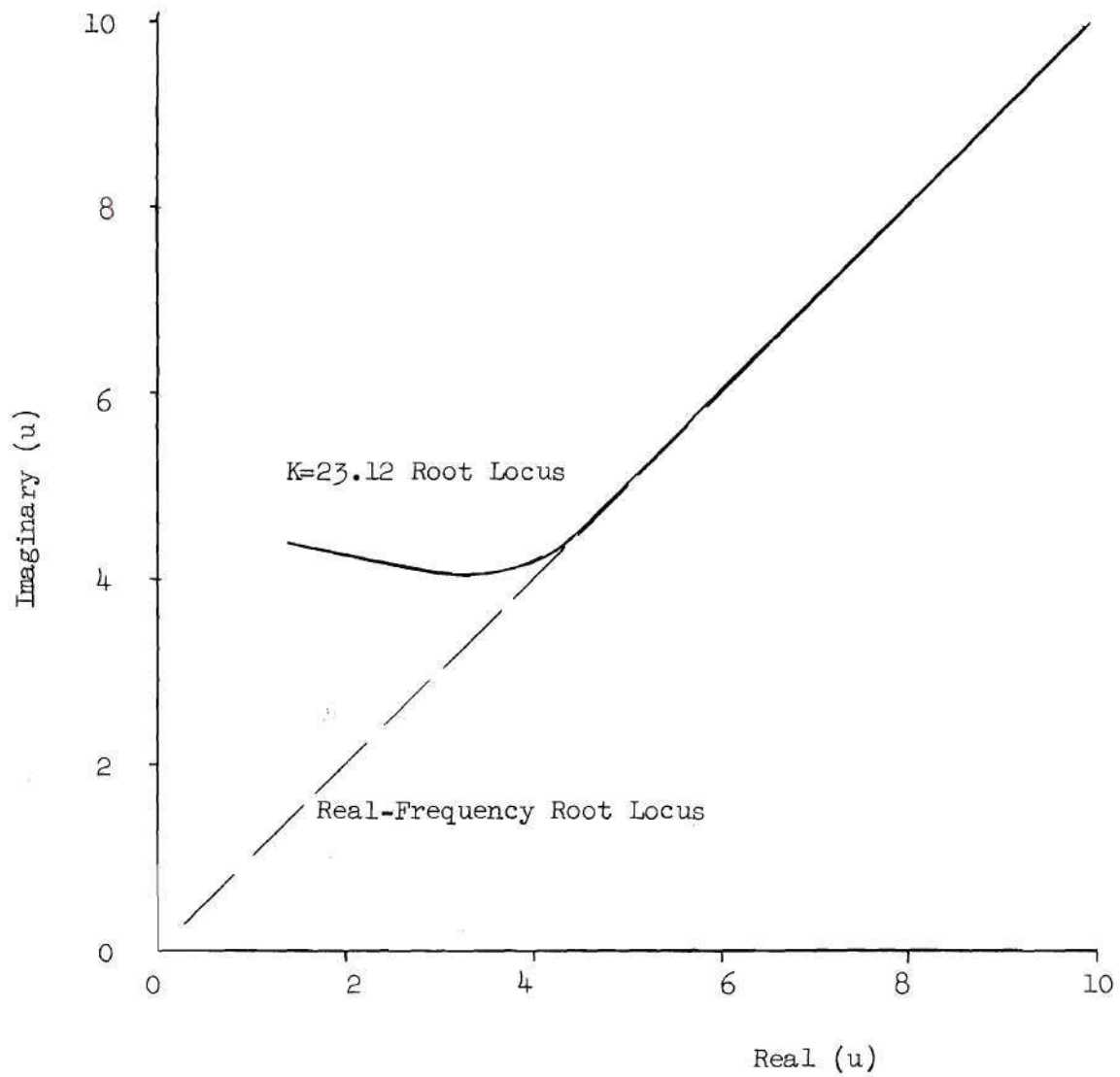


Figure 17.  $u$ -Plane Root Locus for Family of Double-Kelvin Lines Having  $K = 23.12$ .

Figure 17 shows the root locus in the  $u$ -plane for a similar line as the  $r_2/r_1$  ratio is varied about the value required for a real-frequency transmission zero. In this case the  $c_2/c_1$  ratio is held constant and the locus crosses the 45 degree line only once.

Figure 17 is a plot of the root locus for a family of double lines each of which satisfies the  $K = 23.12$  criterion. It can be seen that this root locus approaches the true real-frequency root locus, the 45 degree line, as the magnitude of the root increases.

#### Poles of the Open-Circuit Transfer Function

Poles in the open-circuit voltage transfer function will be produced by the poles of the numerator and zeros of the denominator functions of Equation (3-12). Since the numerator function can be seen to have no internal poles it remains to examine the denominator function for zeros. When the denominator function of the transfer function is set to zero, there is obtained

$$\sinh(A + B)u + K' \sinh(A - B)u = 0 \quad (3-36)$$

where

$$K' = \frac{K_1 - K_2}{K_1 + K_2} \quad (3-37)$$

Since both  $K_1$  and  $K_2$  are greater than zero,

$$-1 > K' > 1 \quad (3-38)$$

Because of the above restriction on the value of  $K'$  and the previous restrictions on  $A$  and  $B$ , the roots of Equation (3-36) lie only on the

imaginary axis in the u-plane. This can be demonstrated as follows.

Let u be replaced by  $x + jy$ . Equation (3-36) can be written as two real variable equations.

$$\cos(A+B)y \sinh(A+B)x + K' \cos(A-B)y \sinh(A-B)x = 0 \quad (3-39)$$

$$\sin(A+B)y \cosh(A+B)x + K' \sin(A-B)y \cosh(A-B)x = 0 \quad (3-40)$$

Rearrange Equations (3-39) and (3-40) to yield

$$\frac{\cos(A+B)y}{\cos(A-B)y} = -K' \frac{\sinh(A-B)x}{\sinh(A+B)x} \quad (3-41)$$

$$\frac{\sin(A+B)y}{\sin(A-B)y} = -K' \frac{\cosh(A-B)x}{\cosh(A+B)x} \quad (3-42)$$

The magnitudes of the right hand members of Equations (3-41) and (3-42) are always less than unity. Therefore, in order to satisfy Equations (3-41) and (3-42) the following inequities must be satisfied.

$$\left| \frac{\cos(A+B)y}{\cos(A-B)y} \right| < 1 \quad (3-43)$$

$$\left| \frac{\sin(A+B)y}{\sin(A-B)y} \right| < 1 \quad (3-44)$$

The complementary nature of the sine and cosine functions precludes the simultaneous satisfaction of the Equations (3-43) and (3-44). If, however  $x=0$ , Equations (3-36) becomes

$$\sin(A+B)y + K' \sin(A-B)y = 0 \quad (3-45)$$

Equation (3-45) can have a real solution in y. Such a real solution lies

on the negative real or imaginary-frequency axis in the  $s$ -plane. Thus it has been demonstrated that the transfer function of the double-Kelvin line has no real-frequency poles.

#### The Frequency Response of the Double-Kelvin Transmission Line

The open-circuit voltage transfer function for the double line, expressed by Equation (3-12), can be written as

$$T(u) = \frac{\sinh(Au) + K \sinh(Bu)}{\sinh(Au) \cosh(Bu) + K \sinh(Bu) \cosh(Au)} \quad (3-46)$$

It has been convenient to examine the behavior of the double line in the  $u$ -domain rather than the  $s$ -domain. The relationships between the independent variables  $u$ ,  $s$ , and  $\omega$ , are

$$u = \sqrt{sr_1c_1\lambda^2} \quad (3-47)$$

$$u = \sqrt{\omega r_1 c_1 \lambda^2} e^{j\frac{\pi}{4}} \quad (3-48)$$

$$\omega = \frac{|u|^2}{r_1 c_1 \lambda^2} \text{ rad/sec} \quad (3-49)$$

The real-frequency behavior of the double line has been shown to be related to the behavior of  $T(u)$  along the 45 degree axis in the  $u$ -plane. Therefore, the frequency response data has been calculated for values of  $u$  lying on the 45 degree axis and are plotted with the magnitude as the abscissa. Equation (3-49) can be used to change the abscissa scale to the real-frequency scale if desired.

The general shape of the amplitude characteristic of the double line transfer function differs significantly from the lowpass characteristic of a single line only when there is a transfer-function zero near the real-frequency axis in the  $s$ -plane. The existence of such a zero has been shown to occur for lines with values of  $K$  near 23.12. Figure 18 shows the attenuation characteristic of a single-Kelvin line and two double-Kelvin lines for comparison. The parameters for the lines are tabulated on the Figure.

The data shown on Figure 19 are from a family of double lines having parameters lying on the  $K = 23.12$  locus of Figure 14. It is noticeable that the depth of the nulls in the transfer functions decreases with the frequency at which the null occurs. As the magnitude of the root of the transfer function decreases, it moves away from the axis of real roots, and the shallow nulls are those caused by roots well off the real-frequency axis.

Double lines having real-frequency zeros but whose values of  $K$  differ from 23.12 behave very much like single lines with external capacitance in series. Such lines have parameters given by the section of the locus shown in Figure 14 which is not part of the  $K = 23.12$  locus. Kaufman's method of analysis and results can be modified to give a good approximate treatment of a line of this type.<sup>13</sup> The frequency response for a family of such lines is shown in Figure 20.

The phase shift characteristics of the open-circuit voltage transfer function of typical double-Kelvin transmission lines are shown in Figure 21. The phase shift characteristic for a single-Kelvin line (curve (a)) is also shown for comparison. The phase shift of a double-

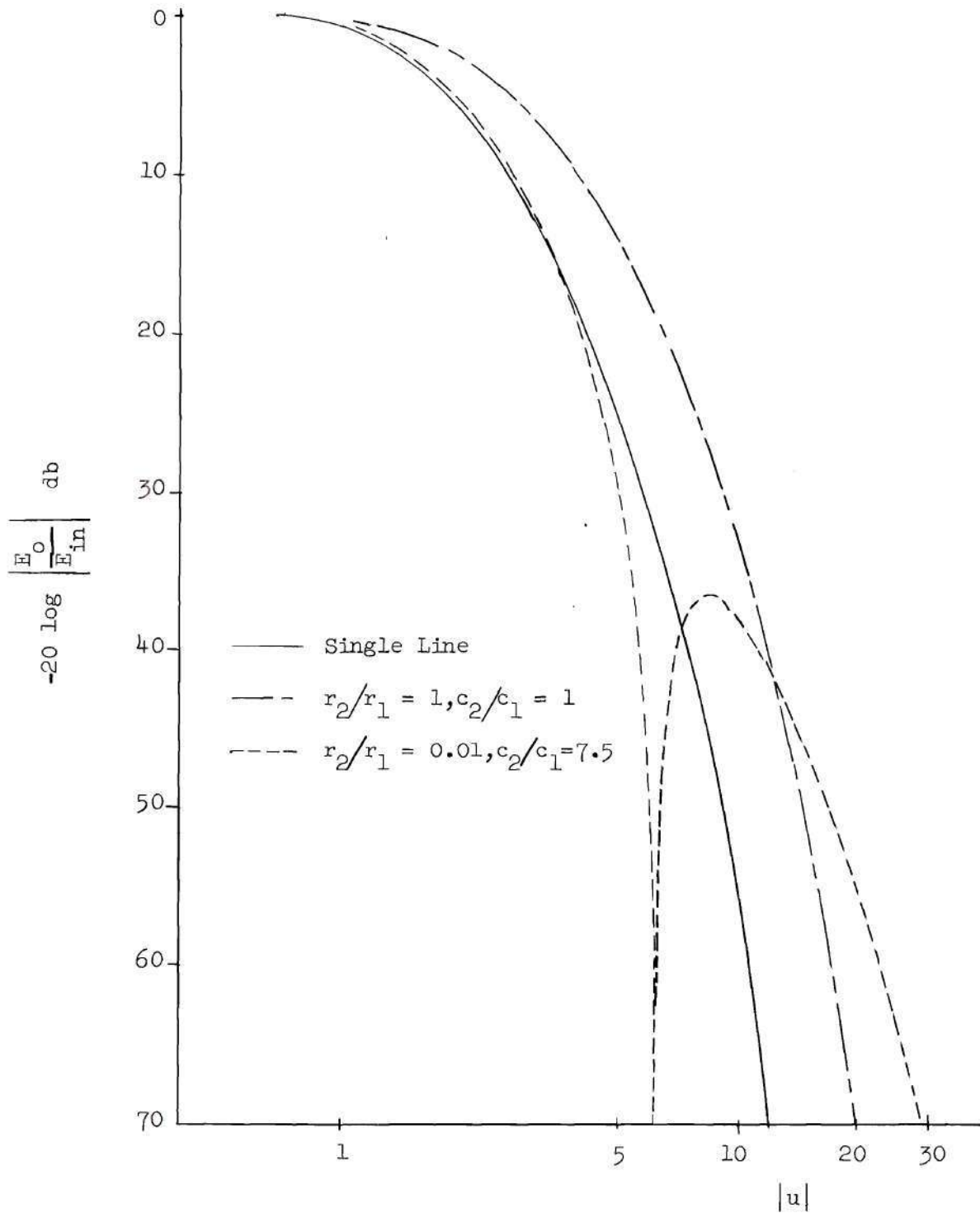


Figure 18. Frequency Response of Single and Double Lines.

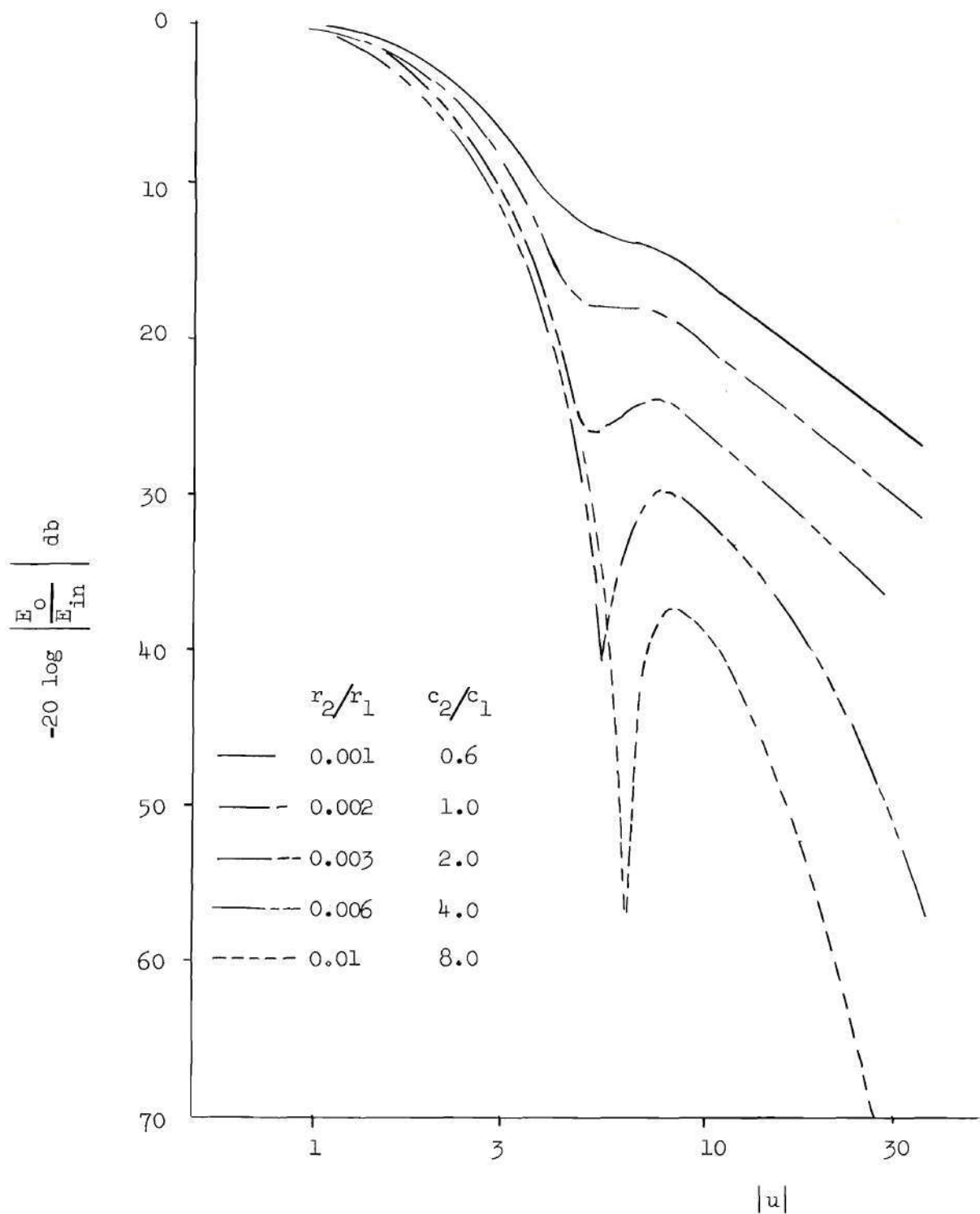


Figure 19. Frequency Response for Family of Double Lines Having  $K = 23.12$ .

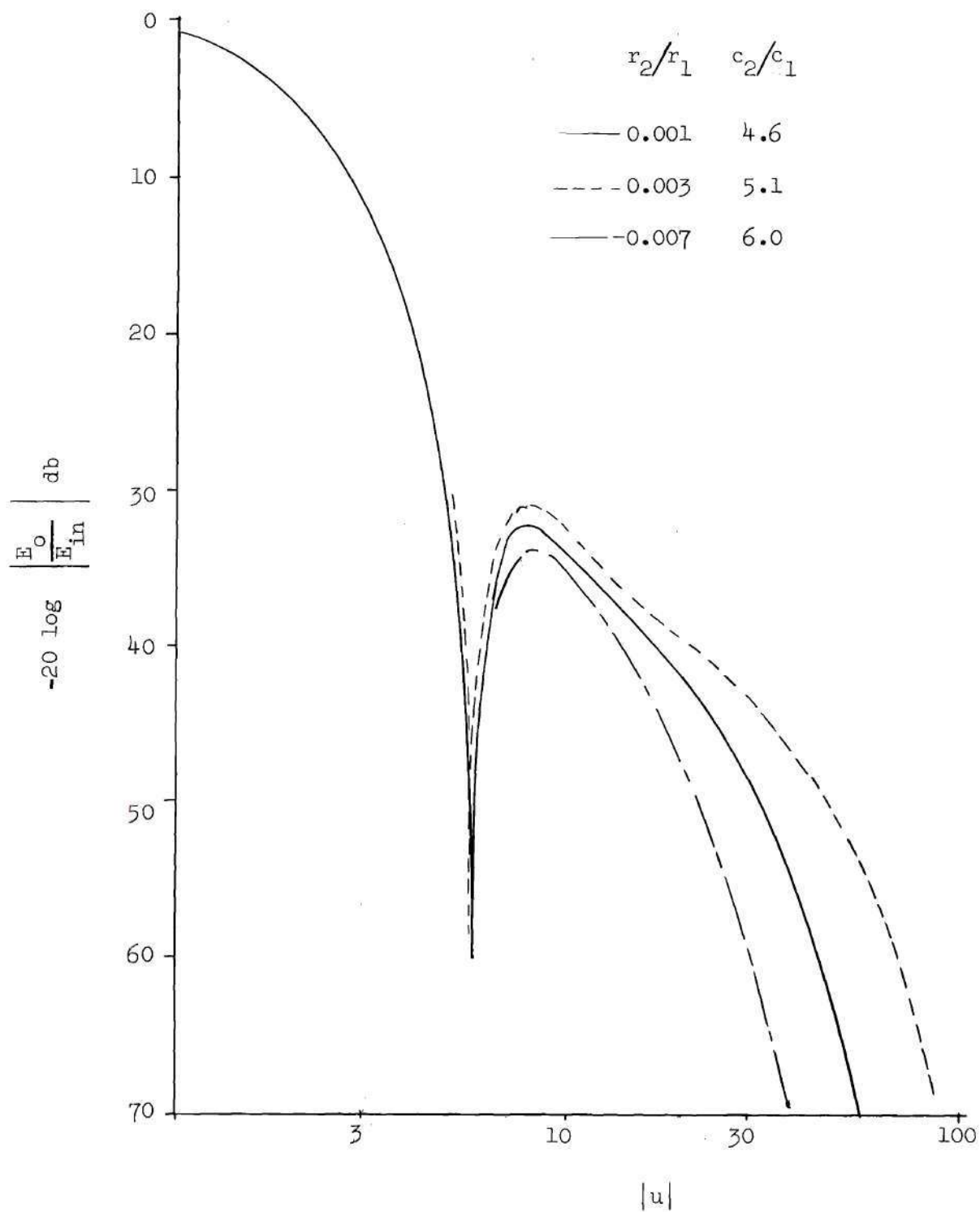


Figure 20. Frequency Response of Three Double Lines with Real-Frequency Zero But Not Having  $K = 23.12$ .

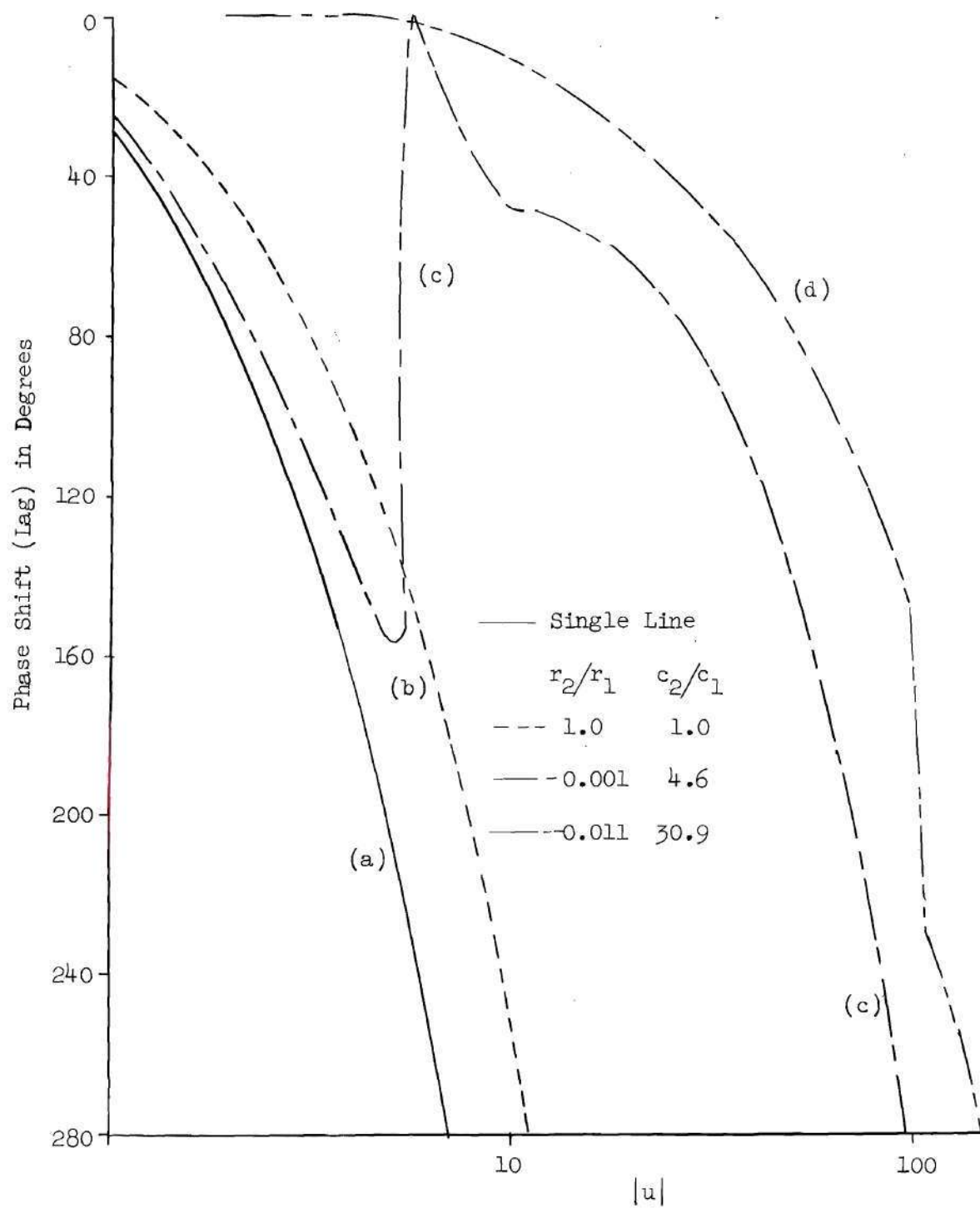


Figure 21. Typical Phase Shift Characteristics for Double Lines.

Kelvin line which has no zero near the real-frequency axis is similar to that of the single line. Curve (b) shows the phase shift of this type line.

A true real-frequency zero in the transfer function causes a discontinuity in the phase shift curve. A near real-frequency zero causes a rapid but continuous change in the phase of the transfer function. The phase shift curve (c) in Figure 21 is for a line with a near real-frequency zero. The amplitude and phase shift for this line are shown in a polar diagram in Figure 22. Notice that the origin of the polar diagram is not encircled by the locus in this case.

Curve (d) in Figure 21 shows phase shift data for a line having a near real zero. In this case the polar plot would encircle the origin and there is a corresponding rapid increase in phase shift.

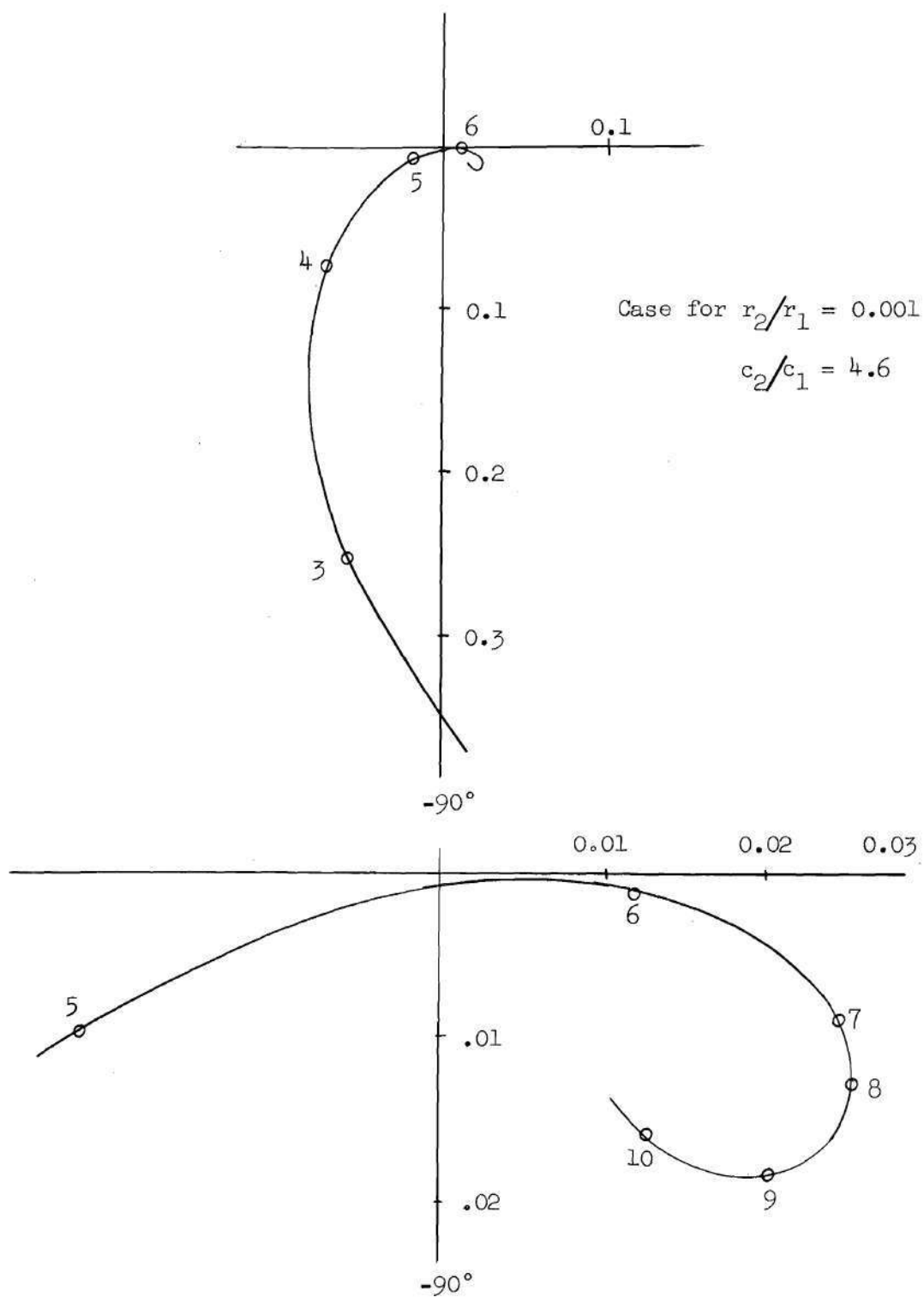


Figure 22. Polar Diagram of the Transfer Function for a Double Line Having a Near Real-Frequency Zero.

## CHAPTER IV

## THE DOUBLE-KELVIN LINE TWOPORT WITH A SERIES ELEMENT

The General Case of Series Impedance

The behavior of the double-Kelvin line twoport when connected in series with a linear and passive circuit element will be investigated. Figure 23 shows the configuration of the circuit to be analyzed.

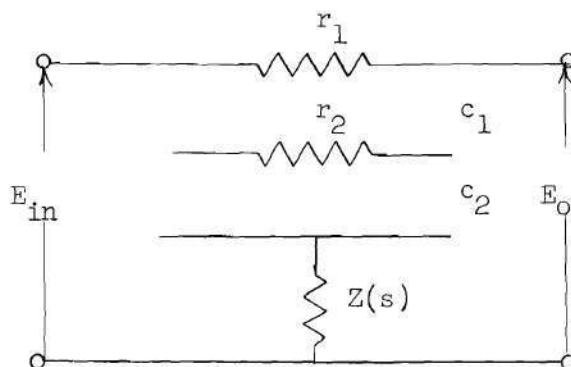


Figure 23. The Double-Line Twoport with Series Element

If the double line is designated as twoport "a" and the impedance  $Z(s)$  is considered as twoport "b," then the open-circuit impedance parameters in the  $s$ -domain of the series twoports are given by the following relationships.<sup>14</sup>

$$z_{11} = z_{11}^a + z_{11}^b = z_{11}^a + Z \quad (4-1)$$

$$z_{12} = z_{12}^a + z_{12}^b = z_{12}^a + Z \quad (4-2)$$

which become, after substitution and simplification

$$z_{11}(s) = \frac{Z(s)(f_9 - f_{10}) \sinh(\alpha\lambda) \sinh(\beta\lambda) + \left(\frac{f_9 r_1}{\beta}\right) \sinh \alpha\lambda \cosh \beta\lambda - \left(\frac{r_1 f_{10}}{\alpha}\right) \sinh(\beta\lambda) \cosh(\alpha\lambda)}{(f_9 - f_{10}) \sinh(\alpha\lambda) \sinh(\beta\lambda)} \quad (4-3)$$

and

$$z_{12}(s) = \frac{Z(s)(f_9 - f_{10}) \sinh(\alpha\lambda) \sinh(\beta\lambda) + \left(f_9 \frac{r_1}{\beta}\right) \sinh(\alpha\lambda) - \left(f_{10} \frac{r_1}{\beta}\right) \sinh(\beta\lambda)}{(f_9 - f_{10}) \sinh \alpha\lambda \sinh \beta\lambda} \quad (4-4)$$

The open-circuit voltage transfer function of the network of Figure 23 is given by

$$T(s) = \frac{Z(s)(f_9 - f_{10}) \sinh(\alpha\lambda) \sinh(\beta\lambda) + \left(\frac{f_9 r_1}{\beta}\right) \sinh(\alpha\lambda) - \left(\frac{f_{10} r_1}{\alpha}\right) \sinh(\beta\lambda)}{Z(s)(f_9 - f_{10}) \sinh(\alpha\lambda) \sinh(\beta\lambda) + \left(\frac{f_9 r_1}{\beta}\right) \sinh(\alpha\lambda) \cosh(\beta\lambda) - \left(\frac{f_{10} r_1}{\alpha}\right) \sinh(\beta\lambda) \cosh(\alpha\lambda)} \quad (4-5)$$

It has been found convenient to investigate the behavior of Equation (4-5) in the  $u$ -plane rather than the  $s$ -plane. The transformations between  $u$  and  $s$  introduced in Chapter III allow Equation (4-5) to be written in the  $u$ -domain as

$$T(u) = \frac{Z_o u \sinh(Au) \sinh(Bu) + K_1 \sinh(Au) + K_2 \sinh(Bu)}{Z_o u \sinh(Au) \sinh(Bu) + K_1 \sinh(Au) \cosh(Bu) + K_2 \sinh(Bu) \cosh(Au)} \quad (4-6)$$

where

$$Z_o = \frac{Z(u)}{r_1 \lambda} \quad (4-7)$$

Notice that Equation (4-6) reduces to Equation (3-12) when  $Z_0$  is zero.

Examination of the open-circuit transfer impedance for the double line, given by

$$z_{12}^a(u) = \frac{r_1 \lambda [K_1 \sinh(Au) + K_2 \sinh(Bu)]}{u \sinh(Au) \sinh(Bu)} \cong \frac{r_1 \lambda K_1}{u \sinh(Bu)} \quad (4-8)$$

indicates the possible choices for  $Z$  to produce a transmission zero. A polar plot for a typical  $z_{12}^a(u)$  for values of  $u$  on the real-frequency axis is sketched in Figure 24.

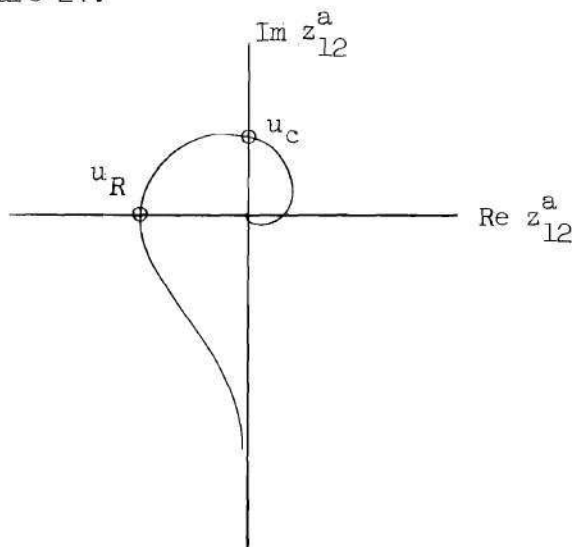


Figure 24. Sketch of Typical  $z_{12}^a(u)$  for the Double-Kelvin Twoport.

The first opportunity to create a transmission zero with a single-element impedance occurs at the point on the sketch of  $z_{12}^a(u)$  marked  $u_R$ . At this frequency a suitable resistance value for  $Z$  will produce a transmission zero.

The second opportunity for a transmission zero with a single element impedance occurs at the frequency marked  $u_c$ . At this frequency a

suitable capacitance will produce a transmission zero.

There is also a third and much higher frequency at which an inductance will produce a zero. However, the amplitude of the transfer function is out of the dynamic range of practical interest before this point is reached.

#### The Case for a Series Resistance

The first element to be considered for Z is a resistance. Let

$$Z_o(s) = R_o = \frac{R}{r_1 \lambda} \quad (4-9)$$

For this case, Equation (4-6) becomes

$$T(u) = \frac{R_o u \sinh(Au) \sinh(Bu) + K_1 \sinh(Au) + K_2 \sinh(Bu)}{R_o u \sinh(Au) \sinh(Bu) + K_1 \sinh(Au) \cosh(Bu) + K_2 \sinh(Bu) \cosh(Au)} \quad (4-10)$$

The series resistance introduces two new terms in the open-circuit voltage transfer function. The new term in the numerator makes it possible to tune the twoport for a real-frequency zero by adjusting the magnitude of R. This is in contrast to the case of the double line of Chapter III which has a real-frequency zero only for selected line parameters.

The approximate conditions for producing a real-frequency zero in the transfer function of Equation (4-10) have been derived. They are valid approximations for lines having  $K_1$  larger than  $K_2$ . An examination of the data shown in Figure 11 of the preceding chapter will show this condition to be satisfied over a large range of line parameters.

Starting with this assumption,  $K_1 > K_2$ , the numerator of Equation

(4-10) when set to zero becomes, after the  $K_2$  term is cast out,

$$R_o u \sinh(Bu) + K_1 = 0 \quad (4-11)$$

The real and imaginary parts of Equation (4-11) are given by Equations (4-13) and (4-14) for values of  $u$  on the real-frequency axis; that is, for

$$u = \frac{u(1+j1)}{\sqrt{2}} \quad (4-12)$$

$$\cos \frac{B|u|}{\sqrt{2}} \sinh \frac{B|u|}{\sqrt{2}} - \sin \frac{B|u|}{\sqrt{2}} \cosh \frac{B|u|}{\sqrt{2}} = \frac{\sqrt{2} K_1}{R_o |u|} \quad (4-13)$$

$$\cos \frac{B|u|}{\sqrt{2}} \sinh \frac{B|u|}{\sqrt{2}} + \sin \frac{B|u|}{\sqrt{2}} \cosh \frac{B|u|}{\sqrt{2}} = 0 \quad (4-14)$$

Equation (4-14) requires, for an approximate real root,

$$|u| \cong (n\pi - \frac{\pi}{4}) \frac{\sqrt{2}}{B} \quad n = 1, 2, 3, 4 \dots \dots \quad (4-15)$$

Under the conditions expressed in Equation (4-15), Equation (4-13) can be satisfied for  $n = 1$  if

$$R_o \cong 0.0569(K_1)(B) \quad (4-16)$$

The approximate frequency of the null in the frequency response due to this real-frequency root can be calculated from

$$\omega_{\text{null}} \cong \frac{9\pi^2}{8r_1 c_1 \lambda^2 B^2} \quad \text{rad/sec} \quad (4-17)$$

When  $K_2$  is not neglected, the numerator of the transfer function can not be solved for a real-frequency zero by any satisfactory approximation. The only method found for locating a zero under this condition is to calculate values of the transfer function in the vicinity of a zero over a range of series resistance values to locate the exact position of the zero and the value of resistance producing the zero. This technique is useful only when a high speed computer is available.

The general pattern of behavior for the double line with series resistance element is shown by the family of characteristics of Figure 25. The curves are for selected values of  $R_0$  starting with zero and including the value causing a real-frequency zero.

Figure 26 is a similar family of transfer functions but for a double line having parameters such that a zero exists in the transfer function near the real-frequency axis when  $R_0 = 0$ . In this example, as  $R_0$  is increased the null is improved. Further increases in  $R_0$  broaden the null and produce a band-elimination characteristic in the transfer function.

The high frequency behavior of the double-line transfer function for the case with an external resistance can be approximated by

$$T(u) \cong \frac{u}{u + \frac{K_1 + K_2}{R_0}} \quad (4-18)$$

However, this expression is not of much practical use because it is valid only when  $u$  is so large as to be of no interest in many examples. The transfer function rises towards unity very slowly because the terms proportional to  $u$  in the numerator and denominator of the transfer function

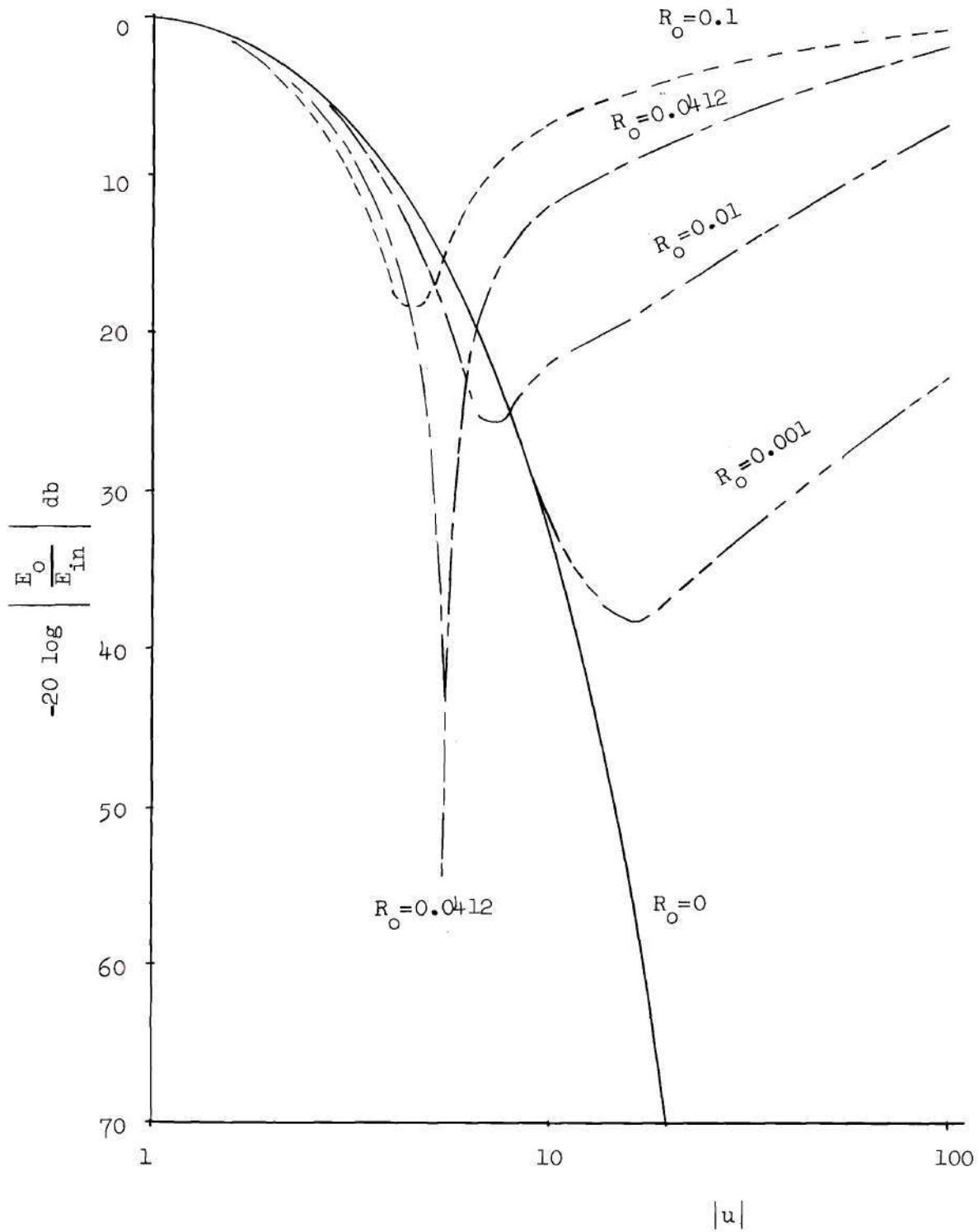


Figure 25. Frequency Response of Double Line with Series Resistance. Case for  $r_2/r_1 = 1.0$  and  $c_2/c_1 = 1.0$ .

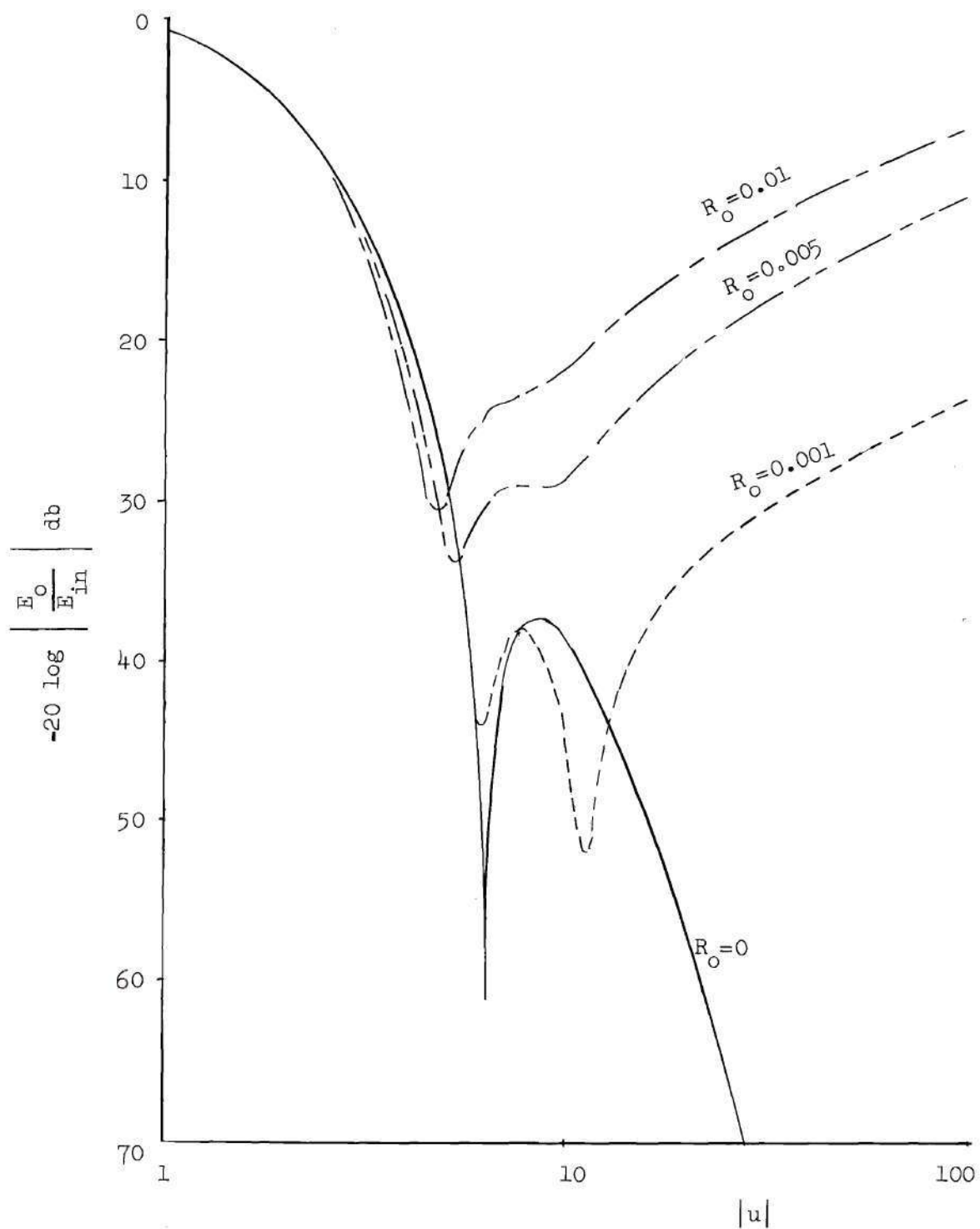


Figure 26. Frequency Response of Double Line with Series Resistance. Case for  $r_2/r_1=0.01$  and  $c_2/c_1=8.0$ .

of Equation (4-10) do not dominate until very large values of  $u$  are reached.

#### The Case for a Series Capacitance

The next case to be analyzed is that for an ideal capacitance connected in series with the double-line twoport. In this case,  $Z(s)$  of Figure 23 is

$$Z(s) = \frac{1}{Cs} \quad (4-19)$$

The open-circuit transfer function in the  $u$ -plane becomes

$$T(u) = \frac{\sinh(Au)\sinh(Bu) + K_1 C_o u \sinh(Au) + K_2 C_o u \sinh(Bu)}{\sinh(Au)\sinh(Bu) + K_1 C_o u \sinh(Au)\cosh(Bu) + K_2 C_o u \sinh(Bu)\cosh(Au)} \quad (4-20)$$

where  $C_o$  is the normalized capacitance given by

$$C_o = \frac{C}{c_1 \lambda} \quad (4-21)$$

The series capacitor modifies the real-frequency response of the twoport in two major ways. First, as was the case with the series resistance element, there is a value of series element for every double line that will produce a real-frequency zero. Second, the external series capacitance causes the high frequency amplitude response to be asymptotic to a -20 db per decade asymptote in the  $u$ -plane. The high frequency phase shift is asymptotic to -45 degrees.

The high frequency behavior of the double line with series capacitor was obtained from Equation (4-20) and is given by

$$T(u) \cong \frac{1}{1 + C_o(K_1 + K_2)u} \quad (4-22)$$

The numerator function of Equation (4-20) can be approximated for a wide range of line parameters while neglecting the  $K_2$  term with respect to the other terms in the numerator. Under the conditions of such an approximation the value of  $C_o$  causing a real-frequency zero and the location of the zero were calculated and are given by

$$C_o \cong 4.57 \frac{B}{K_1} \quad (4-23)$$

$$|u_o| \cong \frac{5.55}{B} \quad (4-24)$$

Equation (4-24) may be transformed to the real-frequency domain yielding a formula for the null frequency

$$\omega_{\text{null}} = \frac{25\pi^2}{8B^2 r_1 c_1 \lambda^2} \text{ rad/sec} \quad (4-25)$$

Typical families of transfer functions have been calculated and are shown in Figures 27, 28, and 29. The values of  $C_o$  have been selected to display the effect of this variable on the transfer function of three double lines. The approximate formulas of Equations (4-23) and (4-24) give satisfactory results for the lines of Figures 27 and 29, but they do not apply to the case shown in Figure 28.

#### The Case for a Series Inductance

The third case to be analyzed is that of an ideal inductance

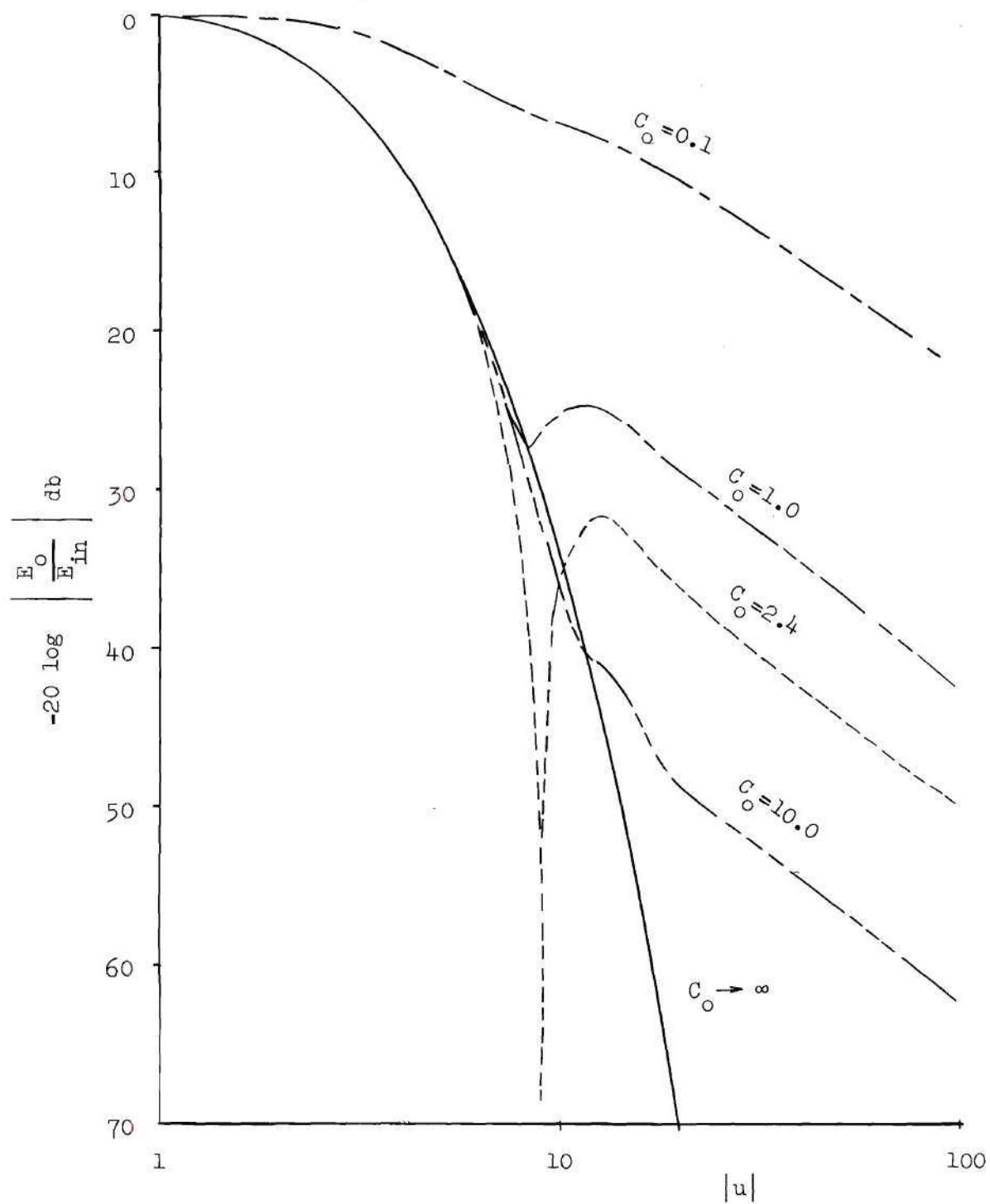


Figure 27. Frequency Response of Double Line with Series Capacitance. Case for  $r_2/r_1=1.0$  and  $c_2/c_1=1.0$ .

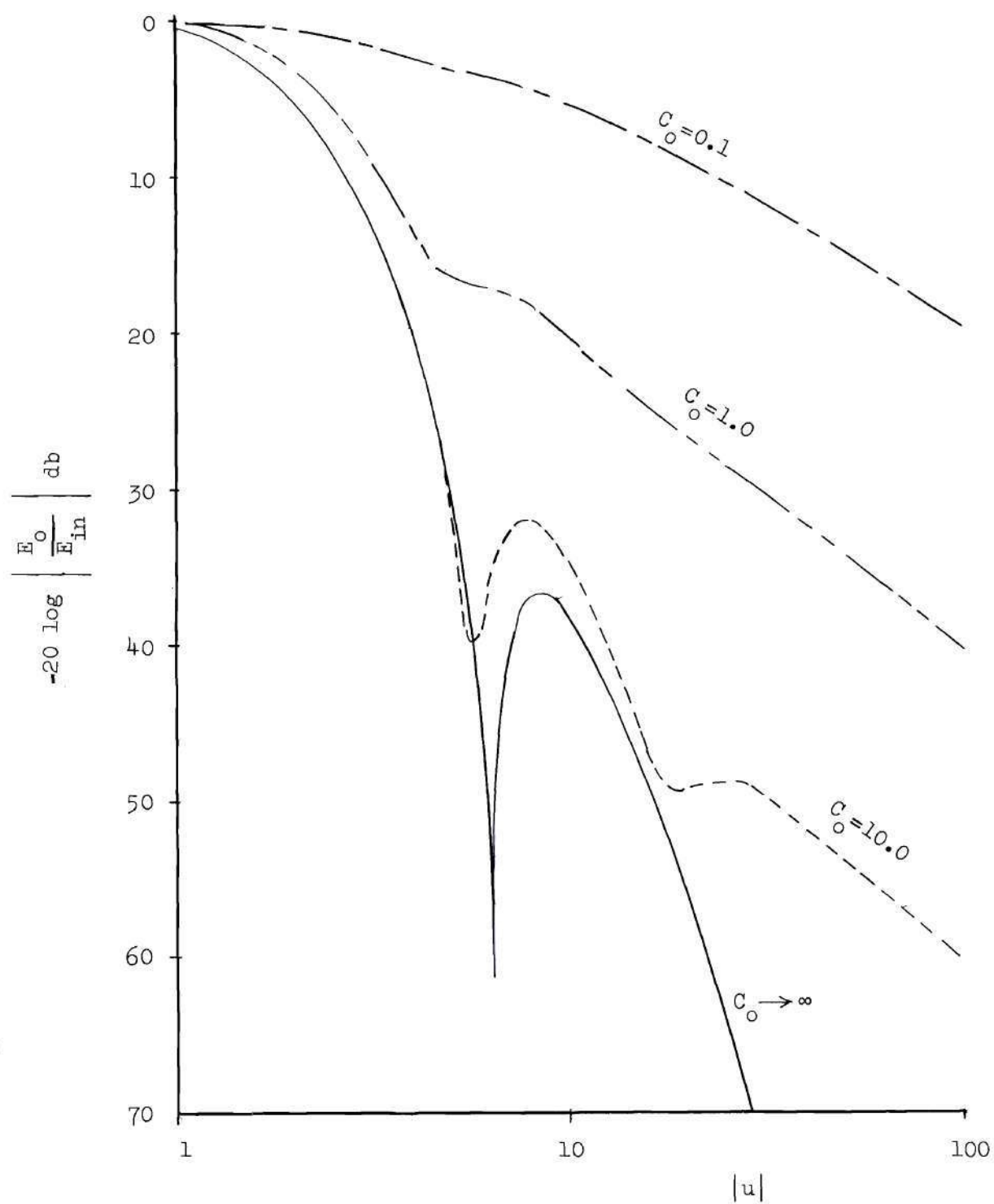


Figure 28. Frequency Response of Double Line with Series Capacitance, Case for  $r_2/r_1=0.01$  and  $c_2/c_1=8.0$ .

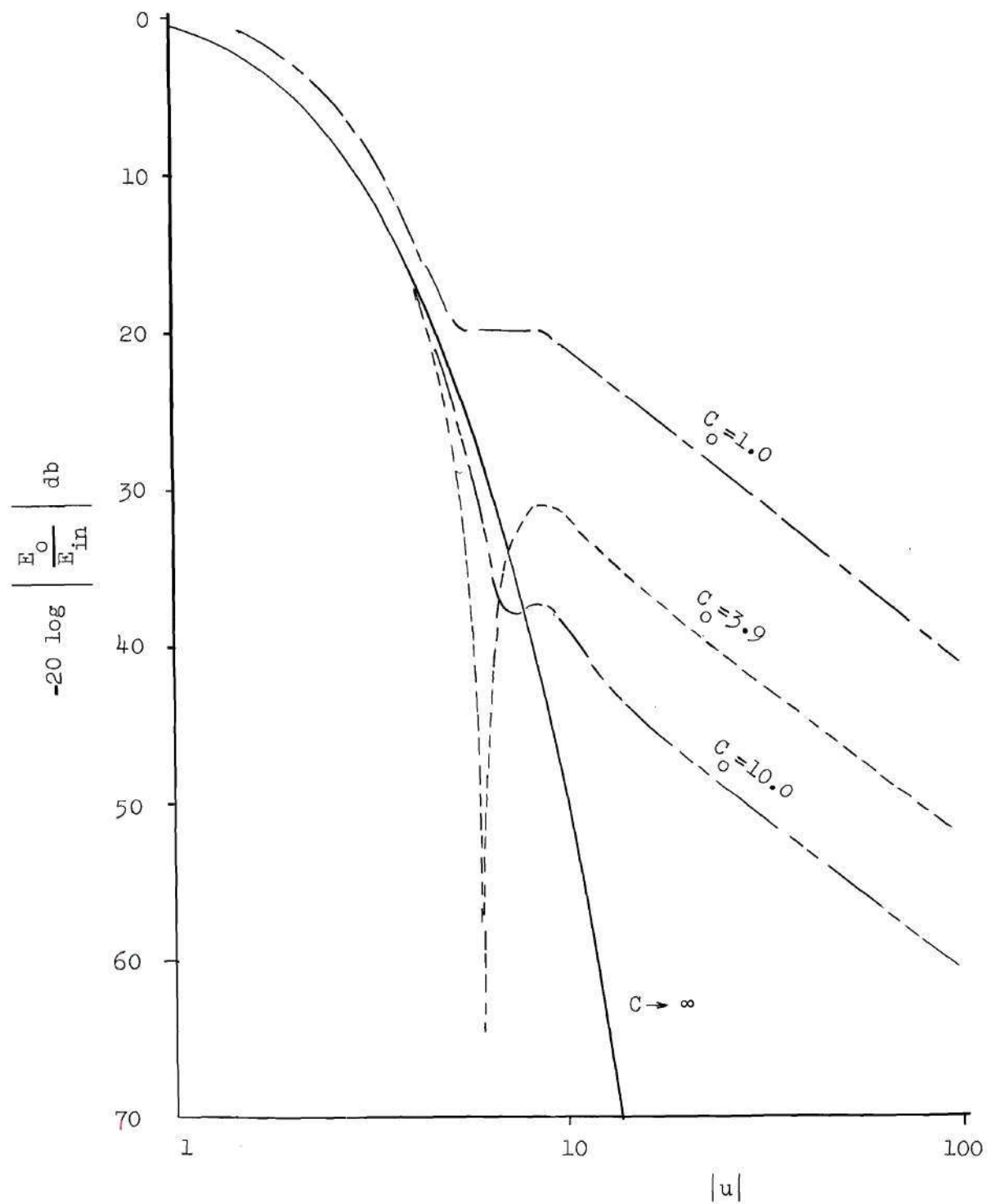


Figure 29. Frequency Response of Double Line with Series Capacitance. Case for  $r_2/r_1=1.0$  and  $c_2/c_1=5.0$ .

connected in series with the double-line twoport. In this case,  $Z(s)$  of Figure 23 is

$$Z(s) = Ls \quad (4-26)$$

Equation (4-6) for the transfer function becomes

$$T(u) = \frac{L_o u^3 \sinh(Au)\sinh(Bu) + K_1 \sinh(Au) + K_2 \sinh(Bu)}{L_o u^3 \sinh(Au)\sinh(Bu) + K_1 \sinh(Au)\cosh(Bu) + K_2 \sinh(Bu)\cosh(Au)} \quad (4-27)$$

where

$$L_o = \frac{L}{r_1^2 c_1 \lambda^3} \quad (4-28)$$

The numerator of Equation (4-27) has been examined for values of  $u$  on the real-frequency axis at which transmission zeros occur. These zeros usually occur at frequencies so high that the attenuation of the twoport is already beyond the dynamic range of practical interest and the addition of the zero makes little difference.

The log-magnitude plots of the transfer function for typical double lines with series inductances are shown in Figures 30, 31, and 32. The essential behavior of these examples is divided into two regions along the abscissa. The low-frequency region is almost unchanged from that of the particular double line without a series element. At some value of  $u$  greater than unity and depending on the series  $L_o$ , the second region begins. In the second region the amplitude characteristic rises sharply to unity at a rate of 60 db per decade with about 3 db overshoot.

The double lines selected for the data shown in Figures 31 and 32

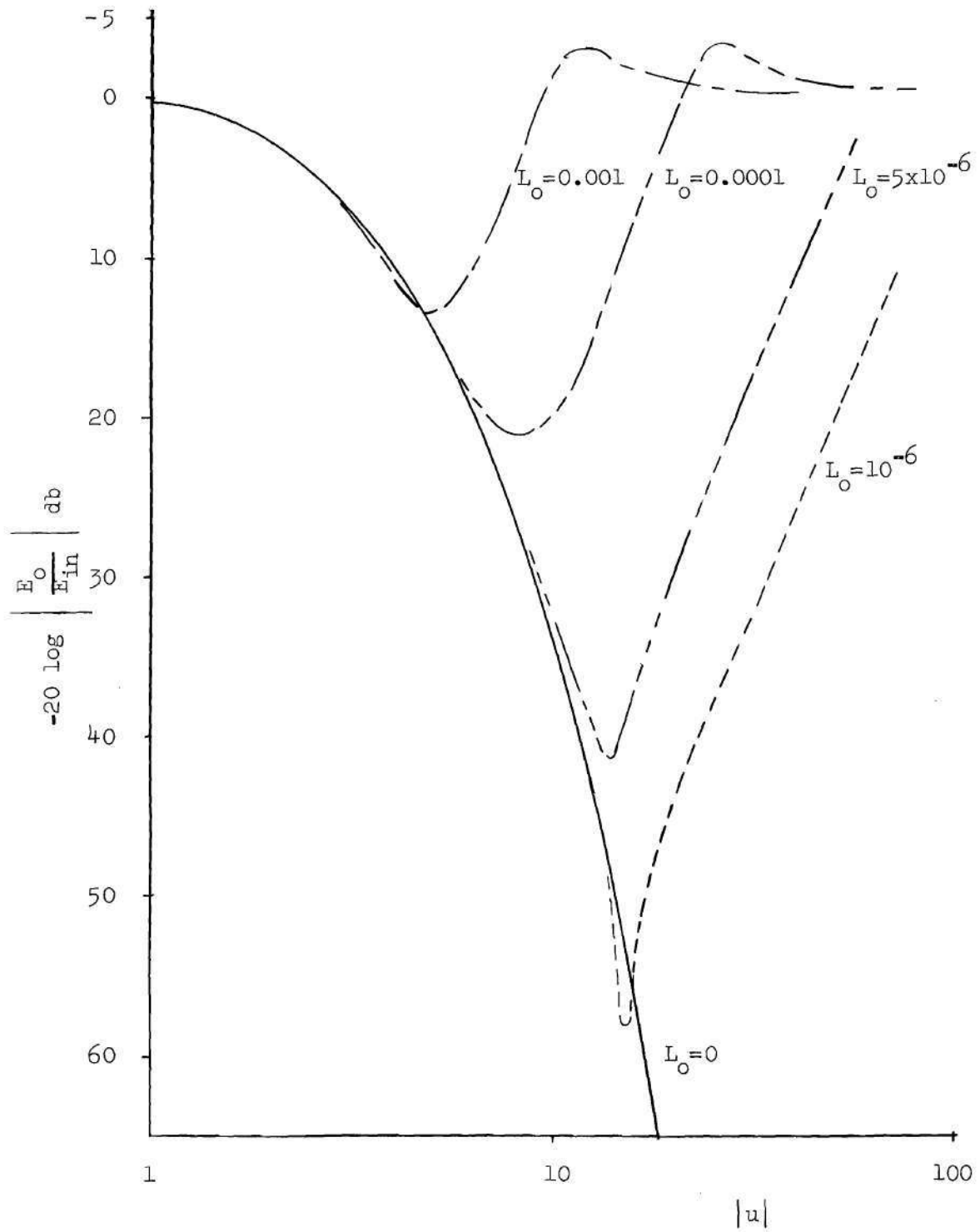


Figure 30. Frequency Response of Double Line with Series Inductance. Case for  $r_2/r_1=1.0$  and  $c_2/c_1=1.0$ .

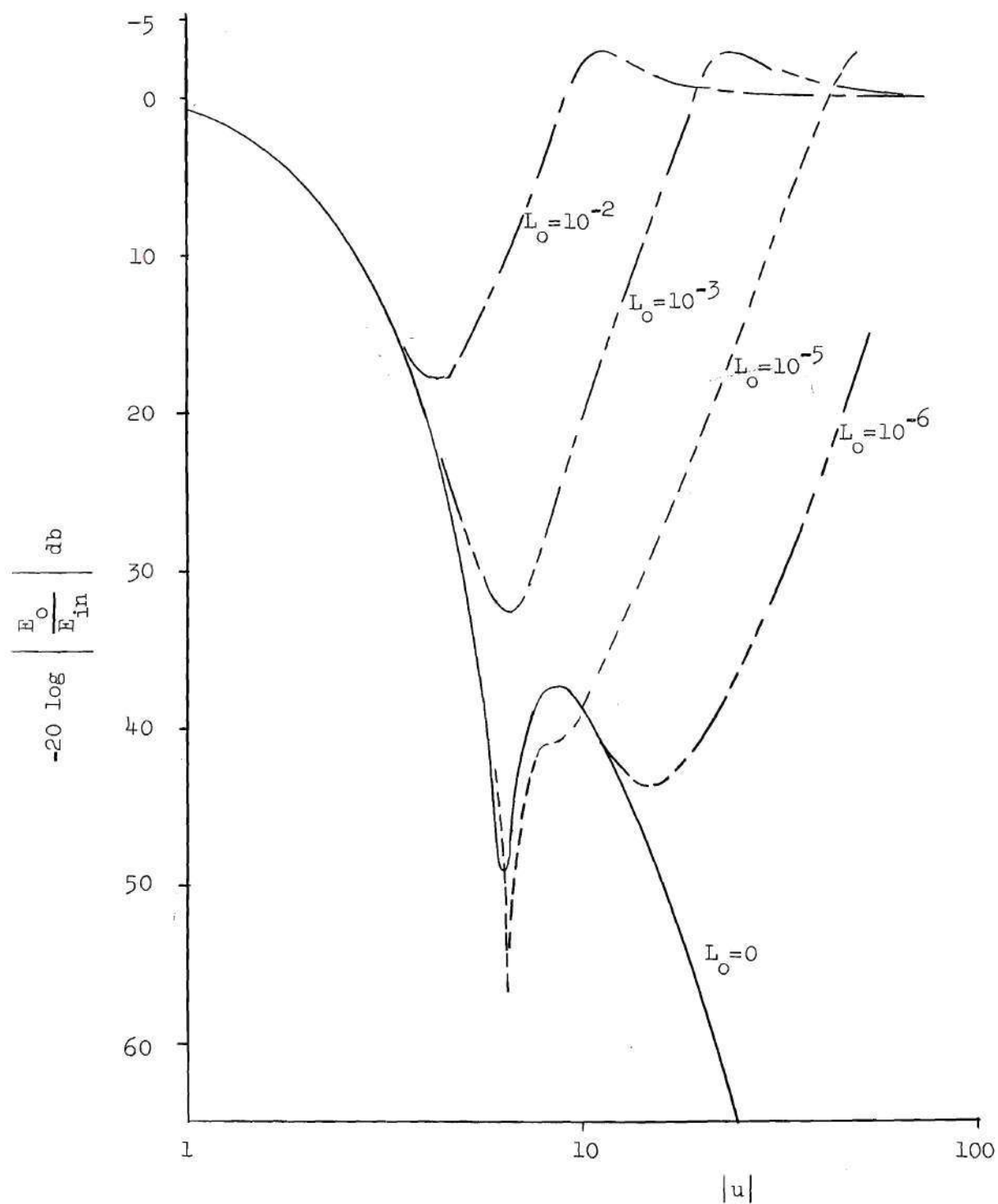


Figure 31. Frequency Response of Double Line with Series Inductance. Case for  $r_2/r_1=0.01$  and  $c_2/c_1=8.0$ .

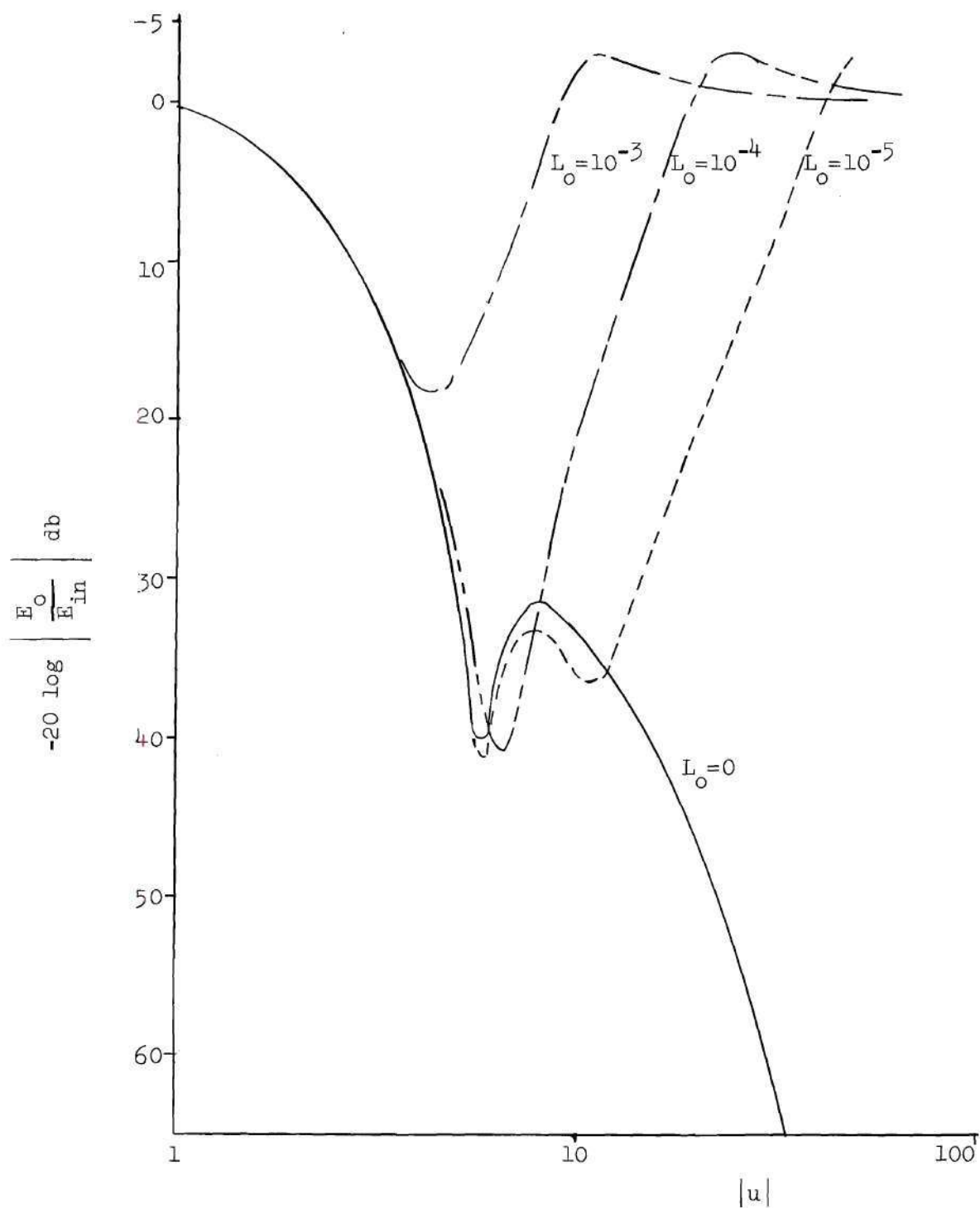


Figure 32. Frequency Response of Double Line with Series Inductance. Case for  $r_2/r_1=0.01$  and  $c_2/c_1=4.7$ .

have parameters which produced a transmission zero on or near the real-frequency axis without series elements. The addition of a series inductance at first sharpens the null for the line of Figure 30 and further increases in inductance move the null frequency away from the real-frequency axis. A small value of inductance seems to introduce a second zero near the real-frequency axis as can be seen in the examples of Figures 30 and 31. In all cases the dominant effect of the series inductance is to return the high frequency gain of the twoport to 0 db at a rate of 60 db per decade in the u-plane.

#### Applications of the Double-Line Twoport

Some of the applications of the double-line twoport are discussed in the following paragraphs. It is assumed that the twoport can be realized in a satisfactory manner and factors such as parameter stability and accuracy, size, weight, and cost are not considered. It is reasonable to expect production techniques for thin-film circuitry to advance to a point in the near future where such circuits will find general application.

#### Low-Pass Filter

The transfer function of the double-line twoport is generally of the low-pass characteristic and similar to that of a single line or a lumped element RC low-pass filter. However, when the parameters of the double line are specified at or near the values required for a real-frequency transmission zero, the attenuation characteristic has a notch along the band edge. The notch makes the double-line filter superior to the other low-pass filters mentioned for some applications. The line constants can be selected to position the null frequency at a point along

the band edge and thereby the filter will offer maximum attenuation at an undesirable signal frequency. Figure 19 illustrates this capability of the double-Kelvin twoport. Formulas suitable for the utilization of this type twoport are developed in Chapter III.

The double-Kelvin twoport with series capacitance also produces a frequency response of the low-pass variety with a null somewhere along the frequency response. A family of such filter characteristics is shown in Figure 27. The approximate location of the null frequency and the value of series capacitance required for the null condition are given in Equations (4-23) and (4-25). This low-pass filter with a notch has the advantage of being somewhat tuneable by varying the magnitude of the lumped series capacitance. However, the high frequency attenuation is asymptotic to a -20 db per decade line as compared to the ever increasing attenuation of the double line by itself.

#### Notch Filter

The double-line twoport with series resistance element produces a transfer function having a sharp null at one frequency very much like a resonant bridged-T twoport. The approximate location of the null frequency and the value of the resistance required for the null are given in Equations (4-15) and (4-16). The character of the null is variable with the series resistance from a very sharp and deep notch to a band-stop shape. This is illustrated by the family of attenuation curves shown in Figure 25. It was possible to obtain -60 db nulls with the experimental filters of this type which were tested during the research.

The double-Kelvin twoport as a frequency selective network has an advantage over the bridged-T network in that it is tuned for the best

null by a single circuit element. The frequency of the null is established by the distributed parameters of the line and is not shifted by the tuning of the series resistance element.

#### Band-Elimination Filter

The double-line twoport with series resistance has a frequency response of the band-elimination shape for some parameter values. For example, by selecting the  $r_2/r_1$  and  $c_2/c_1$  ratios of 0.01 and tuning the series resistance a family of band-elimination characteristics can be generated. They are shown in Figure 33. The high-frequency band edge is not sharp as it approaches a 20 db per decade asymptote in the  $u$ -domain.

The more interesting and novel band-elimination characteristic is obtained when a series inductance is used with the double-Kelvin twoport. In this case, the high frequency asymptote is a 60 db per decade line in the  $u$ -domain. Three sets of frequency response data for such band-elimination filters are shown in Figures 30, 31, and 32. The double-ripple characteristic at the bottom of the stop band, observed for one case in Figure 31, is of special interest. This behavior is obtained when a double-line twoport having a real-frequency zero of its own is used with a small external inductance element.

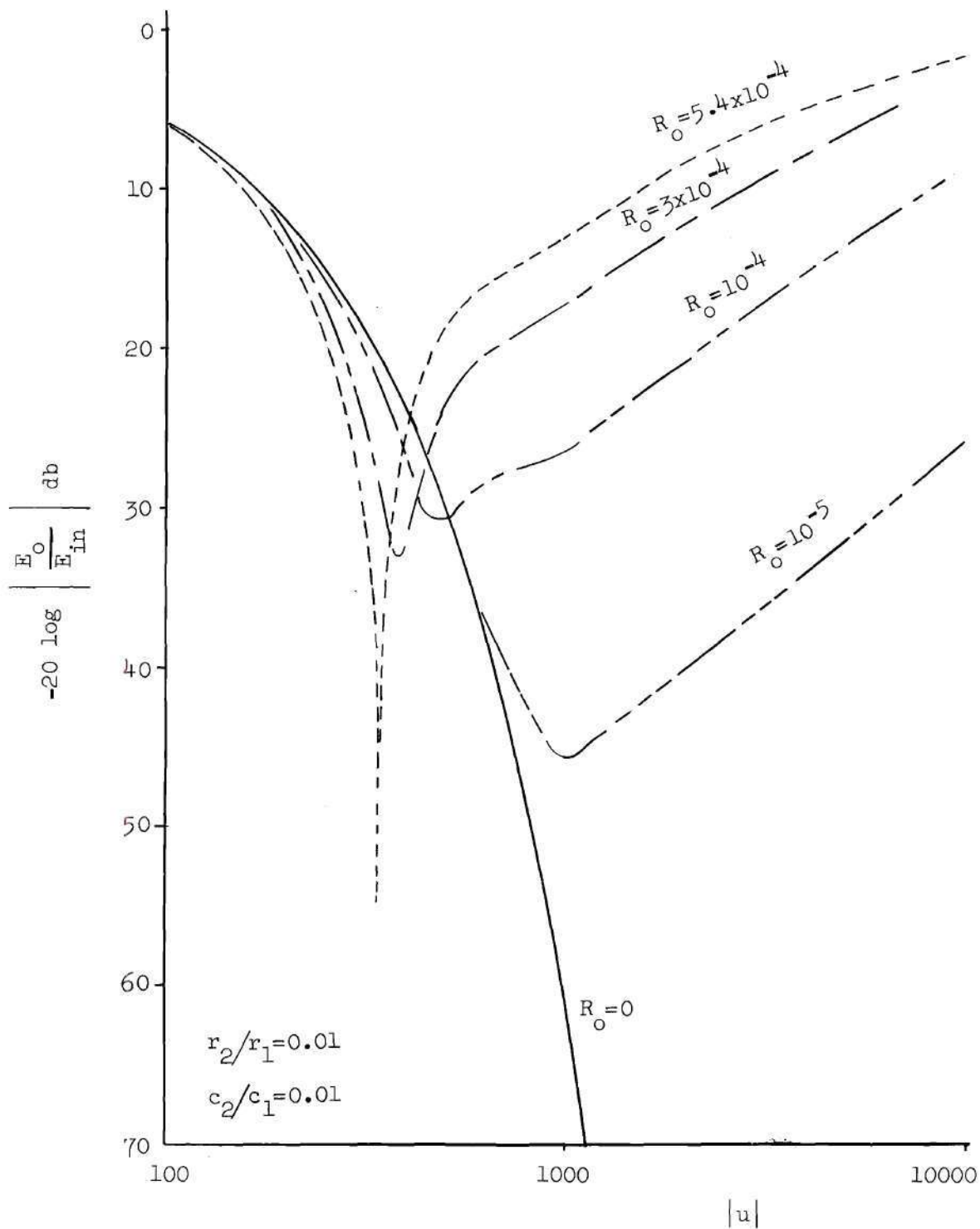


Figure 33. Frequency Response of a Double Line with Series Resistance Giving a Band-Elimination Characteristic.

## CHAPTER V

## EXPERIMENTAL WORK

The double-Kelvin transmission line for utilization as a twoport has been realized in three forms. The first form consists of sections of lumped resistance and capacitance elements connected in tandem to approximate the distributed circuit. The second form utilizes thin-film distributed circuit elements. The third form utilizes parallel plates of resistance and dielectric sheets to form a large model of the thin-film circuit.

The practical advantages of working with lumped circuit elements are well known and therefore the lumped approximate lines were used during the experimental portion of the research whenever they produced a satisfactory approximation of the distributed model. The variance exists between the mathematical model of Chapter II and the lumped circuit model because the boundary conditions are not identical in the two cases.

Thin-film circuit models of the double-Kelvin line were constructed by the Physical Sciences Division of the Engineering Experiment Station at Georgia Institute of Technology. Since the mathematical model of the problem was formulated for the distributed circuit, the thin-film realization produced data more favorable in comparison with the other circuit realizations.

The large parallel-plate model was used to allow versatility in selecting the circuit parameters as it was difficult to obtain specified resistance and capacitance values for thin-film circuits.

### Lumped Constant Realization

It is possible to approximate a double-Kelvin transmission line by connecting lowpass RC-filter sections in a manner as shown in Figure 34.

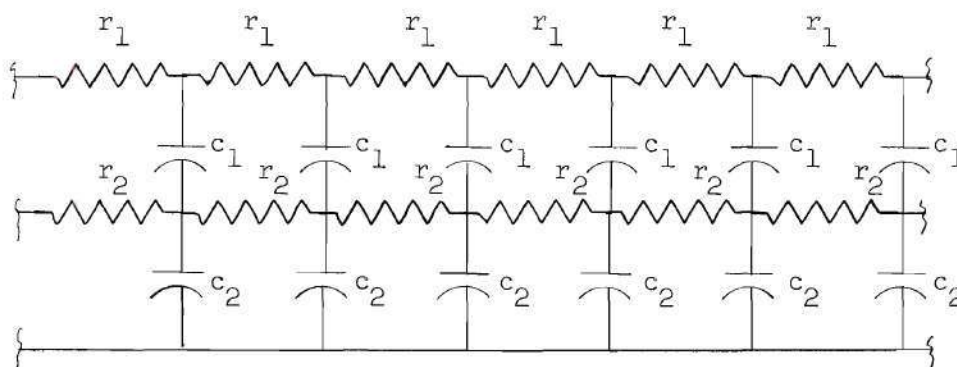


Figure 34. Lumped Approximation of a Double-Kelvin Line.

As the number of elements in the approximate line is increased the lumped approximation approaches the distributed case. The number of sections most commonly used and found to be satisfactory was 10.

The most significant errors in using a lumped line with a finite number of sections to approximate a distributed twoport occur in the phase shift characteristic and the input-output impedances. The phase shift of the lumped line approaches a constant value at high frequencies instead of continuing to increase indefinitely. The input and output conditions of the lumped line do not match those of the distributed line because the lumped line must always begin with a series R or a shunt C.

If the number of lumped sections in the approximation is made large, the phase shift error can be reduced to a negligible value over

the dynamic range of usual interest. However, the error due to the mismatch at the terminals of the line will always exist. This error is most noticeable when a series element is used with the double-Kelvin twoport.

The agreement between transfer function data calculated from Equation (3-12) and measured on a ten section approximate line is shown in Figure 35. The transfer function of this particular line is of the low-pass type and the line parameters were selected to keep the required frequency range of the instrumentation below 4 Mc. Circuit elements having tolerances of 20 per cent or better were used for the construction of the approximate line. In order to determine the effect of the mismatch at the sending end of the line, one set of data were measured on a line beginning with a mid-series or T section, and a second set of data were measured on a line beginning with a mid-shunt or  $\pi$  section. It can be seen in Figure 35 that the calculated data fall somewhere between these two sets of experimental data. The  $\pi$  approximation is better at the low frequency end of the response and the T approximation is better at the high end.

Figure 36 was prepared from calculated and experimental data for a double-Kelvin twoport which has a transmission zero near the real-frequency axis. Reference to the parameter study of Chapter III will show that the parameters of this line, which has a  $c_2/c_1$  of 4.7 and an  $r_2/r_1$  of 0.01, to lie very near the RC locus for real-frequency transmission zeros. This locus is shown in Figure 14. The complex frequency of the transmission zero for this example is calculated to be

$$u_0 = 3.838 + j4.201 \quad (5-1)$$

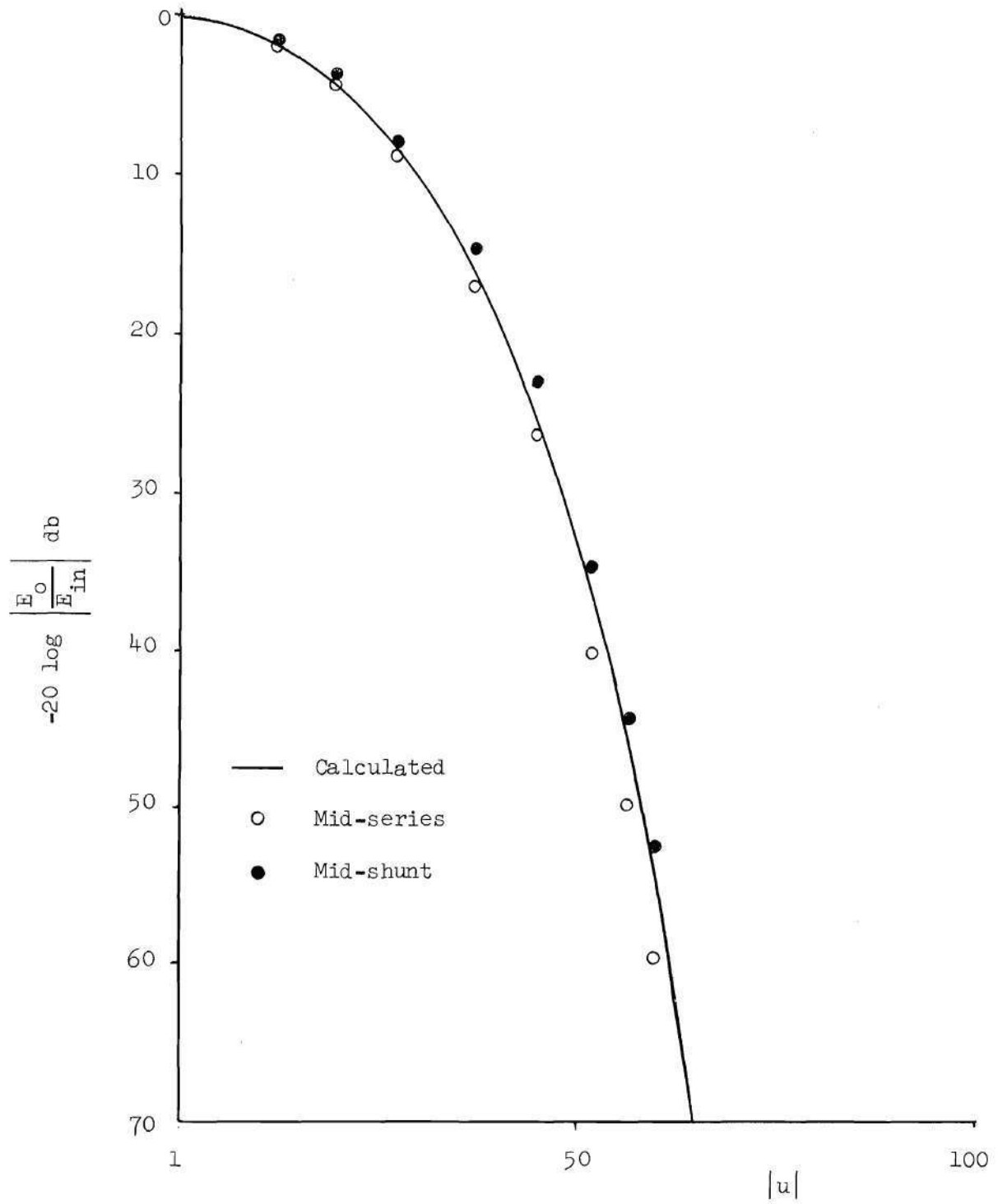


Figure 35. Frequency Response of Lumped Approximate Double Line. Case for  $r_2/r_1=1.0$  and  $c_2/c_1=1.0$ .

This complex u-domain frequency transforms to the s-domain as

$$s_0 = (-2.916 + j32.25) \times 10^4 \quad (5-2)$$

Neglecting the real part of  $s_0$ , the frequency of the transmission zero becomes

$$f_0 \approx 51.32 \text{ Kc} \quad (5-3)$$

The null frequency of the approximate line shown in Figure 36 for which the above calculations were made was measured to be 50.0 Kc.

The analysis of the double-line twoport in series with a resistance was performed in Chapter IV. Figure 38 compares data calculated with the results of this analysis, Equation (4-10), and other data obtained experimentally using lumped-element approximations of the double line. Data for two tests are shown; one test used a double line beginning with a mid-series section and the other used a line beginning with the mid-shunt section. Again, as in the previous tests with the approximate line, the calculated distributed case falls between the two experimental cases. The agreement is very close except at high frequencies where the mid-series case approaches a -10.9 db asymptote and the mid-shunt case approaches a zero db asymptote. An examination of the high frequency equivalent circuits for the two cases shown in Figure 37 will indicate these results to be obvious. The results shown in Figure 38 are in good agreement with the predicted null frequency and series resistance for best null which can be calculated from Equations (4-15) and (4-16).

When used with a series inductance or capacitance the lumped approximate double-line twoport performed well at low values of  $u$  but

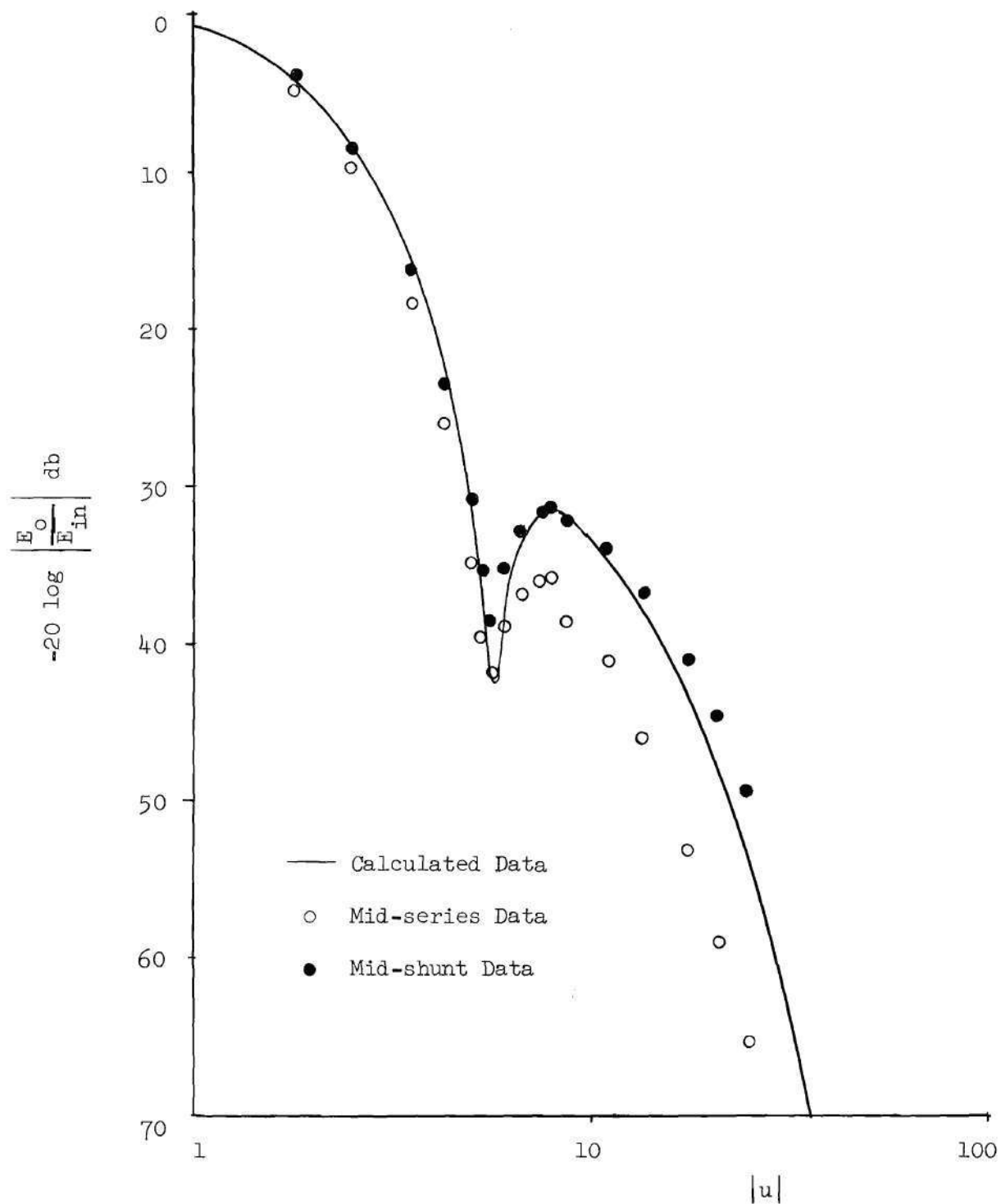


Figure 36. Frequency Response of Lumped Approximate Double Line. Case for  $r_2/r_1=0.01$  and  $c_2/c_1=4.7$ .

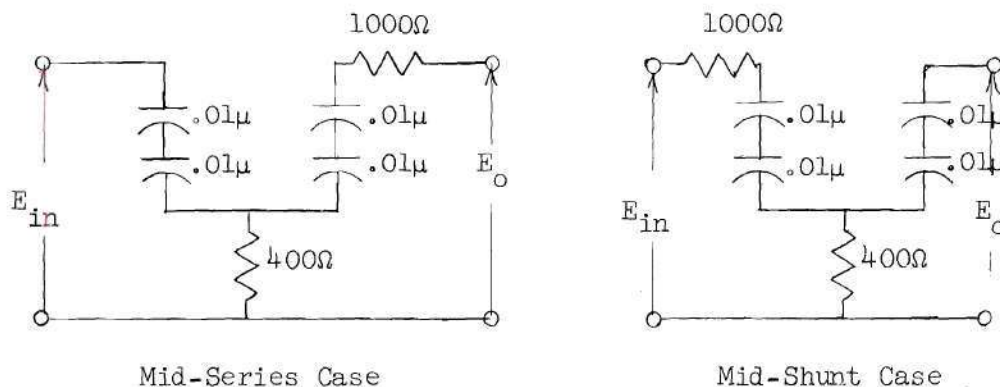


Figure 37. High Frequency Equivalent Circuits for the Approximate Double-Kelvin Line when Used with Series R.

the approximation became very poor as  $u$  was increased above 10. The poor high frequency approximation was caused by the improper boundary conditions which have been previously mentioned. The effect of the improper boundary conditions is specially noticeable when the twoport is connected in series with a reactive circuit element.

Figure 40 shows data from the mid-series and mid-shunt approximate lines compared with the calculated data for the case where the twoport is connected in series with a capacitor of such value so as to produce a real-frequency transmission zero. The value of the capacitance and the frequency at which the null occurs agree with the values predicted by Equations (4-23) and (4-24).

Figure 41 shows experimental and calculated data for an approximate twoport in series with an inductance. The approximate line yields results in good agreement with the calculated results only for low frequencies. The input capacitance of the mid-shunt approximate line resonates with the series inductance to produce a large output voltage. This behavior can be discerned by examining the high-frequency approximate

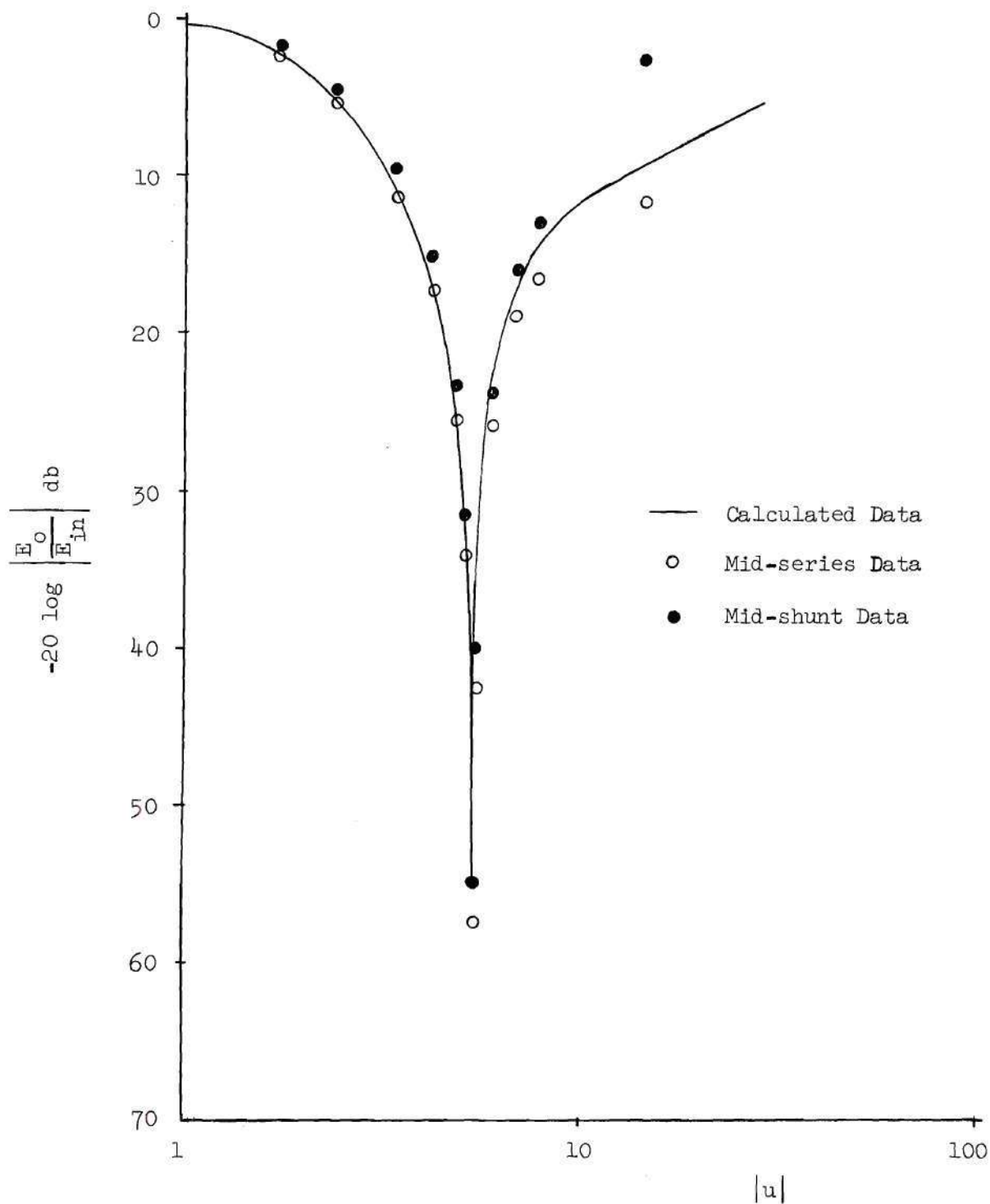


Figure 38. Frequency Response of Lumped Approximate Double Line with Series Resistance. Case for  $r_2/r_1=1.0$  and  $c_2/c_1=1.0$ .

equivalent circuit of Figure 39.

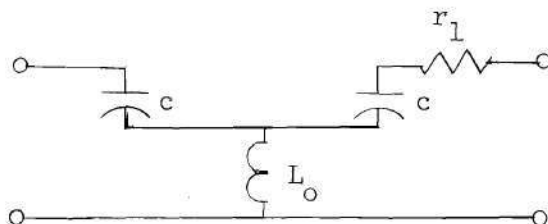


Figure 39. High Frequency Approximate Equivalent Circuit.

#### Thin-Film Realization

Several thin-film double-Kelvin lines were fabricated and transfer function data measured for these twoports. A photograph and model drawing of the thin-film circuit are shown in Figure 42.

Referring to the model of Figure 42, strata 1 and 3 are the resistive films of nichrome. Strata 2 and 4 are the dielectric films of silicon monoxide. Stratum 5 is a near ideal conducting thick-film of aluminum. The substrate is a glass microscope slide. Wire terminals are attached to the ends of strata 1 and 5 with indium solder.

The problems associated with the production and control of thin-film circuits and the measurement of the electrical properties of thin-films are not considered in this research. However, the instability of the electrical characteristics and the lack of accurate data on the electrical parameters of thin-films must be considered when comparing the calculated and experimental data for such circuits. With the available facilities it was extremely difficult to obtain thin-film circuits with the electrical parameters specified in advance. Accurate measurement techniques for the circuit parameters of the thin-film circuits successfully fabricated were lacking. The total resistance from one end

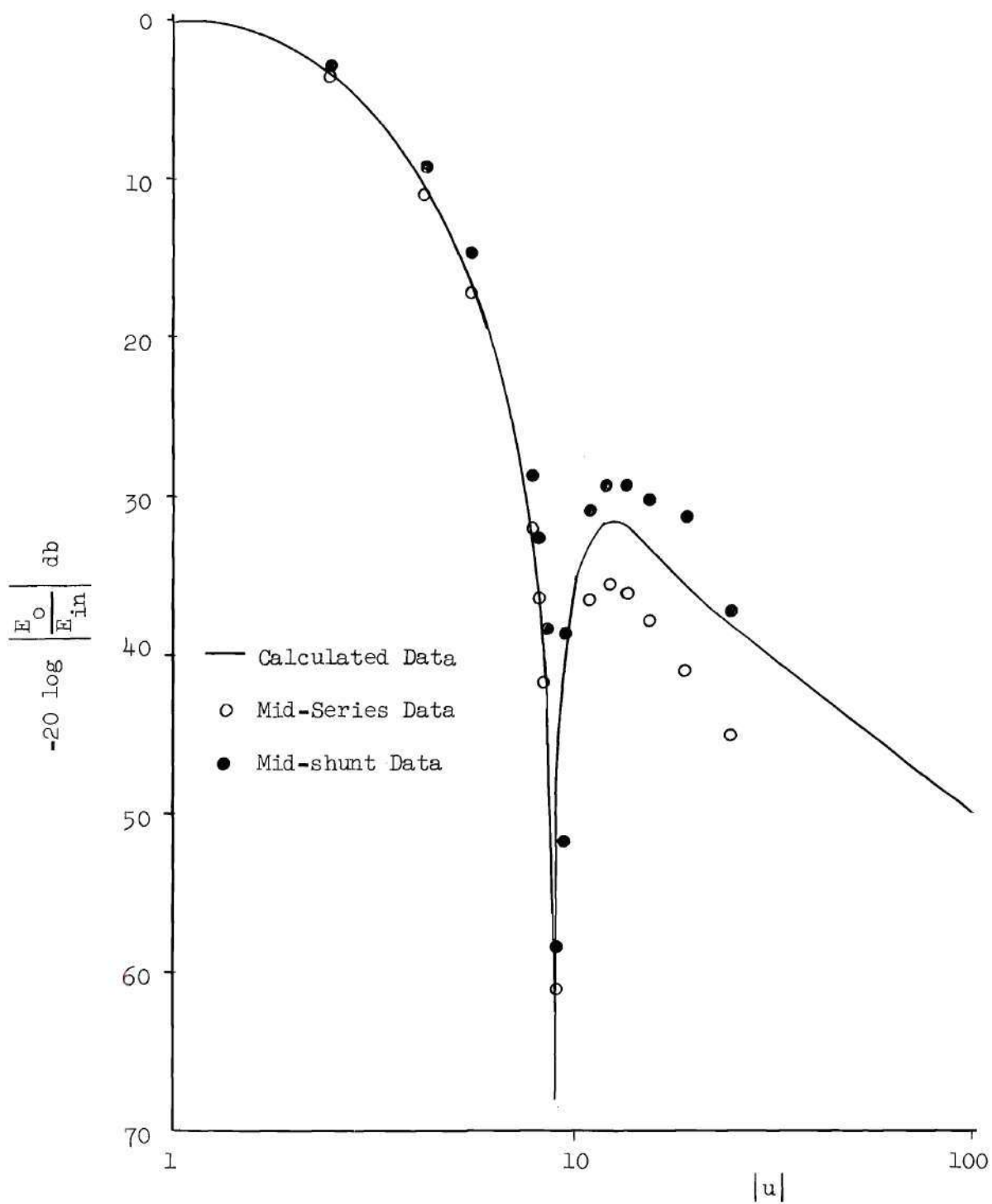


Figure 40. Frequency Response of Lumped Approximate Double Line with Series Capacitance. Case for  $r_2/r_1=1.0$ ,  $c_2/c_1=1.0$  and  $C_0=2.4$ .

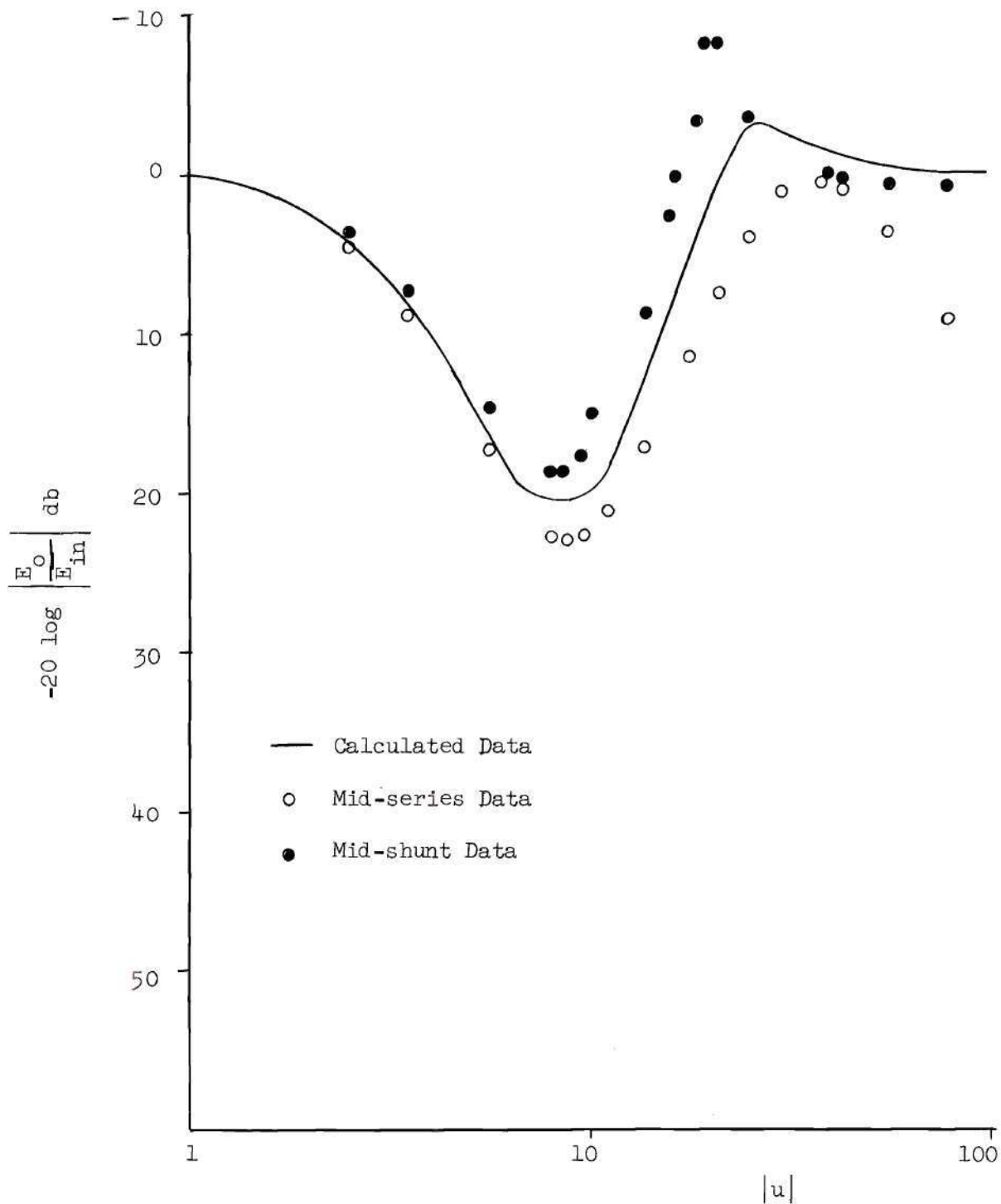
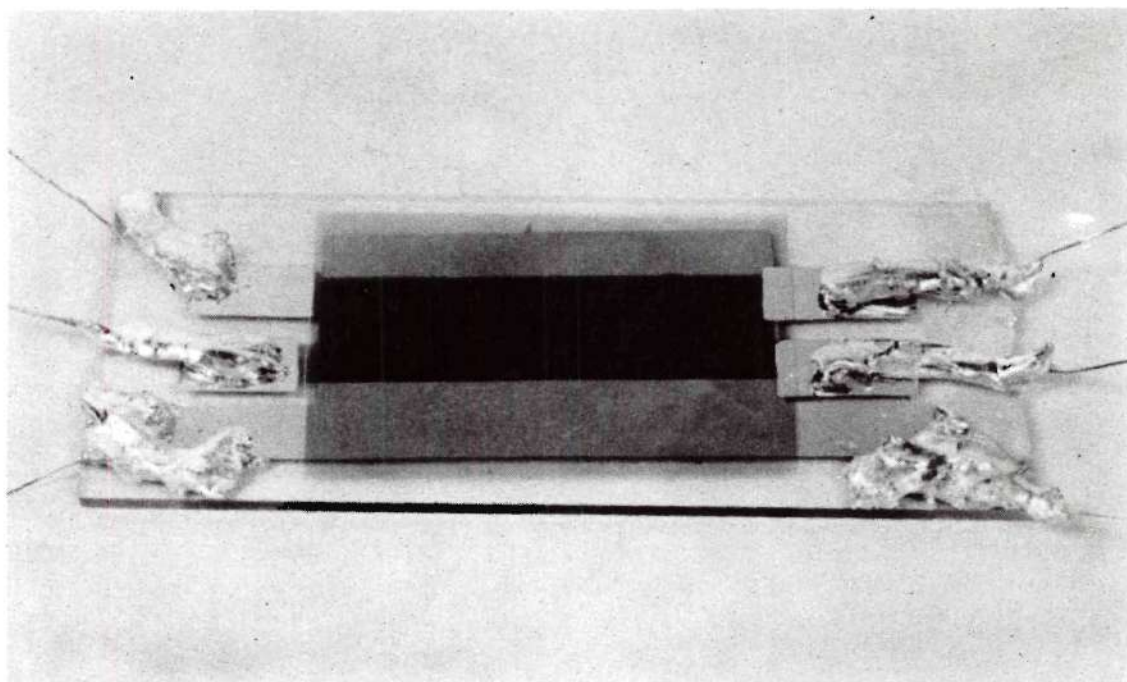
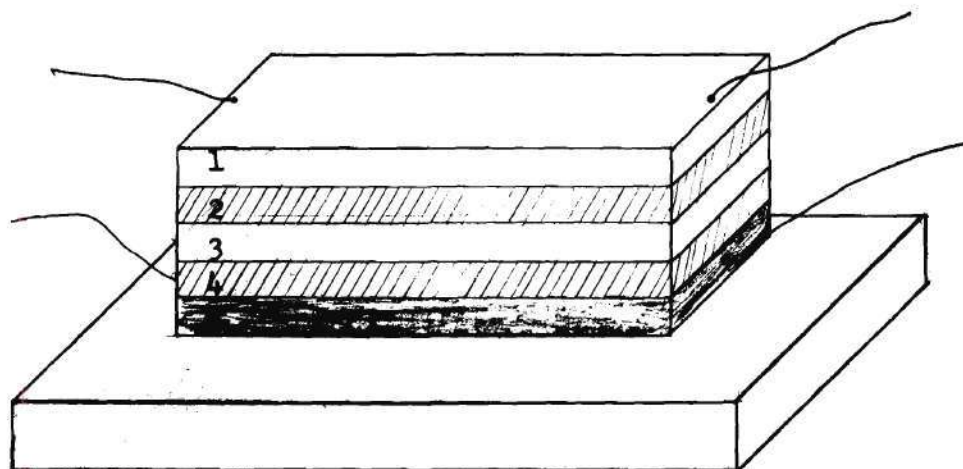


Figure 41. Frequency Response of Lumped Approximate Double Line with Series Inductance. Case for  $r_2/r_1=1.0$ ,  $c_2/c_1=1.0$  and  $L_o=10^{-4}$ .



Photograph



Model

Figure 42. Thin-Film Double Kelvin Transmission Line

of a stratum to the other end of the same stratum was measured on an audio frequency impedance bridge with good results. A nominal capacitance value between strata was obtained using the impedance bridge.

Thin-film resistances are subject to large changes in resistance with time.<sup>15</sup> As the strata age, the resistance increases and this increase is especially severe if the film is very thin as is the case when a high resistance is required. The increase in resistance can be as large as several hundred per cent over a period of a few days. This phenomenon caused difficulty during the experiments by making it difficult to duplicate a given experiment.

Data have been obtained from several thin-film twoports. Figure 43 shows the transfer function for a twoport having an  $r_2/r_1$  ratio of 1.54 and a  $c_2/c_1$  ratio of about 1.15. The calculated transfer function based on these approximate R and C ratios is also shown for comparison. The measured response does not fall off as fast as the calculated response. This discrepancy is due to inaccurate parameter data, particularly for the value of  $c_1\lambda$  which is used to normalize the real-frequency scale to the  $u$  magnitude scale.

Data for another thin-film circuit are shown in Figure 44. This particular twoport has an  $r_2\lambda$  greater than 500 K $\Omega$ . This large stratum resistance made it impossible to measure  $c_1\lambda$  and  $c_2\lambda$  separately. However, the capacitance between strata 1 and 5 was measured and found to be 0.01  $\mu$  fd. This capacitance was assumed to be formed by equal capacitances in series and transfer function data were calculated under this assumption. The calculated data are shown in Figure 44 for comparison with the measured results. This double line behaves as a single line

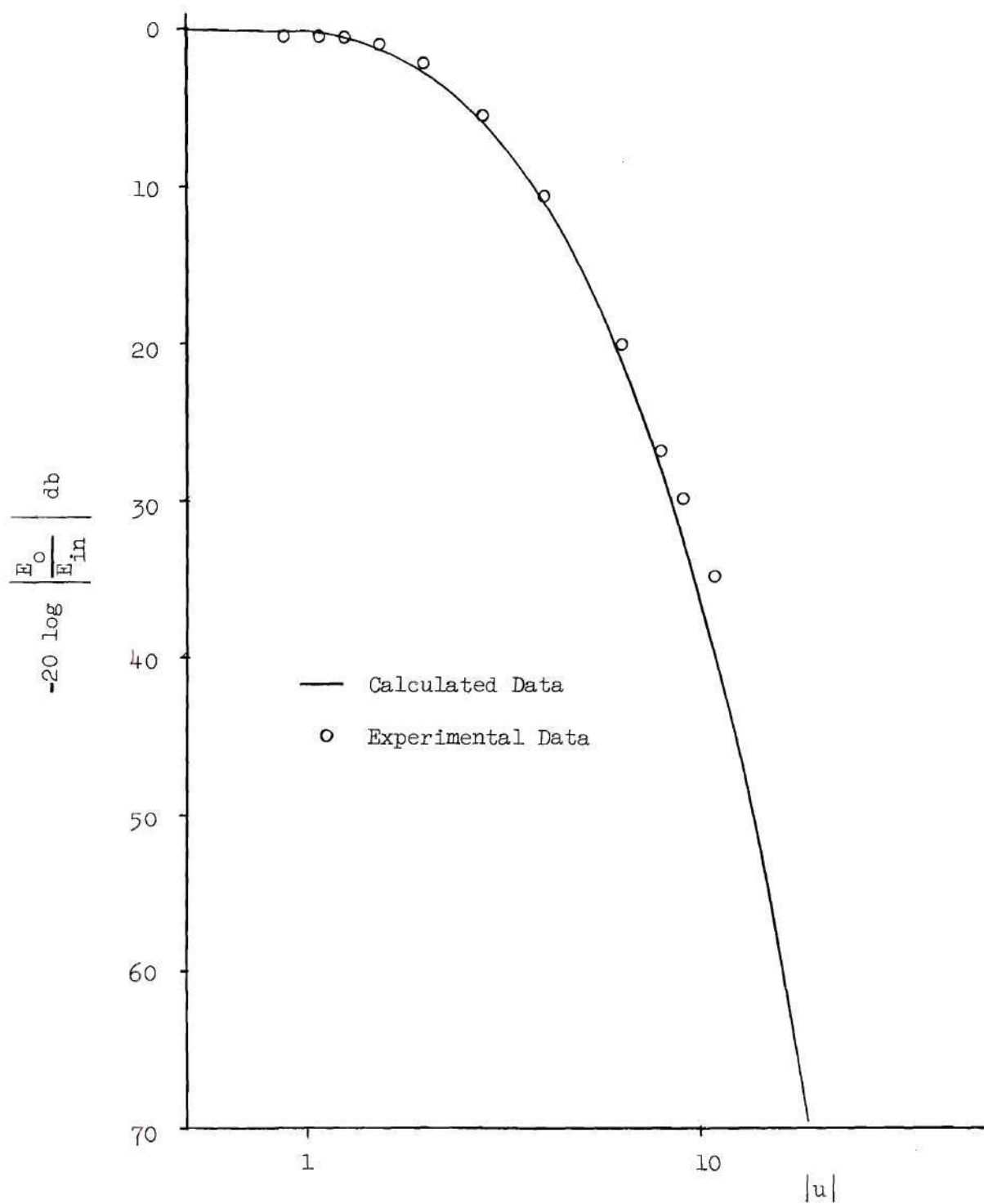


Figure 43. Frequency Response of Thin-Film Double Line.  
Case for  $r_2/r_1=1.54$  and  $c_2/c_1=1.15$ .

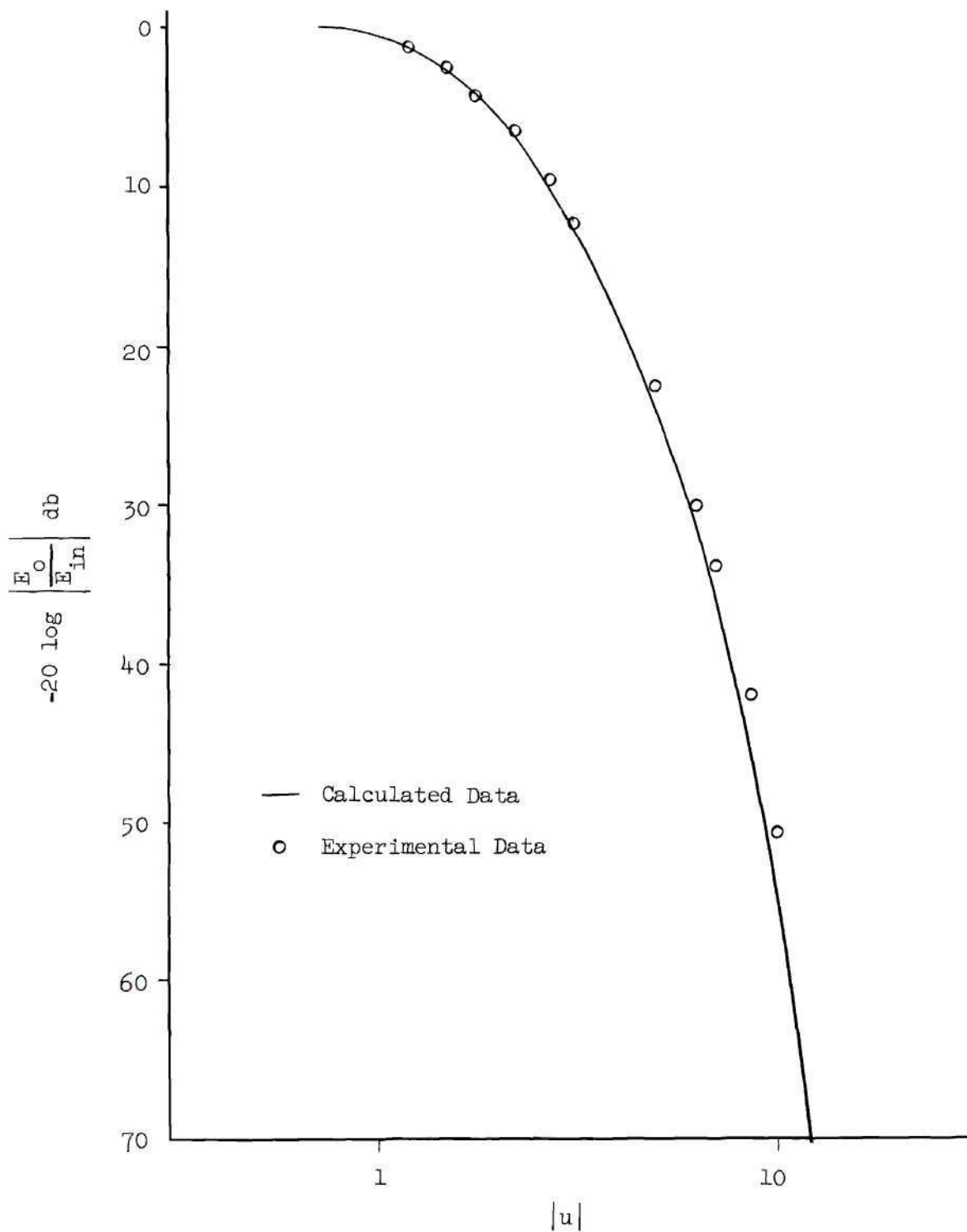


Figure 44. Frequency Response of Thin-Film Double Line. Case for  $r_2/r_1 \rightarrow \infty$  and  $c_2/c_1 = 1.0$ .

because of the large  $r_2/r_1$  ratio.

#### Parallel Plate Circuit Model

The previously mentioned problems associated with the construction and testing of thin-film circuits made it desirable to obtain a more rugged and versatile twoport realization of the double-Kelvin line for experimentation. Large parallel plate models using Teledeltos paper, Mylar film, and aluminum foil were constructed and found to be satisfactory.

The resistance strata were formed with General Electric Type L Teledeltos paper which has a resistance of approximately 2,000 ohms per square. The resistive matter is deposited on a paper base and the entire thickness is 0.004 inches.

The dielectric strata were formed by sheets of DuPont Mylar which is a polyester film. The Mylar used was 0.0006 inches thick and has a relative dielectric constant of 3.12 at 1 Kc and 20° C.<sup>16</sup>

The resistance and dielectric sheets were placed in proper order on a sheet of aluminum foil 0.001 inches thick. The size of the sheets was on the order of 15 cm by 30 cm. Electrodes were painted on the resistive strata with Hanovia No. 13 flexible silver paint. The capacitance between strata achieved was about 12 per cent of that predicted by the parallel-plate capacitance formula. This is not surprising as the pressure plates used were not expected to achieve the 0.0006 inch separation between capacitance plates which is the thickness of the Mylar dielectric.

The results of the tests performed with two of the parallel plate circuits are shown in Figures 45 and 46. The data shown in Figure 45

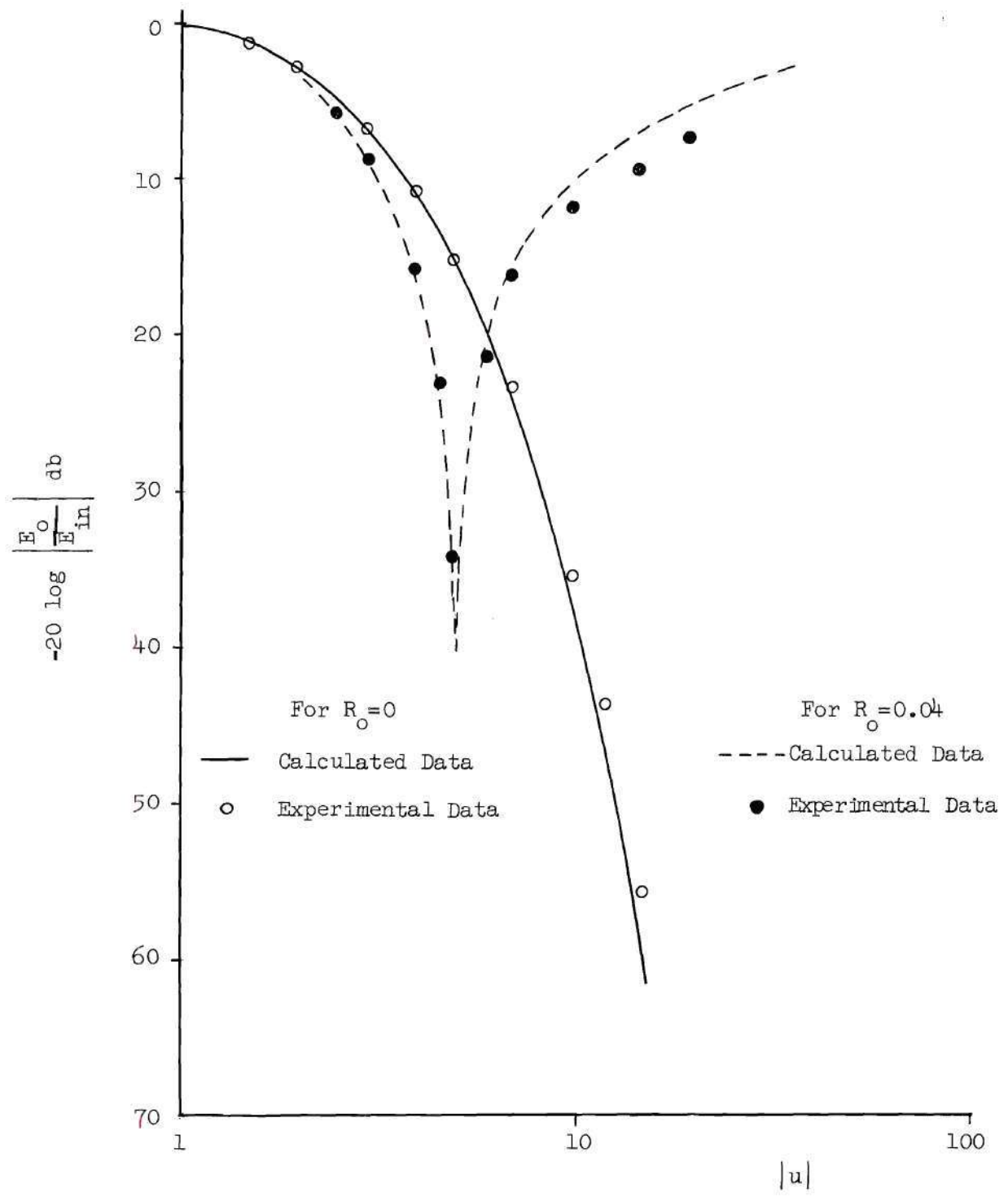


Figure 45. Frequency Response of Parallel Plate Double Line. Case for  $r_2/r_1 = 1.0$  and  $c_2/c_1 = 1.18$ .

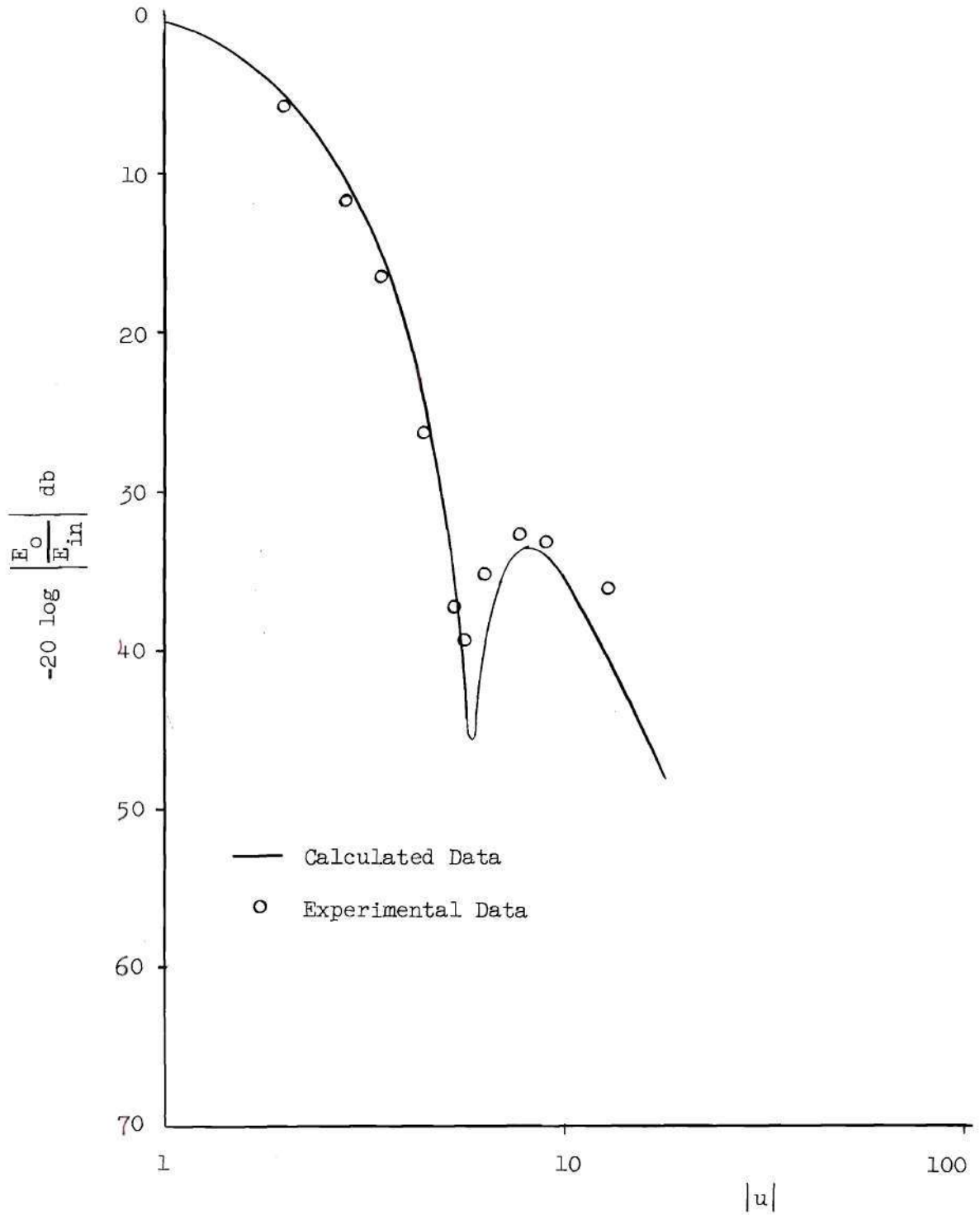


Figure 46. Frequency Response of Parallel Plate Double Line, Case for  $r_2/r_1=0.0117$  and  $c_2/c_1=5.65$ .

were obtained from a line having an  $r_2/r_1$  ratio of 1.00 and a  $c_2/c_1$  ratio of 1.18. Data were calculated using these ratios and are also shown for comparison. Also shown in Figure 45 are the measured and calculated responses of this twoport with a series resistance which has been sized to produce the best null in the frequency response. The general agreement between the calculated and measured data is excellent. The transfer functions were calculated using the relationship expressed in Equation (4-10). The frequency of the null and the value of resistance to produce the best null were calculated using Equations (4-16) and (4-17). The agreement between the calculated and measured results for these two quantities is within 2 per cent for the null and 6 per cent for the resistance.

Figure 46 contains data for a parallel plate twoport having a transmission zero near the real-frequency axis. The line was constructed with an  $r_2$  stratum made of resistance paper coated with conductive paint to reduce the resistance so that the  $r_2/r_1$  ratio between this stratum and a similar one without the paint was 0.0117. The thickness of one dielectric stratum was increased to obtain a  $c_2/c_1$  ratio of 5.65. Examination of Figure 14 shows that a double line with these parameters lies near the RC locus of lines having real-frequency transmission zeros. The measured and calculated transfer functions for this line shown in Figure 46 exhibit the expected dip with good agreement.

## CHAPTER VI

## CONCLUDING REMARKS

Results of the Research

The double-Kelvin transmission line has been analyzed to obtain the open-circuit impedance functions and the open-circuit voltage transfer function for the twoport formed by the line. The transfer function is novel; that is, it differs from the single-Kelvin line, for line parameters lying within the ranges disclosed in the analysis. The existence of lines having a real-frequency transmission zero was derived and the locus of parameters for this family of lines was calculated. Design formulas for the approximate location of the real-frequency zero and the approximate parameters to produce the real-frequency zero have been derived. The double line has been shown to have no internal poles.

The general case for the transfer function of the double-line twoport when connected in series with a linear and passive impedance has been derived. Three special cases of series element were analyzed.

A suitable series resistance was shown to produce a real-frequency transmission zero for any double line. Design formulas for the approximate location of the zero and the approximate value of the series resistance to produce the zero were derived. The high frequency asymptote of the double line with series resistance is 0 db and the general behavior of such a twoport is similar to that of the resonant bridged T.

The double-Kelvin twoport with series capacitance was analyzed.

This configuration produces a low-pass filter with a notch along the band edge. Approximate design formulas for this filter have been derived.

The case of the double line with series inductance has been analyzed. An interesting family of quasi-symmetrical band-elimination filters was demonstrated to have a frequency response with 30 db per decade attenuation along the band edges.

Experimental verification of the analytical results has been performed. Transfer function data were calculated from the formulas derived for the mathematical model of the double line and compared to three physical realizations of the circuit. The three realizations used were the lumped approximate circuit, the thin-film circuit, and the parallel-plate circuit. The best experimental verification was obtained with the parallel-plate circuit.

#### Applications of the Double-Kelvin Line

The double-Kelvin transmission line as a twoport is essentially a low-pass filter. It can, however, be designed to have a real frequency transmission zero along the band edge.

The addition of a single element impedance increases the versatility of the twoport. A series resistance, capacitance, or inductance can be used with the line to obtain a low-pass, band-elimination, or notch filter characteristic. It is also possible to obtain a low-pass characteristic with a notch.

The double-line twoport can be used with suitable active networks to obtain various band-pass characteristics. It also has possible applications as the feedback network in electronic oscillators.

### Recommendations for Future Research

The versatility of the double line was extended by the addition of a series impedance element allowing the production of a real-frequency transmission zero. The zero was possible at a frequency where the transfer impedance of the line was negative-resistive or reactive. However, the attenuation of the line increased so rapidly that only the first two or three axis crossings of the transfer impedance locus were of practical interest. If the series impedance were made more general it would be possible to produce multiple transmission zeros for the twoport. It would also be possible to introduce zeros at points other than those where the locus crosses a major axis. Future investigation is recommended toward this goal.

If the frequency range, over which the dynamic range of the transfer function for the double line remains within practical bounds, could be broadened, additional singularities could be added to the transfer function by the use of higher-order series impedances. The use of tapered lines or cascaded sections of lines toward this goal is suggested.

## A P P E N D I C E S

## APPENDIX I

## DETAILED SOLUTION OF THE DOUBLE-LINE BOUNDARY VALUE PROBLEM

The steady state equilibrium equations for the double line which were derived in Chapter I are

$$\frac{dE_1}{dx} = r_2 I_2 - r_1 I_1 \quad (I-1)$$

$$\frac{dE_2}{dx} = -r_2 I_2 \quad (I-2)$$

$$\frac{dI_1}{dx} = -j\omega c_1 E_1 \quad (I-3)$$

$$\frac{dI_2}{dx} = -j\omega c_2 E_2 + j\omega c_1 E_1 \quad (I-4)$$

Manipulating these equations into triangular form yields

$$\frac{d^4 I_1}{dx^4} - j\omega(r_1 c_1 + r_2 c_2 + r_2 c_1) \frac{d^2 I_1}{dx^2} - \omega^2 r_1 c_1 r_2 c_2 I_1 = 0 \quad (I-5)$$

$$\frac{dI_1}{dx} + j\omega c_1 E_1 = 0 \quad (I-6)$$

$$r_1 I_1 + \frac{dE_1}{dx} - r_2 I_2 = 0 \quad (I-7)$$

$$-j\omega c_1 E_1 + \frac{dI_2}{dx} + j\omega c_2 E_2 = 0 \quad (I-8)$$

The characteristic determinant for the system of Equations (I-1) through (I-4) reduces to

$$\Delta = D^4 - j\omega(r_1c_1+r_2c_2+r_2c_1)D^2 - \omega^2r_1c_1r_2c_2 \quad (\text{I-9})$$

The system of equations is therefore independent and there are four arbitrary constants in the general solution.

Solving Equation (I-5) for  $I_1$  gives

$$I_1 = A_1e^{-\alpha x} + A_2e^{-\beta x} + A_3e^{\alpha x} + A_4e^{\beta x} \quad (\text{I-10})$$

where  $A_1, A_2, A_3$  and  $A_4$  are arbitrary constants and  $\alpha$  and  $\beta$  are the roots of the characteristic equation obtained by setting expression (I-9) equal to zero.

$$D^2 = \frac{j\omega(r_1c_1+r_2c_2+r_2c_1)}{2} \left\{ 1 \pm \sqrt{1 - \frac{4r_1c_1r_2c_2}{(r_1c_1+r_2c_2+r_2c_1)^2}} \right\} \quad (\text{I-11})$$

$$D = \pm \sqrt{j\omega \frac{(r_1c_1+r_2c_2+r_2c_1)}{2} \left\{ 1 \pm \sqrt{1 - \frac{4r_1c_1r_2c_2}{(r_1c_1+r_2c_2+r_2c_1)^2}} \right\}} \quad (\text{I-12})$$

Introducing the new parameters  $\tau$  and  $\beta_r$ , the four roots of the characteristic equation are written

$$D_{1,2,3,4} = \pm \sqrt{j\omega\tau (1 \pm \beta_r)} \quad (\text{I-13})$$

The  $\alpha$  and  $\beta$  of Equation (I-10) are

$$\alpha = \sqrt{j\omega\tau (1 + \beta_r)} \quad (\text{I-14})$$

$$\beta = \sqrt{j\omega\tau (1 - \beta_r)} \quad (\text{I-15})$$

where

$$\tau = \frac{1}{2} (r_1 c_1 + r_2 c_2 + r_2 c_1) \quad (\text{I-16})$$

$$\beta_r = \sqrt{1 - \frac{4r_1 c_1 r_2 c_2}{(r_1 c_1 + r_2 c_2 + r_2 c_1)^2}} \quad (\text{I-17})$$

and  $\beta_r$  is always real because

$$(r_1 c_1 + r_2 c_2 + r_2 c_1)^2 > 4r_1 c_1 r_2 c_2 \quad (\text{I-18})$$

Solving Equation (I-6) for  $E_1$  using Equation (I-10) gives

$$E_1 = \frac{\alpha}{j\omega c_1} A_1 e^{-\alpha x} + \frac{\beta}{j\omega c_1} A_2 e^{-\beta x} - \frac{\alpha}{j\omega c_1} A_3 e^{\alpha x} - \frac{\beta}{j\omega c_1} A_4 e^{\beta x} \quad (\text{I-19})$$

Equations (I-7), (I-10), and (I-19) yield a solution for  $I_2$ .

$$I_2 = \left[ \frac{r_1}{r_2} - \frac{\alpha^2}{j\omega r_2 c_1} \right] A_1 e^{-\alpha x} + \left[ \frac{r_1}{r_2} - \frac{\beta^2}{j\omega r_2 c_1} \right] A_2 e^{-\beta x} + \left[ \frac{r_1}{r_2} - \frac{\alpha^2}{j\omega r_2 c_1} \right] A_3 e^{\alpha x} + \left[ \frac{r_1}{r_2} - \frac{\beta^2}{j\omega r_2 c_1} \right] A_4 e^{\beta x} \quad (\text{I-20})$$

Equations (I-10), (I-19), and (I-20) substituted into Equation (I-8) gives

$$\begin{aligned}
&= \frac{r_2}{\alpha} \left[ \frac{r_1}{r_2} - \frac{\alpha^2}{j\omega r_2 c_1} \right] A_1 e^{-\alpha x} + \frac{r_2}{\beta} \left[ \frac{r_1}{r_2} - \frac{\beta^2}{j\omega r_2 c_1} \right] A_2 e^{-\beta x} \quad (\text{I-21}) \\
&- \frac{r_2}{\alpha} \left[ \frac{r_1}{r_2} - \frac{\alpha^2}{j\omega r_2 c_1} \right] A_3 e^{\alpha x} - \frac{r_2}{\beta} \left[ \frac{r_1}{r_2} - \frac{\beta^2}{j\omega r_2 c_1} \right] A_4 e^{\beta x}
\end{aligned}$$

Introducing a functional notation and writing Equations (I-10), (I-19), (I-20), and (I-21) in matrix form simplify the evaluation of the arbitrary constants  $A_1$ ,  $A_2$ ,  $A_3$ , and  $A_4$ .

$$\begin{bmatrix} f_1(x) & f_2(x) & f_3(x) & f_4(x) \\ f_5(x) & f_6(x) & f_7(x) & f_8(x) \\ f_9(x) & f_{10}(x) & f_{11}(x) & f_{12}(x) \\ f_{13}(x) & f_{14}(x) & f_{15}(x) & f_{16}(x) \end{bmatrix} \begin{bmatrix} A_1 \\ A_2 \\ A_3 \\ A_4 \end{bmatrix} = \begin{bmatrix} I_1(x) \\ E_1(x) \\ I_2(x) \\ E_2(x) \end{bmatrix} \quad (\text{I-22})$$

The functions in the square matrix represent the corresponding functions in Equations (I-10), (I-19), (I-20), and (I-21). They are listed in Table I-1 for reference.

Applying the boundary conditions

$$I_1(\lambda) = 0 \quad (\text{I-23})$$

$$I_2(0) = 0 \quad (\text{I-24})$$

$$I_2(\lambda) = 0 \quad (\text{I-25})$$

$$E_1(0) + E_2(0) = E_{in} \quad (\text{I-26})$$

to the matrix equation and simplifying to eliminate some of the functions

produce

$$\begin{bmatrix} f_1(\lambda) & f_2(\lambda) & f_3(\lambda) & f_4(\lambda) \\ f_9(0) & f_{10}(0) & f_9(0) & f_{10}(0) \\ f_9(0)f_1(\lambda) & f_{10}(0)f_2(\lambda) & f_9(0)f_3(\lambda) & f_{10}(0)f_4(\lambda) \\ \frac{r}{\alpha} & \frac{r_1}{\beta} & -\frac{r_1}{\alpha} & -\frac{r_1}{\beta} \end{bmatrix} \begin{bmatrix} A_1 \\ A_2 \\ A_3 \\ A_4 \end{bmatrix} = \begin{bmatrix} 0 \\ 0 \\ 0 \\ E_{in} \end{bmatrix} \quad (\text{I-27})$$

For convenience, the following notation will be used to indicate the value of a function at the sending end of the line.

$$f_k(x)_{x=0} = f_k \quad (\text{I-28})$$

Utilizing this notation, Equation (I-27) becomes

$$\begin{bmatrix} e^{\alpha\lambda} & e^{-\beta\lambda} & e^{\alpha\lambda} & e^{\beta\lambda} \\ f_9 & f_{10} & f_9 & f_{10} \\ f_9 e^{-\alpha\lambda} & f_{10} e^{-\beta\lambda} & f_9 e^{\alpha\lambda} & f_{10} e^{\beta\lambda} \\ \frac{r_1}{\alpha} & \frac{r_1}{\beta} & -\frac{r_1}{\alpha} & -\frac{r_1}{\beta} \end{bmatrix} \begin{bmatrix} A_1 \\ A_2 \\ A_3 \\ A_4 \end{bmatrix} = \begin{bmatrix} 0 \\ 0 \\ 0 \\ E_{in} \end{bmatrix} \quad (\text{I-29})$$

The determinant of the coefficients for Equation (I-29) after evaluation and simplification is

$$\Delta = 4(f_9 - f_{10}) \left( \frac{r_1}{\beta} f_9 \sinh(\alpha\lambda) \cosh(\beta\lambda) - \frac{r_1}{\alpha} f_{10} \sinh(\beta\lambda) \cosh(\alpha\lambda) \right) \quad (\text{I-30})$$

Solving for the arbitrary constants produces

$$A_1 = \frac{-2E_{in} f_{10} (f_9 - f_{10}) \epsilon^{\alpha\lambda} \sinh(\beta\lambda)}{\Delta} \quad (I-31)$$

$$A_2 = \frac{2E_{in} f_9 (f_9 - f_{10}) \epsilon^{\beta\lambda} \sinh(\alpha\lambda)}{\Delta} \quad (I-32)$$

$$A_3 = \frac{2E_{in} f_{10} (f_9 - f_{10}) \epsilon^{-\alpha\lambda} \sinh(\beta\lambda)}{\Delta} \quad (I-33)$$

$$A_4 = \frac{-2E_{in} f_9 (f_9 - f_{10}) \epsilon^{-\beta\lambda} \sinh(\alpha\lambda)}{\Delta} \quad (I-34)$$

After substituting these values for the constants, Equations (I-10), (I-19), (I-20) and (I-21) can be written after simplification

$$I_1(x) = E_{in} \frac{f_9 \sinh(\alpha\lambda) \sinh(\lambda-x)\beta - f_{10} \sinh(\beta\lambda) \sinh(\lambda-x)\alpha}{\frac{r_1}{\beta} f_9 \sinh(\alpha\lambda) \cosh(\beta\lambda) - \frac{r_1}{\alpha} f_{10} \sinh(\beta\lambda) \cosh(\alpha\lambda)} \quad (I-35)$$

$$I_2(x) = E_{in} \frac{f_9 f_{10} \sinh(\alpha\lambda) \sinh(\lambda-x)\beta - f_9 f_{10} \sinh(\beta\lambda) \sinh(\lambda-x)\alpha}{\frac{r_1}{\beta} f_9 \sinh(\alpha\lambda) \cosh(\beta\lambda) - \frac{r_1}{\alpha} f_{10} \sinh(\beta\lambda) \cosh(\alpha\lambda)} \quad (I-36)$$

$$E_1(x) = E_{in} \frac{f_6 f_9 \sinh(\alpha\lambda) \cosh(\lambda-x)\beta - f_5 f_{10} \sinh(\beta\lambda) \cosh(\lambda-x)\alpha}{\frac{r_1}{\beta} f_9 \sinh(\alpha\lambda) \cosh(\beta\lambda) - \frac{r_1}{\alpha} f_{10} \sinh(\beta\lambda) \cosh(\alpha\lambda)} \quad (I-37)$$

$$E_2(x) = E_{in} \frac{f_9 f_{14} \sinh(\alpha\lambda) \cosh(\lambda-x)\beta - f_{10} f_{13} \sinh(\beta\lambda) \cosh(\lambda-x)\alpha}{\frac{r_1}{\beta} f_9 \sinh(\alpha\lambda) \cosh(\beta\lambda) - \frac{r_1}{\alpha} f_{10} \sinh(\beta\lambda) \cosh(\alpha\lambda)} \quad (I-38)$$

Also an expression for the voltage between the top and bottom strata is given by

$$E(x) = E_{in} \frac{\alpha f_9 \sinh(\alpha\lambda) \cosh(\lambda-x) \beta - \beta f_{10} \sinh(\beta\lambda) \cosh(\lambda-x) \alpha}{\alpha f_9 \sinh(\alpha\lambda) \cosh(\beta\lambda) - \beta f_{10} \sinh(\beta\lambda) \cosh(\alpha\lambda)} \quad (I-39)$$

since

$$(f_6 + f_4) = \frac{r_1}{\beta} \quad (I-40)$$

and

$$(f_5 + f_{13}) = \frac{r_1}{\alpha} \quad (I-41)$$

When Equation (I-39) is evaluated for

$$x = \lambda \quad (I-42)$$

the open-circuit voltage transfer function is

$$T(s) = \frac{\alpha f_9 \sinh(\alpha\lambda) - \beta f_{10} \sinh(\beta\lambda)}{\alpha f_9 \sinh(\alpha\lambda) \cosh(\beta\lambda) - \beta f_{10} \sinh(\beta\lambda) \cosh(\alpha\lambda)} \quad (I-43)$$

Multiplying this equation by  $\frac{r_1}{\alpha\beta}$  yields

$$T(s) = \frac{\frac{r_1 f_9}{\beta} \sinh(\alpha\lambda) - \frac{r_1 f_{10}}{\alpha} \sinh(\beta\lambda)}{\frac{r_1 f_9}{\beta} \sinh(\alpha\lambda) \cosh(\beta\lambda) - \frac{r_1 f_{10}}{\alpha} \sinh(\beta\lambda) \cosh(\alpha\lambda)} \quad (I-44)$$

Since  $u = \sqrt{s r_1 c_1} \lambda^2$ , the following changes in parameters and variables can be made.

$$\alpha\lambda = Au \quad (I-45)$$

$$\beta\lambda = Bu \quad (I-46)$$

$$\frac{r_1 f_9}{\beta} = K_1 \quad (\text{I-47})$$

$$-\frac{r_1 f_{10}}{\alpha} = K_2 \quad (\text{I-48})$$

The transfer function can be written in terms of the new variable  $u$

$$T(u) = \frac{K_1 \sinh(Au) + K_2 \sinh(Bu)}{K_1 \sinh(Au) \cosh(Bu) + K_2 \sinh(Bu) \cosh(Au)} \quad (\text{I-49})$$

A summary of the notation introduced follows in Table 1.

Table 1. Summary of Notation Introduced in Appendix I

---

$\Delta$	The Characteristic Determinant
$A_1, A_2, A_3, A_4$	Arbitrary Constants
$D_1, D_2, D_3, D_4$	The Roots of the Characteristic Equation

$$\tau = \frac{1}{2} (r_1 c_1 + r_2 c_2 + r_2 c_1)$$

$$\beta_r = \sqrt{1 - \frac{4r_1 c_1 r_2 c_2}{(r_1 c_1 + r_2 c_2 + r_2 c_1)^2}}$$

$$\alpha = \sqrt{j\omega\tau(1+\beta_r)}$$

$$\beta = \sqrt{j\omega\tau(1-\beta_r)}$$

$$f_1(x) = \epsilon^{-\alpha x}$$

$$f_2(x) = \epsilon^{-\beta x}$$

$$f_3(x) = \epsilon^{\alpha x}$$

---

(Continued)

Table 1. (Continued)

$$f_4(x) = e^{\beta x}$$

$$f_5(x) = \frac{\alpha}{j\omega c_1} e^{-\alpha x}$$

$$f_6(x) = \frac{\beta}{j\omega c_1} e^{-\beta x}$$

$$f_7(x) = -\frac{\alpha}{j\omega c_1} e^{\alpha x}$$

$$f_8(x) = -\frac{\beta}{j\omega c_1} e^{\beta x}$$

$$f_9(x) = \left[ \frac{r_1}{r_2} - \frac{\alpha^2}{j\omega r_2 c_1} \right] e^{-\alpha x}$$

$$f_{10}(x) = \left[ \frac{r_1}{r_2} - \frac{\beta^2}{j\omega r_2 c_1} \right] e^{-\beta x}$$

$$f_{11}(x) = \left[ \frac{r_1}{r_2} - \frac{\alpha^2}{j\omega r_2 c_1} \right] e^{\alpha x}$$

$$f_{12}(x) = \left[ \frac{r_1}{r_2} - \frac{\beta^2}{j\omega r_2 c_1} \right] e^{\beta x}$$

$$f_{13}(x) = \frac{r_2}{\alpha} \left[ \frac{r_1}{r_2} - \frac{\alpha^2}{j\omega r_2 c_1} \right] e^{-\alpha x}$$

$$f_{14}(x) = \frac{r_2}{\beta} \left[ \frac{r_1}{r_2} - \frac{\beta^2}{j\omega r_2 c_1} \right] e^{-\beta x}$$

$$f_{15}(x) = -\frac{r_2}{\alpha} \left[ \frac{r_1}{r_2} - \frac{\alpha^2}{j\omega r_2 c_1} \right] e^{\alpha x}$$

$$f_{16}(x) = -\frac{r_2}{\beta} \left[ \frac{r_1}{r_2} - \frac{\beta^2}{j\omega r_2 c_1} \right] e^{\beta x}$$

$$\tau' = \frac{1}{2} \left( 1 + \frac{r_2}{r_1} + \frac{r_2 c_2}{r_1 c_1} \right)$$

(Continued)

Table 1. (Continued)

---

$$A = \sqrt{\tau' + \sqrt{(\tau')^2 - \frac{r_2 c_2}{r_1 c_1}}}$$

$$B = \sqrt{\tau' - \sqrt{(\tau')^2 - \frac{r_2 c_2}{r_1 c_1}}}$$

$$K_1 = \frac{A^2 - 1}{B(A^2 - B^2)}$$

$$K_2 = \frac{1 - B^2}{A(A^2 - B^2)}$$

---

APPENDIX II

COMPUTATIONAL METHOD FOR THE ROOTS OF  
TRANSCENDENTAL EQUATIONS

The method used for computing the roots of the transcendental equations discussed in the research is the Newton-Raphson iteration generalized for two variables.<sup>17</sup> The independent variables in this case are the real and imaginary parts of the complex-frequency variable.

The Newton-Raphson method for one variable uses an approximate root and improves this root to produce in most cases an improved approximate root. The well known recurrence formula for this process is

$$x_{k+1} = x_k - \frac{f(x_k)}{F'(x_k)} \quad (\text{II-1})$$

The error in the approximation tends to be proportional to the square of the error in the previous approximate root when the process is converging satisfactory.

The Newton-Raphson process as applied to a function of a complex variable is outlined in the following paragraphs.

Starting with the function of a complex variable,  $F(u)$ , it is written as the sum of two real functions of two real variables

$$F(u) = f(x,y) + j g(x,y) \quad (\text{II-2})$$

Now the zeros of the function  $F(u)$  are the simultaneous zeros of the two functions

$$f(x,y) = 0 \quad (\text{II-3})$$

$$g(x,y) = 0 \quad (\text{II-4})$$

Expanding Equations (II-3) and (II-4) in Taylor series about the point  $(x,y)$  and neglecting all terms above the linear terms yields

$$f(x,y) = 0 = f(a,b) + (x-a)f_x(a,b) + (y-b)f_y(a,b) \quad (\text{II-5})$$

$$g(x,y) = 0 = g(a,b) + (x-a)g_x(a,b) + (y-b)g_y(a,b) \quad (\text{II-6})$$

Now replacing  $(a,b)$  with  $(x_k, y_k)$  and  $(x,y)$  with  $(x_{k+1}, y_{k+1})$  produces the desired recurrence formulas.

$$(x_{k+1} - x_k)f_x(x_k, y_k) + (y_{k+1} - y_k)f_y(x_k, y_k) = -f(x_k, y_k) \quad (\text{II-7})$$

$$(x_{k+1} - x_k)g_x(x_k, y_k) + (y_{k+1} - y_{k+1})g_y(x_k, y_k) = -g(x_k, y_k) \quad (\text{II-8})$$

The following notation is introduced.

$$(x_{k+1} - x_k) = X_{\text{cor}} \quad (\text{II-9})$$

$$(y_{k+1} - y_k) = Y_{\text{cor}} \quad (\text{II-10})$$

$$f(x_k, y_k) = F1 \quad (\text{II-11})$$

$$f_x(x_k, y_k) = F2 \quad (\text{II-12})$$

$$f_y(x_k, y_k) = F3 \quad (\text{II-13})$$

$$g(x_k, y_k) = G1 \quad (\text{II-14})$$

$$g_x(x_k, y_k) = G2 \quad (\text{II-15})$$

$$g_y(x_k, y_k) = G3 \quad (\text{II-16})$$

Equations (II-7) and (II-8) are written in matrix form and solved for the corrections which can then be applied to  $(x_k, y_k)$  to obtain  $(x_{k+1}, y_{k+1})$ .

$$\begin{bmatrix} F2 & F3 \\ G2 & G3 \end{bmatrix} \begin{bmatrix} X_{\text{cor}} \\ Y_{\text{cor}} \end{bmatrix} = \begin{bmatrix} -F1 \\ -G1 \end{bmatrix} \quad (\text{II-17})$$

$$X_{\text{cor}} = \frac{G1 \cdot F3 - F1 \cdot G3}{F2 \cdot G3 - F3 \cdot G2} \quad (\text{II-18})$$

$$Y_{\text{cor}} = \frac{G2 \cdot F1 - F2 \cdot G1}{F2 \cdot G3 - F3 \cdot G2} \quad (\text{II-19})$$

Equations (II-18) and (II-19) have been programmed for the Burroughs 220 digital computer for the transcendental functions discussed in Chapters III and IV. In the case of the numerator of Equation (3-12), given by

$$F(u) = \sinh(Au) + K \sinh(Bu)$$

an extensive study of the root locus was made using the described method. The results of this study appear in Chapter III.

## BIBLIOGRAPHY

1. Thomson, Sir William, Mathematical and Physical Papers, Vol. II, Cambridge University Press, 1884, pp. 41-174.
2. Kennelly, A. E., Tables of Complex Hyperbolic and Circular Functions, Harvard University Press, 1913.
3. Kaufman, W. M., "Theory of a Monolithic Null Device and Some Novel Circuits," Proceedings of the Institute of Radio Engineers, Vol. 48, No. 9, pp. 1540-1945, September 1960.
4. Castro, P. S., "Microsystem Circuit Analysis," Electrical Engineering, Vol. 80, No. 7, pp. 535-542, July 1961.
5. Happ, W. W., and Castro, P. S., "Distributed Parameter Circuit Design Techniques," LMSC 6-59-61-1, Lockheed Missile and Space Company, Palo Alto, California.
6. Carson, J. R., "Propagation of Periodic Currents over Nonuniform Lines," Electrician, Vol. 861, No. 10, pp. 272-273, March 1921.
7. Starr, A. T., "The Nonuniform Transmission Line," Proc. of IRE, Vol. 20, No. 6, pp. 1052-1063, June 1932.
8. Edson, W. A., "Tapered Distributed RC Lines for Phase-Shift Oscillators," Proc. of IRE, Vol. 49, No. 6, pp. 1021-1024, June 1961.
9. Su, K. L., Trigonometric RC Transmission Lines, To be published in the I.E.E.E. Convention Record, Vol. 11, 1963.
10. Golomb, M., and Shanks, M., Elements of Ordinary Differential Equations, New York, McGraw-Hill Book Company, Inc., 1950, pp. 191-221.
11. Happ, W. W., and Castro, P. S., op. cit., pp. 3-5.
12. Truxal, J. G., Automatic Feedback Control System Synthesis, New York, McGraw-Hill Book Company, 1955, p. 190.
13. Kaufman, W. M., op. cit.
14. Guillemin, E. A., Synthesis of Passive Networks, New York, John Wiley and Sons, Inc., 1957, p. 191.
15. Holland, L., Vacuum Deposition of Thin Films, New York, John Wiley and Sons Inc., 1956, p. 249.

16. Bjorksten Laboratories, Polyesters and Their Applications, New York, Reinhold Publishing Corporation, 1956, p. 221.
17. Hildebrand, F. B., Introduction to Numerical Analysis, New York, McGraw-Hill Book Company, Inc., 1956, pp. 447-48.

## VITA

Joseph Morris Googe, the son of Paul H. and Edith M. Googe, was born in Savannah, Georgia, on August 15, 1927. He was married to Miss Betty R. Buntyn in 1949, and they now have three sons.

He attended public schools in Savannah and graduated from Savannah High School in 1945. Later he attended the Georgia Institute of Technology, receiving the Bachelor of Electrical Engineering degree in 1951 and the Master of Science degree in Electrical Engineering in 1952.

Mr. Googe served as an Electronic Technician in the United States Navy from 1946 through 1948. He was employed as an engineer by ARO, Incorporated, Tullahoma, Tennessee, from 1951 until 1956. During 1956 and 1957 he was employed by the Lockheed Aircraft Corporation, Marietta, Georgia. In 1957 he became an Assistant Professor of Electrical Engineering at the Georgia Institute of Technology, resigning that position in 1962 to accept a Ford Foundation Fellowship.

Mr. Googe is a Senior Member of the Institute of Electrical and Electronics Engineers. He is a Deacon in the Presbyterian Church in The United States.